



UNIVERSITY OF CENTRAL FLORIDA

**EEL 4914 – Senior Design I, Summer 2021**  
**Portable Surface Plasmon Resonance Sensor for**  
**Immunoglobulin G Antibody Testing**

Group 2

Robert Ballentine, Photonics Engineering

Robin Howell, Photonics Engineering

James Henderson, Computer Engineering

# Table of Contents

1. Project description .....	4
1.A Defined Project.....	4
1.B Motivation .....	6
1.C Project Goals and Objectives.....	6
2. Requirements.....	7
2.A Features .....	7
2.A.1 Basic Features .....	8
2.A.2 Advanced Features.....	10
2.A.3 Stretch Features .....	10
2.B List of Requirement Specifications .....	11
2.C Table of Specifications .....	11
2.D House of Quality .....	12
3. Device Illustration.....	14
4. Project Research.....	15
4.A Existing Products.....	15
4.A.1 Smartphone Based SPR Sensor using Multimode Optical Fiber.....	16
4.A.2 Smartphone Based SPR Sensor using an External LED.....	17
4.A.3 Prism-coupled Method for SPR Sensors.....	18
4.B Optical Fiber for Wave Propagation.....	19
4.C Light Sources .....	19
4.C.1 LED as a Light Source .....	19
4.C.2 Laser Diode as a Light Source .....	20
Table x. Comparison of Laser Diodes to Purchase.....	22
4.D Physical Optics .....	23
4.D.1 Neutral Density Filter .....	23
4.D.2 Wavelength Filters.....	24
4.D.3 Linear Polarizer.....	27
4.D.4 Right-Angle N-BK7 Glass Prism .....	27

4.E CMOS Sensor and Microcontroller for SPR Detection .....	28
4.F SPR Sensor Surface .....	29
4.G SPR Sample Preparation .....	30
4.H SPR Sensor Accuracy .....	31
4.I Power Delivery .....	32
4.J 3D-Printed Housing and Mounts .....	33
4.J Software Solutions .....	34
5. Constraints and Standards .....	37
5.A Constraints .....	38
5.A.1 Financial .....	38
5.A.2 Environmental .....	38
5.A.3 Social .....	39
5.A.4 Political .....	39
5.A.5 Ethical .....	39
5.A.6 Health and Safety .....	39
5.A.7 Manufacturability .....	40
5.A.8 Software Compatibility .....	40
5.A.9 Sustainability .....	40
5.A.10 Covid and the Global Semiconductor Shortage .....	41
5.A.11 Time Constraints .....	41
5.A.12 Storing and Handling of Biological Samples .....	42
5.B Standards .....	44
5.B.1 Laser Safety .....	45
5.B.3 Communication Standards .....	47
5.B.4 Software Standards .....	48
5.B.7 Chemical Laboratory Safety in Academic Institutions .....	49
5.B.7.1 Personal Protective Equipment (PPE) .....	50
5.B.7.2 Maintaining an Organized Environment .....	51
5.B.7.3 Labeling Chemicals .....	51
5.B.7.4 Cleaning Glassware and Disposal of Chemicals .....	52
5.B.7.5 Safety Procedures for Using Electrical Equipment .....	54
5.B.7.6 Refrigerating Chemical or Biological Samples .....	54

6.	Project Hardware Design Details.....	55
6.A	Design Calculations.....	55
6.A.1	Optical Design Calculations.....	55
6.A.2	Electrical Design Calculations.....	53
6.B	Initial Designs and Related Diagrams.....	57
6.B.1	Initial Design Idea – Smartphone Based SPR Sensor.....	58
6.B.1.1	Light Source Design.....	60
6.B.1.2	SPR Detector Design.....	61
7.	Project Testing and Prototype Construction.....	61
7.A	Hardware Testing.....	62
7.A.1	Microcontroller and Power Supply Testing.....	62
7.A.2	3D Printed Housing / Mounts.....	68
7.A.3	Laser Diode Testing.....	72
7.A.4	Simulating the Surface Plasmon Resonance Curve.....	76
7.A.5	Power Optimization using Software.....	73
7.B	Prototype Construction.....	79
7.B.1	Determining the Polarization of our Incident Light.....	85
7.B.2	Investigating the Properties of our SPR Chip.....	92
7.C	Software Testing.....	85
8.	Block Diagrams.....	94
9.	Bill of Materials.....	96
10.	Project Milestones.....	97
11.	Conclusion.....	98
	Appendix A – References.....	100
	Appendix B – Permissions.....	101

## 1. Project description

### 1.A Defined Project

Surface plasmon resonance, or SPR for short, is an optical effect that can measure the binding of molecules in real time without labels. The SPR sensor is a biological sensor used to measure the kinetics and affinity of the interactions within the

sample. These interactions can be seen through dips in spectral intensity as a light source interacts with a dielectric film layered with the analyte.

The goal of this device is to create a more affordable, easily readable, and portable sensor for commercial use that is controlled using a software application. This will be done using an optical set up that detects the surface plasmon interactions through changes in the light source's intensity. This change in intensity will be detected using an external CMOS sensor camera that will be controlled using a microcontroller unit. The captured images from the camera will be transmitted via Wi-Fi to a compatible device where the detectable information will be extrapolated and displayed through a self-developed android application. The application will display various characteristics and information pertaining to the processed information from the sensor. A 532 nm focused laser diode will be the light source of choice for this experiment. The beam will undergo slight modifications before the light propagates through the prism and interacts with SPR sensor chip attached to the prism's uppermost face. Before the beam reflects off the first mirror, it will experience a filtering of both wavelength, polarization, and overall light intensity. A neutral density filter with optical density of 1.0 will allow only 10% of the light to be transmitted, reducing the output power of the laser diode from 10 milliwatt to 1 milliwatt to ensure the SPR and CMOS sensor are not oversaturated. A bandpass filter with a center wavelength of 532nm to maintain uniformity in laser light, and a polarizing filter to make all the light linear and p polarized. This means that the light's electric field is polarized to be parallel to the plane of incidence. This will lessen the amount of light traveling at different angles, reducing the divergence within the initial region of the system. Linear polarized light is an asset for this project because linear polarized light operates under the constraint of a single dimensional vector plane for propagation. This light will bounce off two mirrors before it enters the prism. For surface plasmon resonance to occur, light needs to penetrate the surface the SPR chip is attached to at an angle greater than the critical angle of the glass prism's face. It was calculated that a simple angle such as  $90^\circ$  allow for surface plasmons to be detected through detection of evanescent waves. This angle will be produced from placing the two mirrors at different angles. The first mirror will have a  $45^\circ$  tilt, sending the beam to the second mirror that has an angle of  $135^\circ$ . The mirrors will be attached to wedge-like platforms throughout the body of the 3D printed housing. The prism of choice is a right-angle flint (N-BK7) prism that lacks coating. The lack of coating is important to note as the risk of not attuning the light with filters before arriving at the interface would result in the targeted data being contaminated with unwanted information generated within the diode. After the excitation occurs, the light will be guided directly onto the CMOS sensor. The CMOS sensor will capture one image every 0.5 seconds over a 600 second interval. After the images are captured, the CMOS sensor will transmit the images via Wi-Fi to the compatible device. Once the images are transmitted, the application will process the images to determine the changes in intensity during the SPR sensing process and convert the data into user-friendly graphs that inform when molecular binding began, ended, or did not occur.

This document describes the design process of the SPR sensor. The report begins with a device description and the motivation behind choosing the sensor, as well

as the initial goals and objectives. The requirements and specifications of the device follow. A research section will be included to describe the process of choosing different optical components including a comparison between different technology compatible with the device. The research section will also describe the benefits of each component in the system. Following the research, a section describing the standards and constraints of the device will be introduced. The following section will be dedicated towards describing the hardware and software design of the device, including the process of 3D printing components and housing. The document will then include information on the administrative aspect of the project. This includes a timetable for the paper and the development of the device and financing. The end of the report will include a conclusion, references, and an appendix if necessary.

## **1.B Motivation**

There are various questions that exist that can be solved from the SPR detection method. Such questions include: Are pesticides lingering on produce? Is there contamination in a body of water? Does my food contain traces of salmonella? As mass production of perishables become more and more processed, these are important things to be aware of before consumption. Yet the challenge for many SPR sensors are their price and portability. Commercial SPR sensors can cost thousands of dollars and are not well designed for many remote and low-income locations. The need for low-cost yet high quality devices is crucial for the democratization of medical services. Therefore, we propose to develop a compact SPR sensor that can be attached to a compatible device to provide rapid, on-site detection while significantly reducing the manufacturing cost of the SPR sensor itself.

## **1.C Project Goals and Objectives**

The proposed idea for this project is to create a portable, accurate, and low-cost SPR sensor that can be easily controlled using various devices. For this idea to come to fruition, the main goals and objectives must be defined to provide direction in the development of our product. The four main goals for our portable SPR sensor are as follows:

1. Cost
2. Portability
3. Consumer Friendly
4. Accuracy

The first goal of the device is to build a product that is at a more affordable price range compared to commercial SPR sensors in the market today. The average price of a commercial SPR sensor is \$40,000 which limits the use of this technology to only those with large budgets. Our device would allow for lower-income or remote locations

that may not have the necessary expenses to be able to build or use our SPR sensor to understand molecular interactions of antibodies or other substances.

The second goal is to allow our device to be portable for easy use in remote locations. To do this, a battery-powered power supply unit will be used as a power source for our laser diode and microcontroller using two 9V Alkaline batteries. With this goal, our device can be used in locations where power from a wall outlet may not be available.

The third goal is to create a device that is simple and easy to use for a consumer. This goal will be achieved in multiple ways. First, our design will use a prism as the SPR sensing location in order to keep the optical components separate from the solution to be tested so the sensor can easily be replaced by the consumer. Second, the software application to control the SPR sensor will be accessible for Windows, Android, Linux, iOS, and MacOS devices. This will allow our final product to be compatible with various devices, allowing the consumer to control the device from multiple platforms.

The fourth goal is to develop an SPR sensor that is as accurate if not more so than previous SPR sensors available. Researchers in China in 2015 developed a smart phone based SPR sensor which was able to detect samples of bovine immunoglobulin G as small as 47.4 nanomolar and compared it to a commercial SPR sensor which could detect the same analyte in concentrations as small as 15.7 nanomolar [Liu, Y. citation]. The goal for our device is to be able to accurately detect samples of bovine immunoglobulin G to at least 47.4 nanomolar and at most 15.7 nanomolar. To achieve this goal, high precision optical components were chosen to ensure majority of the emitted light from our source is controlled throughout the system.

## **2. Requirements**

### **2.A Features**

During the initial planning of any design, it is necessary to decide on the main features of the project one hopes to accomplish. These features provide a detailed explanation of the main functions of the final product and how they aid in accomplishing the goals set by the entire team. The features are separated into three sections: basic features, advanced features, and stretch features. Basic features are the set attributes we will accomplish for our project at the end of Senior Design II. These features will be detailed in their explanations to properly express the final design ideas from each team member. Advanced features are ideas for upgrading our project that would enhance the functionality of our product but may not be possible to accomplish given the allotted time. Stretch features are ideas to take our project to the next level if it were to become a marketable product. It would place our device at the same level as commercial SPR

sensors but would require even more time to accomplish. The following sections will describe the three features and the benefits they bring to our final idea.

### **2.A.1 Basic Features**

The basic features of our project will describe each optical, electrical, and computer component required for our final design. This project is primarily optical, with some systems and electrical engineering to create a fully functional SPR sensor. A 532 nm laser diode will be connected to a microcontroller that will allow the software application to communicate with the system and determine when the laser turns on or off. An external CMOS sensor camera will be connected to the microcontroller unit and will be used as the detector for our SPR sensor. Throughout the experiment, the camera will capture one image at the end of the optical system every 0.5 seconds at a 1600 x 1200-pixel resolution. This will provide us with the necessary data to determine when molecular binding of the analyte to the ligand is taking place. A battery-powered power supply unit will be used as a power source for our laser diode and microcontroller. The power supply will consist of two 9V Alkaline batteries. One 9V battery will power the microcontroller unit while the other will provide power to the laser diode. Two separate batteries will ensure that there is sufficient power given to both the microcontroller unit and the laser diode so that the input voltage to our laser diode remains constant. This is crucial to the success of our project due to any fluctuations in the intensity of our laser diode can corrupt our data. The light from the laser diode will be manipulated by a 532 nm bandpass filter and linear polarizer. The bandpass filter will filter out any infrared wavelengths in the emitted light from our laser diode that was used to pump our gain medium to create stimulated emission, therefore ensuring we have monochromatic light throughout of SPR sensor. The linear polarizer is crucial to create surface plasmon excitation, as it allows only light that is linearly polarized parallel to the plane of incidence to interact with our SPR sensor. Two mirrors will then be used to direct the light onto a right-angle prism. This is where the surface plasmon detection occurs. By angling our incident beam to a 45-degree angle using mirrors, we can create the phenomenon called total internal reflection as the beam hits the right-angle prism. This coupling of the light using the prism creates a perfect situation where surface plasmon excitation can occur as most of the energy from our incident light will be absorbed at a particular angle, defined as the resonance angle, by the metal/dielectric interface on our SPR chip. This leads to a decrease in intensity of our received light onto the CMOS camera. The decrease in intensity of our received light indicates that excitation occurred, and molecular binding took place.

For our experiment, we will observe the molecular binding of Staphylococcus Protein A (SPA) and bovine immunoglobulin G (IgG). Due to the interactions between SPA and IgG, SPA is commonly used to for antibody testing and disease diagnosis. The SPA will be previously immobilized to an SPR chip that will be purchased from a



manufacturing facility, while the IgG will be in various liquid concentrations with the buffer solution phosphate-buffer saline. Phosphate-buffer saline (PBS) is a common salt solution used for cell culture applications to remove the molecular binding in an SPR chip. The IgG concentrations will be placed into the sample chamber which contains our Protein A immobilized SPR chip glued to the base of our prism. The purpose of testing various concentrations of our IgG solution with PBS is to provide an accurate representation of the sensitivity of our SPR sensor as molecular binding occurs. PBS is used to clean an SPR sensor after use by removing the molecular binding that occurred on the sensor surface. As the concentration of IgG is increased, we can gain a better understanding of our SPR sensor's sensitivity to the molecular binding occurring with SPA and IgG. The expected outcome of our experiment is to see an increase in our relative intensity of the SPR sensor's response as we increase the concentration of IgG in our solution, which indicates its sensitivity to detecting IgG being bound to SPA. Our goal is to create an SPR sensor that can detect IgG concentrations as low as 7.11 micrograms combined in 1 mL of PBS buffer solution. The decision to test concentrations as low as 7.11 micrograms was based on a previous smartphone SPR sensor created in 2015 that was able to detect IgG concentrations as low as 47.4 nanomolar [Lui, Y. citation]. To convert 47.4 nanomolar to micrograms, Equation 1 below was used. Knowing that the typical molecular weight of IgG is 150,000 g/mol, we were able to calculate that our goal concentration level of IgG we should be able to detect would be around 7.11 micrograms.

$$M = C \times V \times W$$

Equation 1: Conversion of concentrations from molarity to grams.

Mass in grams (M) is equal to the concentration per liter (C) of the solution, multiplied by the volume in liters (V) which is multiplied by the molecular weight in grams per molarity (W).

A software application will be developed to turn on the SPR sensor and analyze the captured images from the external CMOS sensor camera. The application will control both the external laser diode and camera to capture one image every 0.5 seconds of the reflected light from the SPR sensor during a 600 second interval while surface plasmon excitation is occurring. A custom-programmed application will be used to map the relative intensity profile of the received images and display them in a graphical form, providing the user with the change in relative intensity over time. Initially we will use MATLAB for testing the image processing methods then transition to an software-based application with processing methods influenced from the MATLAB functions. The application will be able to analyze the increase or decrease in relative intensity and provide the user with information on what time interval molecular binding begins, ends, and if no binding occurred at all. The application will also allow the user to test various concentrations of the same sensing element to then provide a graph containing the various relative intensity changes over time for the different concentrations. This would easily allow the user to determine which concentration created the most molecular binding from their experiment. The final application will also

be designed for compatibility with Windows, Linux, iOS, and MacOS to provide a more versatile product.

### **2.A.2 Advanced Features**

An advanced feature we would like to implement into our final design is a flow cell that would be attached to our SPR sensing location. A flow cell is a tube designed for liquid samples to continuously flow through using a pump. A pump is attached to two small holes on the flow cell and pushes the liquid sample through at a certain flow rate. This is beneficial for samples that can be damaged by light sources or for samples that are changing their concentration. Many SPR sensors that we have researched contained flow cells to allow for a constant flow of the sample across the SPR sensing location, which aids in the molecular binding process. One such example was in a 2015 smartphone based SPR sensor created in China [Liu, Y. citation], which used optical fiber as its SPR sensing location and placed the flow cell around the exposed core of the fiber that contained the gold film functionalized with immobilized Protein A. Another example is a smartphone based SPR sensor created in Turkey in 2016 [Guner, H. citation], which used a flow cell to pump mouse IgG antibodies onto a SPR sensor chip designed using a Blu-ray disk coated with silver and gold nanoparticles. Both examples utilized a flow cell in their final design due to the constant flow rate of the analyte solution allowing for more molecular binding to occur on the SPR sensing location. A flow cell is a very practical addition to an SPR sensor as it allows for a more accurate reading of the analyte solution to occur due to the constant movement of the solution across the SPR sensor itself.

### **2.A.3 Stretch Features**

A stretch feature for our design would be to upgrade the pump connected to the flow cell to automatically pump our phosphate-buffered saline solution or bovine immunoglobulin G solution into the flow cell and drain it once SPR detection is complete. The idea is very similar to commercial SPR sensors, such as the OpenSPR by the company Nicoya, which contains plastic bottles on the outside of the SPR sensing device where the buffer and analyte solutions can be added by the user. These bottles are attached to the sensing location of the SPR device with tubes that, when the pump is activated, will transfer their solution into the sensing location at a constant flow rate. A third bottle would be used to transfer the waste solution that is no longer needed after SPR detection is complete. An example image of the OpenSPR by Nicoya can be seen below in Figure 1.



**Figure 1.** OpenSPR Surface Plasmon Resonance Sensor by Nicoya [approval for image from Nicoya pending]

## 2.B List of Requirement Specifications

The following requirement specifications for a successful SPR sensor are as follows:

- Power consumption must be under 10 watts.
- Fast response time from external camera to software application.
- Camera must be able to capture one image every 0.5 seconds during a 600 second interval.
- Transmission range will be around 10 meters.
- Simple, consumer-friendly graphical user interface for software application.
- SPR sensor should be able to detect concentrations of IgG as low as 47.4 nanomolar combined in 1 mL of PBS buffer solution, or 7.11 micrograms per 1 mL of IgG/PBS solution.
- Voltage must be regulated to ensure laser output remains constant with no fluctuations in intensity.
- Application to control SPR sensor will be compatible with Windows, Android, Linux, iOS, and Mac OS.

## 2.C Table of Specifications

Table 1 below illustrates the specifications for the main optical, computer, electrical, and biological components that will be used in our SPR sensor.

Item	Specifications
Right-Angle Prism	<b>Material:</b> N-BK7 (K9) glass <b>Surface Flatness:</b> $\lambda/8$ <b>Surface Quality:</b> 40-20 <b>Dimensions:</b> 20x20x20 mm <b>Coating:</b> none
Bandpass Filter	<b>Material:</b> LB1 green glass <b>Center Wavelength:</b> 532 nm <b>Dimensions:</b> 25 mm diameter, 2 mm thickness
Plano Mirror(s)	<b>Material:</b> technical glass, A-Class

	<b>Dimensions:</b> 12 mm diameter <b>Coating:</b> none
Polarizing Beam Splitter	<b>Beamsplitter Material:</b> N-SF1 <b>AR Coating Range:</b> 420-680 nm <b>Surface Quality:</b> 40-20 <b>Surface Flatness:</b> < $\lambda/4$ at 633 nm <b>Extinction Ratio:</b> $T_p:T_s > 1000:1$ <b>Transmission Efficiency:</b> $T_p > 90\%$ <b>Reflection Efficiency:</b> $R_s > 99.5\%$
Laser Diode	<b>Center Wavelength:</b> 532 nm <b>Output Power:</b> 10 mW <b>Beam Divergence:</b> 0.1-2 mradian <b>Dot Diameter:</b> <25 mm at 10 m <b>Working Voltage:</b> 3V-5V DC
Absorptive Neutral Density Filter	<b>Optical Density:</b> 1.0 <b>Optical Density Tolerance:</b> +/- 4% at 546.1 nm <b>Transmission:</b> 10.0% at 546.1 nm <b>Dimensions:</b> 25.4 mm diameter, 0.9 mm thickness <b>Wavelength Range:</b> 400-900 nm <b>Damage Threshold:</b> 30 W//cm <sup>2</sup> for CW <b>Surface Quality:</b> 60-40 scratch-dig <b>Surface Flatness:</b> $\leq 2\lambda$ at 632.8 nm
Microcontroller and CMOS Sensor	<b>Resolution:</b> 1600x1200 pixels <b>Module Development Board:</b> ESP32-CAM <b>Microcontroller Chip:</b> ESP32 <b>Camera Module:</b> OV2640 <b>Camera Lens Diameter:</b> 5 mm <b>Energy Efficiency:</b> 5 mA LPM <b>Extra Features:</b> Wi-Fi enabled, compliant with Wi-Fi 802.11b/g/n/e/i and Bluetooth 4.2 standards
SPR Sensor Chip	<b>Dimensions:</b> 9x9x0.3 mm <b>Functionalized Chemical Group:</b> Protein A
Phosphate-Buffered Saline Solution	<b>Form:</b> liquid <b>Concentration:</b> 10X <b>pH Level:</b> 7.4
Immunoglobulin G	<b>Form:</b> liquid <b>Target:</b> Bovine <b>Host:</b> Goat <b>Antibody Format:</b> Whole IgG <b>Specificity:</b> IgG (H+L) <b>Conjugate:</b> Unconjugated <b>Clonality:</b> Polyclonal

**Table 1.** Table of Specifications for Optical, Electrical, Computer, and Biological Components

## 2.D House of Quality

A House of Quality diagram provides a guide for communicating both the marketing and engineering requirements for a project. It allows one to easily visualize what is considered a crucial parameter based on the particular need for the project and how it could work for or against the needs of the marketing or engineering team. It is difficult to describe what a customer means by quality, with each product and consumer

different from the other. Many times this leads to producing items that are costly and missing key functions that were not noticed during the initial planning. This is why diagrams such as House of Quality are so important: they provide a map for planning the cheapest yet most efficient product possible. A good House of Quality ensures that each component chosen for the product is meeting both the marketing and engineering goals agreed to by each party. The following table below shows a crossover between engineering requirements and marketing requirements for our SPR sensor and how each requirement correlates with one another.

			<b>Engineering Requirements</b>				
			<b>1.Transmission Range</b>	<b>2.Detector Response Time</b>	<b>3.Power Draw</b>	<b>4.Data Storage Space</b>	<b>5.Cost</b>
			+	+	-	+	-
<b>Marketing Requirements</b>	<b>1.Transmission Range</b>	+	↑↑	↓↓	↓	○	↓
	<b>2.Moderate Power Consumption</b>	-	○	○	↑	↓	↑
	<b>3.SPR Measurement Accuracy</b>	+	○	↑↑	↑	↑↑	↓↓
	<b>4.Simple GUI</b>	+	○	○	○	↓	↑↑
	<b>5.Cost</b>	-	↑	↑↑	↓	↓↓	↑↑
<b>Target</b>			~10 m	0.5 s	< 10 W	~256 MB	\$600

**Table 2.** House of Quality Diagram

Legend:

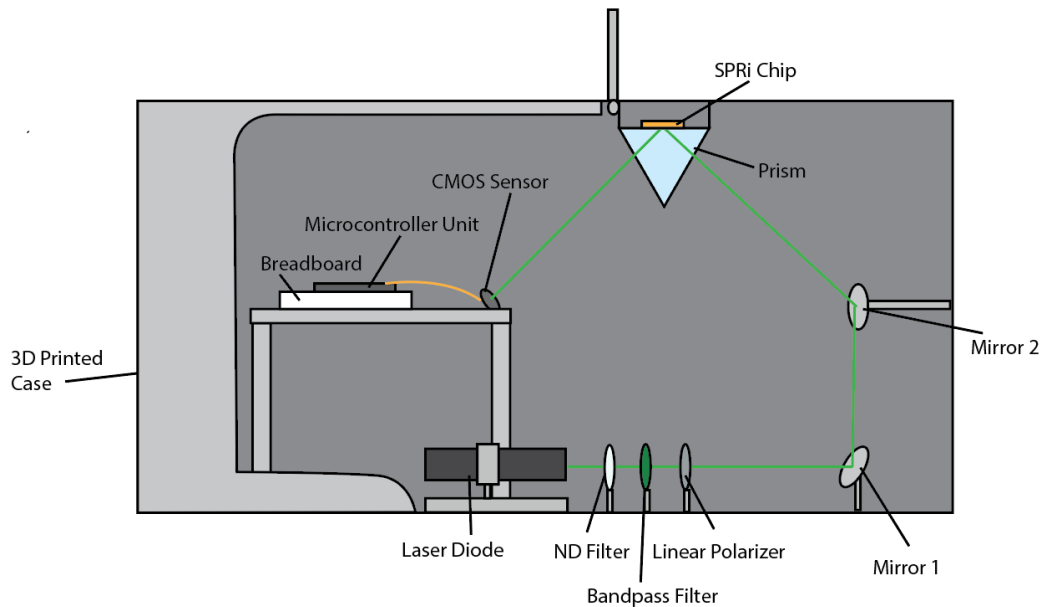
- ↑↑ Strong Positive Correlation
- ↑ Positive Correlation
- ○ No Correlation
- ↓↓ Strong Negative Correlation
- ↓ Negative Correlation

Table 2 illustrates the House of Quality designed for our portable SPR sensor. The House of Quality allows for us to easily visualize the necessary requirements from both a marketing and engineering standpoint to ensure our device is as successful as possible. Marketing requirements explain what is essential for our SPR sensor to achieve success from a marketing standpoint, while the engineering requirements illustrate what is essential for success from an engineering standpoint. Transmission Range for both marketing and engineering describe how far the wireless device can be positioned and still communicate with our SPR sensor using Wi-Fi. Allowing for the device to have a large transmission range is beneficial for both marketing the device to consumers and for allowing the device to work reliably from an engineering perspective. Moderate Power Consumption in the marketing requirements correlates with Power Draw for engineering requirements, as both should be low to ensure we have a long battery life for our SPR sensor. Other similar requirements include Cost which should be low for both marketing and engineering to provide users with an affordable device when compared to commercial SPR sensors.

Some requirements have a negative correlation with one another, as can be seen with SPR Measurement Accuracy in marketing requirements and Cost in engineering requirements. As is to be expected, a higher accuracy of our SPR sensor would allow our product a competitive edge when competing with more expensive SPR sensors on the market today. However, to obtain higher accuracy, many components such as the laser, prism, and CMOS sensor would need to be of a higher quality in order to achieve the precision accuracy many commercial SPR sensors can achieve. It then becomes a trade-off when designing the device on how accurate our final product can be while still maintaining a low budget. These negative correlations should be carefully considered when designing our product in order to find the right balance between both the management and engineering requirements.

### **3. Device Illustration**

This section provides an illustration of an ideal device for our surface plasmon resonance sensor, as can be seen in Figure 1 below. This image provides a visual representation of the final product with all the included components. As we perform tests and experiments, certain functions and components illustrated may change as we determine the most productive and cost-efficient form our final design will take.



**Figure 3.** Illustration of SPR Sensor device

## 4. Project Research

In this section, we discuss the decision-making process that occurred in the amalgamation of the surface plasmon resonance sensor. We discuss various technologies and design ideas used by previous SPR sensors and the benefits and concerns their approach has on the final product. Through our research of various mobile SPR sensors, we were able to design a product that meets our needs for the completion of the project. Additionally, we discuss improvements we've made on past design ideas that will ensure our final product is more efficient and consumer friendly.

### 4.A Existing Products

The following sections will describe various existing products we have researched that are similar to our final design. The purpose of this research was to gain a better understanding of the challenges designing a low-cost SPR sensor can bring and the multiple methods past designers have used to overcome these challenges. From our research, we were able to decide on which of these methods would be the most beneficial for our particular goals and constraints while also improving upon their original designs.

#### 4.A.1 Smartphone Based SPR Sensor using Multimode Optical Fiber

In the early days of our project, our design for a low-cost surface plasmon resonance sensor centered around utilizing a smartphone device as the controller, light source, and detector for the SPR sensor itself. In doing so, much of the cost would be mitigated and allow us to spend more money on other aspects of our product. One study conducted in China in 2015 gave us our initial ideas on how a smartphone can be used to detect molecular binding [Lui, Y citation]. In this study, a smartphone based SPR sensor was developed using intensity modulation to monitor the light intensity of the LED source during molecular binding. In their device, the flashlight LED of the smartphone device was used as the light source for the SPR sensor. A schematic of their final design as well as an image of the finished product can be seen in Figure 2.

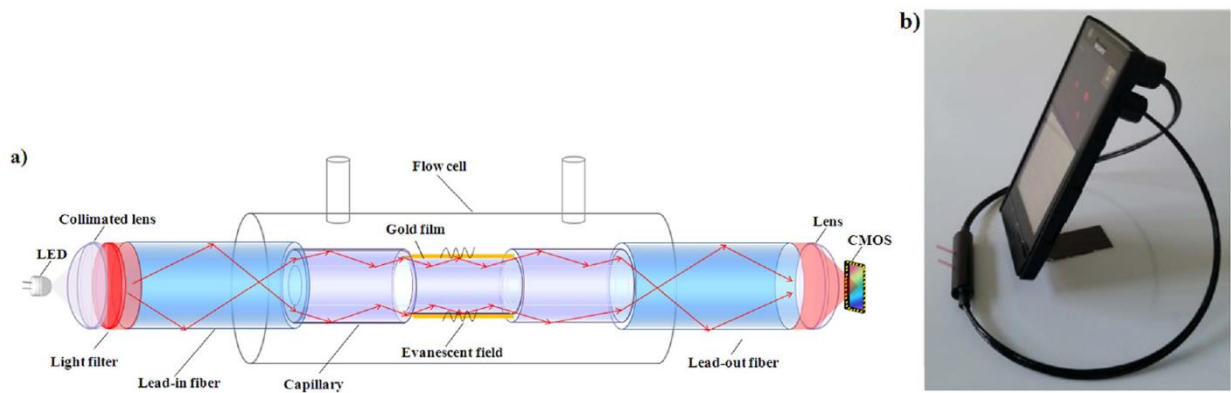


**Figure 2.** Instrumentation of the smartphone based SPR imaging biosensor. (a) Schematic of the smartphone based SPR sensor, (b) Image of final SPR sensor installed on Android smartphone. The above work is licensed under a Creative Commons Attribution 4.0 International License and is free for public redistribution.

A collimating lens was placed after the LED on the smartphone camera to collimate the incoming light into the multimode optical fiber. For intensity modulation, the light source needed to be of one central wavelength. The white light of a flashlight LED is made of multiple wavelengths which needed to be filtered out before travelling through the optical fiber. Therefore, a bandpass filter with central wavelength of 590 nm was placed after the collimating lens. The optical fiber was used as the sensor location for the SPR device by exposing the core of the fiber and coating the exposed core with gold nanoparticles. The gold nanoparticles were functionalized with Protein A, the ligand used in the experiment, and a flow cell encased the entire section where the core of the fiber was exposed. The camera of the smartphone device was used as a detector, which would capture one image every 0.5 seconds to measure the variation in intensity seen during molecular binding. The final device proved to be able to detect concentrations of bovine immunoglobulin G as low as 47.4 nanomolar. While this was not as sensitive a detection level as commercial SPR sensors, which with the same analyte and ligand were able to detect concentrations as low as 15.7 nanomolar, the



device does have the advantages of being much more portable and lower cost compared to a commercial SPR sensor.

#### 4.A.2 Smartphone Based SPR Sensor using an External LED

It was apparent from our research that many smartphone based SPR sensors would use the LED flashlight on the smartphone itself as the light source for the excitation to occur. But after careful consideration, we decided that having the light source be separate from the smartphone device would be much more beneficial to our final design. A separate light source from the device would allow us to manipulate the optical path to fit our needs, as opposed to constraining ourselves to have the light from the smartphone be redirected back onto the camera of the smartphone. One example of using an external LED as their light source was a study done in Turkey in 2016 [Guner, H citation]. In this experiment, a green LED with a central wavelength of 520 nm was used as the light source and was directed towards the SPR sensing location using multimode optical fiber and a beam splitter plate. A schematic of the final device and two images of the finished product can be seen below in Figure 3.

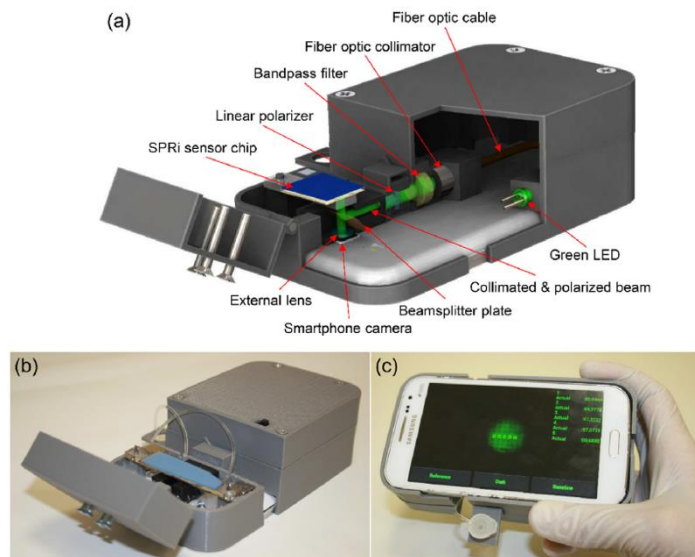


**Figure 3.** SPR Imaging Platform with a Smartphone. (a) Schematic illustration, (b) Image of final product, (c) Image of application for monitoring.

*Reprinted with permission from Copyright Clearance Center's RightsLink service.*

The optical fiber would direct the emitted light from the LED towards a bandpass filter and a linear polarizer to ensure the incident light was correctly polarized and had a central wavelength of 520 nm for intensity modulation. After this, the light was directed onto the sensing location of the SPR sensor. The SPR sensing location used a lab made SPR chip which used a Blue ray disk coated with gold and silver nanoparticles and functionalized with RAM IgG antibodies that were immobilized onto its surface. A

beam splitter was placed in the optical path to direct half of the light onto the Blue ray disk SPR chip and the other half onto the camera of the smartphone device. The light directed onto the SPR chip would experience surface plasmon excitation which would cause a dip in its intensity. The reflective surface of the Blue ray disk would allow the light to then be redirected into the beam splitter and into the camera of the smartphone device where it could record a video of the intensity changes seen by the SPR sensor during the experimentation.

### 4.A.3 Prism-coupled Method for SPR Sensors

The two products mentioned previously both used multimode optical fiber for wave propagation of their incident light. The purpose of this was to ensure their final product was more compact compared to commercial SPR sensors. However, the traditional method of a prism based SPR sensor commonly used for commercial devices is a much simpler setup that provides a high level of sensitivity to the device. To accomplish this, a method called angle-resolved SPR detection is used where molecular binding is measured based on the changes in the resonance angle observed when the refractive index of the sample material changes. Figure 4 below illustrates a device using angle-resolved SPR that can be attached to a smartphone device [Lertvachirapaiboon, C. citation].

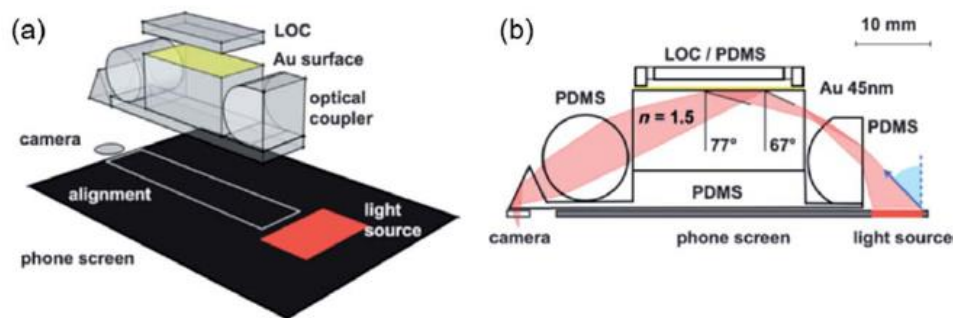


**Figure 4.** Angle-resolved SPR for smartphone application. (a) 3D schematic of disposable device, (b) 2D schematic of experimental light path.

*Reprinted with permission from Copyright Clearance Center's RightsLink service.*

Although this device does not use a prism in its optical path, it uses the idea of angle-resolved SPR detection and the light is manipulated using the refractive index of the various materials used. For this device, a disposable component was assembled to be placed on the front camera of a smartphone for molecular binding detection. The light source used was the screen of the cell phone itself instead of the LED flashlight as has been previously used. The disposable component was made of PDMS and epoxy, which has a particular refractive index that allowed the light to be redirected onto the gold coated surface where the SPR sensing would take place. This device provided us with ideas on how one can use 3D printed components or other materials such as

prisms to direct your incident light in a way where one could observe angle-resolved SPR detection. It also showed us how we could design an optical path that is compact for our final product without the need for optical fiber.

## **4.B Optical Fiber for Wave Propagation**

To avoid the traditional method of a prism based SPR sensor for surface plasmon excitation, many mobile SPR sensors utilized multimode or single mode optical fiber as the optical coupling element for wave propagation [Lui, Y. citation]. This method allows for a more compact and simple optical system for the incident light to be directed onto the SPR sensing region. However, the SPR sensor is installed directly onto the optical fiber by depositing a metal layer onto an exposed portion of the fiber core. An SPR sensor contains a disposable component where the molecular binding takes place. After a certain number of experiments, the optical fiber would require replacement and the metal layer deposited once again. A more consumer-friendly approach would be to avoid requiring any optical realignment for reuse of the product. Our final product will utilize a prism-based system where the phenomenon of total internal reflection enables surface plasmon excitation, thus removing the complication of disrupting the optical path whenever SPR sensor replacement is required. The prism-based system will be discussed more in detail in section 3.D.4 below.

## **4.C Light Sources**

Semiconductor devices are the most important discoveries for modern technology. Semiconductors are an essential component in electronic devices, allowing the positive advancement of society. In SPR sensing surface plasmon resonance detection only occurs at certain spots along the noble metal thin film attached to the prism. As the light propagates through the prism, it will contact the film at the angle of total internal reflection, causing some of the light to be absorbed into the film, minimizing the light intensity. When the wave vector of the incident light, or momentum of photons matches the wavelength of the surface plasmons, the electrons resonate. This is the reason for the technique's name. This section will discuss two variations of a semiconductor technology, a light emitting diode and a laser diode.

### **4.C.1 LED as a Light Source**

Past SPR sensors that utilized LEDs as a light source include a smartphone based SPR sensor developed in Turkey in 2016 [Guner, H. citation]. In this experiment, a green LED with central wavelength at 520 nm was coupled to a multimode fiber which was directed onto a bandpass filter with a central wavelength of 520 nm and full width half maximum wavelength of 10 nm. A polarizer was placed afterwards to only allow transverse magnetically polarized light into the system, where it was then directed onto

an SPR sensor chip created with a Blu-ray disk coated with silver and gold nanoparticles. A multimode fiber was chosen to direct the light to capture as much of the LED light as possible, but even using optical fiber leads to some loss of light from the wide spread of the LED itself. Using an LED as the SPR sensor's light source is beneficial because LEDs are affordable and easy to install into a circuit board. A simple circuit would be enough to make the device operational. A monochromatic LED is important to use to prevent any inconsistency regarding the dip in intensity. This means that a specific wavelength of light must be chosen in place of a modern commercial white LED.

LEDs typically have a turn on voltage of 0.7 volts and are operated using a DC power source. The LED consumes the current from the power source to produce light. The power of LEDs can be plotted with respect to the input current to determine the threshold current of the LED. Due to the cost of a pre collimated LED light source, an unmounted LED would be ideal for the development of a lower cost system.

An LED is not the chosen light source for this device because the photons generated from spontaneous emission do not have a fixed direction. The lack of direction would result in a loss of optical power as the light must be focused on a specific direction to enter the optical system, however an LED can be focused using a collimating lens. A collimating lens induce uniformity on the light before the gold film within the SPR sensor chip absorbs the light to indicate biological interactions within the sample. A lens placed directly in front of the CMOS sensor would be necessary to focus the light into the sensor to analyze and display the transmitted data.

#### **4.C.2 Laser Diode as a Light Source**

The laser in this device is a diode pumped solid state neodymium doped YAG (nd:YAG) laser. When a beam passes through an nd:YAG crystal, the light changes into infrared light that has a wavelength of 1064 nanometers. To achieve an emitted wavelength of 532 nanometers, this laser undergoes a process called second harmonic generation. Second harmonic generation is a nonlinear process of doubling the light's frequency. As a result of doubling the frequency, the wavelength is halved. When the intensity of light is high enough, the electric field vibrations stemming from the optical wave can produce nonlinear interactions in certain crystals. The laser uses a potassium titanyl phosphate (KTP) as it's nonlinear crystal to create second harmonic generation

A laser diode module can be used as the light source for SPR sensing. This device requires a collimated beam to interact with the thin film of metal for uniform data collection so using a laser diode can be seen as a more optimal light source than an LED as an LED requires a bit more optical manipulation to utilize the style of light desired. A few options for diodes will be analyzed in this section.

The first laser diode in question is a 532-nanometer diode pumped solid state laser from the vendor Laserlands. This vendor is based out of Wuhan China and has certifications from the Food and Drug Administration to authorize the production and distribution of laser equipment for international distribution. This laser diode is a class IIb laser and operates between 10 and 50 milliwatts. It is to be noted that the margin of error for the output power range is unknown, so while testing the 10-milliwatt laser diode, it was found that the output power was ranged around 19 or so milliwatts. This may be an item distribution mistake or a technological mistake from the vendor if Laserlands sent the incorrect equipment. This laser has a divergence ranging from 0.1 to 2 milliradians and has a light bending rate of 1.5 millimeters at 5 meters. For long range applications this laser diverges too much as a 2 milliradian divergence at 5 meters results in a beam diameter of around 12 millimeters making the diameter at 10 meters around 25 millimeters. The divergence is also dependent on the diameter of the laser diode module's aperture. Another important characteristic necessary for the device is laser module size. The dimensions of this module are 18mm x 75mm. This module is small enough to fit within the 3D printed casing without occupying a great amount of space, and large enough for adjusting in accordance with what is necessary for the finished product. A heatsink is directly installed into the laser diode to direct heat flow away from the diode. The heatsink moves any heat generated from the laser diode away to prevent damage. If this were not installed directly into the module, it would be placed into the circuit board that is going to power the diode. Another important characteristic about this diode module is that it has a fixed focus. This removes the importance of using a collimating or a focusing lens as the laser beam will be focused uniformly as it travels through the system. The duty cycle of the diode is two hours on and five minutes off. This means that the module can operate continuously for two hours before it begins operating intermittently. The module will begin operating as normal after being powered off for an estimated five minutes. This makes it a decent choice for imaging as the device will require the laser to operate consecutively in ten to twenty minute intervals to collect images of the light's intensity.

Another laser diode that was considered is another 532-nanometer diode pumped solid state laser offered from Thorlabs. The part number is DJ532-10. This diode is labeled as having a 10-milliwatt output power but realistically ranges between 10 and 20 milliwatts. The wavelength ranges from 531 to 533 nanometers. The operating current ranges from 220 to 250 milliamps, and the operating voltage ranges from 1.9 to 2.2 volts. The beam divergence ranges between 12 to 15 milliradians. Compared to the first diode, the divergence of this diode is not as feasible for long distance use. This diode is bare and needs to be connected to a circuit to operate. The reason this diode was considered is the threading on the front of the diode encasing. This would allow for easy alignment as this diode could be threaded into a pre aligned mount that was 3D printed inside the encasing.

The third laser diode that was considered is a 532-nanometer fixed focus diode pumped solid state laser from Edmund Optics. This class IIIb diode has an output power of 10 milliwatts and has a wavelength tolerance of 1 nanometer. The beam diameter is typically 1 millimeter divergence is less than 1 milliradian. The minimal divergence from this laser diode makes it appealing but the dimensions of the diode limit the amount of space for other optics within the housing. The dimensions of this laser diode are 15mm x 90mm which is slightly longer than the first laser diode. The operating voltage for this diode is 5 volts, which is more than the second laser diode. This diode has a modulation frequency that ranges between 0 to 10 kilohertz. Modulating the light is not necessary for this device and would potentially result in important data not being collected.

The fourth laser diode that was considered is a 532-nanometer dot module from a third-party vendor on Ebay. The power output of this device is stated to be 100 milliwatts, defining it as a class IIIb laser. The working voltage of this diode is 3 to 3.7 volts, and the working current is less than 250 milliamps. The working characteristics of this diode are like the second diode discussed but has a slightly higher voltage requirement. This diode would need to be installed into a circuit to operate. The aperture of the diode has threading around the outside making it an easy install into the housing for easy alignment, and the dimensions are 12mm x 35mm making this diode small enough to fit within the housing.

A fifth laser diode will be considered for the device but will only be used in the optical prototype demonstration at the end of the first part of the senior design capstone sequence. This diode is a 5-milliwatt laser with similar specifications to the laser diode discussed above from Edmund Optics. More information about the importance of this diode is listed below in section 13.B.

Table 3 below displays similarities between the four diodes that assisted in deciding which was more desirable for the device.

Diode Vendor	Pricing (USD)	Divergence (milliradian)	Power (milliwatt)	Dimensions (millimeter)
Laserlands	18.00	0.1-2	10-20	15 x 75
Thorlabs	160.15	12	10-20	9.5 x 7.6
Edmund Optics	325.00	<1	10	15 x 90
3 <sup>rd</sup> Party on Ebay	17.00	Not listed	100+	12 x 35

**Table 3.** Comparison of Laser Diodes to Purchase.

The diode that was purchased was the one from Laserlands. This laser diode is the best choice for the device taking the pricing of each diode into consideration. The diode from the 3<sup>rd</sup> party vendor was considered because of the pricing and dimensions

but as the divergence was not listed in the specifications was too big of a risk as this could interfere with data collection.

## **4.D Physical Optics**

The following below will be a detailed description of the physical optics that were chosen to align the laser beam into the CMOS sensor. The beam will pass through a neutral density filter. A neutral density filter will prevent a percentage of light from passing through the system to lower the optical power of the beam to prevent any irreparable damage on either the SPR sensor or the CMOS sensor. A bandpass filter of 532 nm will be placed directly behind of the neutral density filter to ensure that any unwanted noise will be filtered out before the light interacts with the CMOS sensor, ensuring that the recorded data will be uniform in wavelength. A linear polarizer will be following the bandpass filter to ensure that the beam is linearly polarized parallel to the plane of incidence. Following the polarizer, the beam will bounce off two mirrors, one angled at 45 degrees, and the other at 135 degrees. The mirrors will send the beam directly into a right-angle prism at a 90-degree angle to send the light into the SPR sensor chip to record the kinetic reaction of the analyte and ligand. A third mirror will be placed horizontally in such a way the propagating light reflects off at a 45-degree angle after leaving the prism to direct the light into the CMOS sensor. Below we will discuss the importance of our neutral density filter, bandpass filter, linear polarizer, and right-angle prism and why each component was specifically chosen for our final product.

### **4.D.0 Filters**

The next few passages will discuss the filters necessary to optimize the devices efficiency pertaining to the path of light, as well as assist in promoting laser safety. An analysis of the laser diode will be made to determine what optical density value for a neutral density filter will be necessary to install to prevent any damage to the external CMOS sensor. The types of optical wavelength filters will be discussed to determine the most optimal component for the device pertaining to filtering unwanted noise.

#### **4.D.1 Neutral Density Filter**

The neutral density filter chosen is dependent on the output power of the device's laser diode. The laser diode will emit an output power of 10 milliwatts, a significant amount of power that can cause irreparable damage to the SPR and CMOS sensor. The Laser Institute of America recommends for a 532 nm continuous wave laser emitting 10 milliwatts of output power that a neutral density filter of optical density 1.0 should be used to avoid damage. The recommendation is based on the Guidelines for

Implementing a Safe Laser Program (ANSI Z136 Standards). The relation between transmitted percentage and the optical density value can be seen in Equation 2 below.

$$Transmission\ percentage = 10^{-OD} * 100\%$$

**Equation 2.** Relation of transmitted light to optical density.

As can be seen in Figure 4, an optical density of 1.0 ensures only 10% of the light is transmitted at a 546-nanometer wavelength, which in response, reduces the output power of the diode from 10 milliwatts to around 1 milliwatt which is an acceptable range for the CMOS sensor. As the optical density filter purchased has a test wavelength of 546 nanometers, it is safe to assume that by using the graph above, the actual absorption rate for the optical density filter may be slightly higher for a 532-nanometer beam but may also be negligible. This optical density filter does not approach the power threshold of the external camera but is still detectable. This allows ease of operation with respect to safety and efficiency for the type of laser purchased. There are a variety of optical density filters that are applicable to different scenarios. If the laser diode had a higher output power or the camera was more sensitive to the intensity of light and had a lower power threshold another optical density value would be preferred but for this device a neutral density filter with an optical density of 1.0 is a safe choice.

#### 4.D.2 Wavelength Filters

The SPR sensor will utilize the intensity modulation method, which monitors the intensity of the reflected light from the sensing location at a constant wavelength. For a solid-state laser diode to emit a wavelength range of 532 nm, an infrared 808 nm diode is pumped into a neodymium doped (Nd:YAG) crystal to emit a 1064 nm infrared beam. The 1064 nm beam is then pumped into a nonlinear potassium titanyl phosphate (KTP) crystal which will emit the 532 nm light at the output facet. Due to these various pumping wavelengths, our optical system may detect multiple wavelengths other than the desired 532 nm. To filter out these undesired wavelengths, the device has the versatility to use a short pass, long pass, or bandpass filter. Table 2 below illustrates the considered choices for the three types of filters.

Filter Type	Glass Type	Peak Transmission Range
Short pass	BG39	350-600 nanometers
Long pass	JB510	510 nanometers
Bandpass	LB1	525 nanometers

**Table 4:** Considered Choices for Wavelength Filters for the SPR Sensor



A short pass filter allows for shorter wavelengths, starting at 0 until a certain threshold wavelength to transmit through the filter. Once the light passes beyond that threshold wavelength, the amount of transmitted light begins to decline drastically until the amount of transmission percentage becomes nonexistent. The light that is not transmitted is either reflected or absorbed, depending on the type of coating that is on the filter. The transmission spectra of a short pass filter can be seen in Figure 5.

## BG39



**Figure 5:** A short pass filter's transmission spectra with respect to wavelength (Ebay)

A long pass filter is the opposite of a short pass filter. At shorter wavelengths, the transmission percentage of light is nonexistent and grows as the wavelength value increases. At a certain wavelength, the transmission percentage will begin to increase dramatically until the wavelength value transmits all the incoming light. The transmission spectra of a long pass filter can be seen in Figure 6.

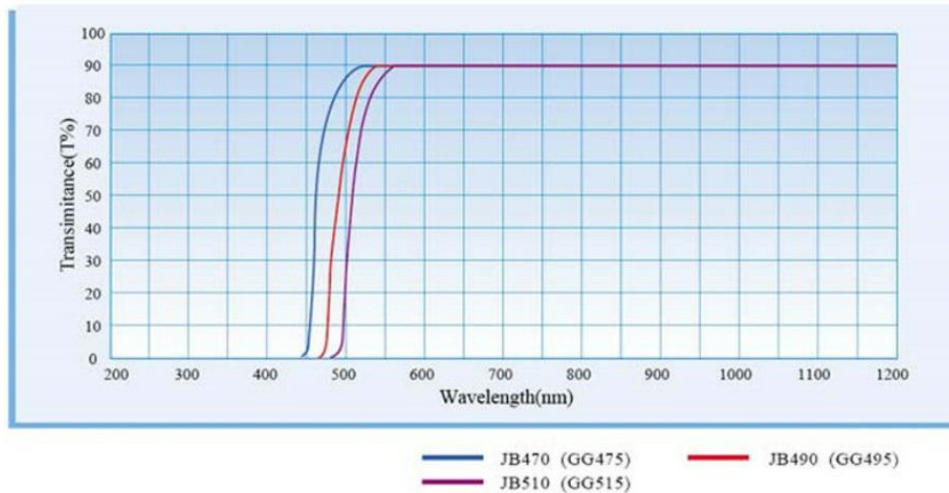


**Figure 6:** A long pass filter's transmission spectra with respect to wavelength. The graph has multiple products displayed to compare the different transmission spectrums differing in wavelength for an ease of understanding. (Ebay)

A bandpass filter is a mixture of short pass and long pass filters. A bandpass filter transmits a specified range of wavelengths. If a light source has a wavelength outside of this range, the amount of transmitted light will be almost nonexistent. The range of wavelengths that transmit light can be as small as less than one angstrom to a few hundred nanometers. The transmission spectra of a bandpass filter can be seen in Figure 7.

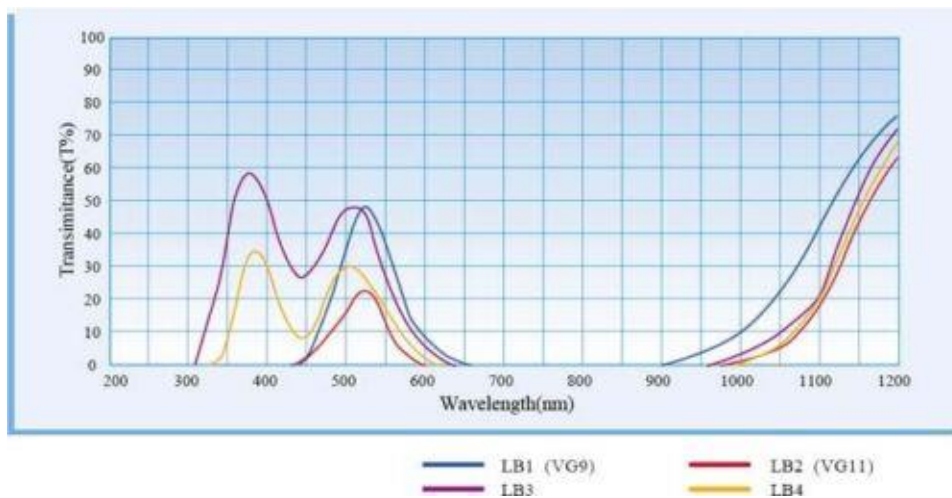


**Figure 7:** Bandpass filter's transmission spectra with respect to wavelength. Multiple similar products are also displayed on the graph for comparison of products for ease of understanding to purchase the appropriate product. (Ebay)

It was determined that a 532 nm bandpass filter be placed in the optical path before interaction with the SPR sensing location to ensure that the beam is monochromatic in the 532 nm wavelength range. The other filters are compatible with the device and will be switched out if necessary. The main reason for a potential swap

is if the amount of transmitted light is too low with taking the neutral density filter into consideration. If the amount of transmitted light ranges from 10 to 12 percent of the laser's initial output power, the bandpass filter will reduce that percentage to 5 or 6 percent according to the bandpass filter graph above. In this scenario it would be ideal to swap the bandpass filter out for the short pass filter to avoid damaging the CMOS sensor. If the short pass filter does not transmit enough light than the long pass filter will be used as the filter of choice.

### **4.D.3 Linear Polarizer**

Surface plasmon excitation occurs when incident light at a certain angle stimulates electrons at the interface between metal and a dielectric material. This surface plasmon polariton, which is a combined excitation of surface plasmons and photons, is an electromagnetic wave that propagates in the parallel direction to the dielectric material. The surface plasmon polariton cannot be excited simply by unpolarized incident light, but instead requires the incident light to be polarized parallel to the dielectric material so the two waves can combine. To manipulate the incident light to become polarized, a linear polarizer can be used to polarize the light parallel to the plane of incidence. This will allow for surface plasmon excitation to occur when the polarized incident light interacts with the surface plasmon polariton wave. Another alternative will be a polarizing beam splitter to ensure that the amount of S polarized light that travels through the system is limited by the polarization being split. The beam splitter is designed to allow S polarized light to exit perpendicular to the system. This would ensure that the light contacting the gold film is linear P polarized light.

### **4.D.4 Right-Angle N-BK7 Glass Prism**

The most widely used design for SPR sensing is through the Kretschmann geometry for total internal reflection. This configuration uses an incident wave, polarized parallel to the plane of incidence, and directs it onto a prism at an angle larger than the calculated critical angle. This creates the phenomenon of total internal reflection, where all the light is reflected off the prism and none is transmitted through the glass material. SPR sensors take advantage of this phenomenon by depositing a noble metal layer onto the side of the prism where the light is reflected off. By doing so, majority of the light is no longer reflected but instead will travel through the metal layer and excite the surface plasmon polariton wave located between the metal and dielectric layers. To ensure total internal reflection occurs, the glass material of the prism must be chosen carefully. The most common material for optical experiments is N-BK7 due to the purity of its raw ingredients used in the manufacturing process. This allows for a smooth transition and low absorption of the light entering the material, which leads to a refractive index of around 1.5. Utilizing Snell's Law, one can determine the critical angle

of N-BK7 glass in air which is calculated to be 41.8 degrees. Total internal reflection only occurs when the incident angle of light is larger than the critical angle when travelling from a medium of high refractive index to a medium of low refractive index. Therefore, if our incident light is angled at 45 degrees, total internal reflection will occur inside our prism. To ensure our reflected light is directed at a 90 degrees angle, a right-angle prism was chosen. This allows for the light to easily be directed onto our CMOS sensor camera for detection of the surface plasmon excitation to occur. Another crucial component to consider in a prism is its surface quality and surface flatness. Surface quality is how many imperfections on the surface of the optical component, such as bubbles, fractures in the glass, and any defects in the coating. A scratch-dig surface quality of 40-20 is recommended for powerful lasers and imaging systems to ensure the light scattering is reduced to a minimum. Surface flatness is a measure of the flatness of your optical surface, usually measured in fractions of a reference wavelength. This is tested by placing the flat, polished surface of the optical component next to a reference surface. A monochromatic light source is directed through the optical component and dark and light bands, known as interference fringes, can be visualized on the reference surface. The amount of curvature seen in the spacing between the fringes is indicative of the surface flatness, with straight lines indicating a high surface flatness. The prism chosen for our SPR sensor contains a surface flatness of  $\lambda/8$ , which is a relatively high standard for general laboratory use. For our purposes, a surface flatness of  $\lambda/8$  is an acceptable range since our SPR sensor does not require a very precise surface flatness to create surface plasmon excitation.

#### **4.E CMOS Sensor and Microcontroller for SPR Detection**

The initial design of our project was to utilize the CMOS camera of a smartphone as the detector for the SPR sensing system. Upon further investigation, we concluded that our project would benefit from removing the smartphone from the optical path altogether. To increase the compatibility of the SPR device, a decision was made to remove the 3D printed smartphone mount that would otherwise position the rear-camera lens for proper lining with the laser. This way the smartphone running the software can be free to move within the transmission range of the microcontroller. This also provides the added benefit of our SPR sensor becoming adaptable to various types of smartphones regardless of its camera's location. However, this provided a new challenge where we had to provide a standalone image sensor to record the data from the laser and upload the images to a webserver for the application to retrieve and process. When choosing a camera module, specifications like capture rate, array size, power consumption, sensor size, and output format were the most important for the accuracy of the processed data. The ESP32 was the first microcontroller that stood out for its low power mode efficiency, low price point, reliability, and wireless features such as Bluetooth low-energy (BLE) and Wi-Fi. Until 2018, ESP32 could not support a parallel camera interface but with the addition of pseudostatic RAM (Random Access

Memory), this became possible and enhanced the microcontrollers functionality for IoT applications and even artificial intelligence.

With the microcontroller unit selected and because of its newly redesigned parallel camera interface support, there are a lot of varying options for a CMOS sensor. OmniVision, a leading CMOS image sensor manufacture, has 30 years of experience in the industry and become very popular for its system on chip CMOS image sensors. During the inception of our project, we wanted to use a smartphone's internal CMOS image sensor but as said before, we scrapped that idea for the sake of compatibility and an easier user experience. The iPhone 5 uses the OV2C3B unit which was the main source of influence to find the manufacture and incorporate their image sensors into our SPR device. Our priority requirement for an imaging sensor would be fast processing and reaction time and one that makes use of the digital video port, a parallel source synchronization camera interface with 8-bit data signals. This interface specifically is very friendly with low-end ARM microprocessors such as the ESP32. In contrast, a similar functionality would only exist on high-end MIPI processors. The OV2640 camera module was first on the list and for many reasons. What influenced our decision the most was the JPEG encoder onboard the camera module, it off-loads the processing power in order to reduce the memory footprint on the microcontroller. For a comparison, the max resolution for this camera module is 1600 x 1200 pixels. A typical raw format in RGB656 would be just over 3.5 MB of memory space but with JPEG compression, it would only occupy 150 KB: almost x25 compression ratio.

#### **4.F SPR Sensor Surface**

Surface plasmon resonance can be successfully monitored on multiple different types of substrates under the condition of a dielectric film coated on a surface of the substrate. It is a requirement to have the dielectric material be in contact with a noble metal, such as gold or silver, to create surface plasmon excitation. The noble metal will capture the light being reflected off its surface at a certain angle, termed the resonance angle, and excite the mobile electrons that oscillate on the surface of said metal. The wave created by the mobile electrons will combine with the wave of the incident light and create a dip in intensity observed by the SPR detector.

After careful consideration, the noble metal chosen for our SPR sensor was gold. This is due to the oxidation of silver can lead to complications when reusing the SPR sensor surface for multiple experiments. It was also decided to purchase an SPR sensor chip for our experiment instead of creating our own, due to the time consuming and delicate process of depositing the noble metal evenly onto the sensing location and immobilizing the ligand to be used in our experiment. If the noble metal is not evenly distributed, it can lead to incorrect data and an inconsistent location of our resonance angle.

## 4.G SPR Sample Preparation

To obtain measurements that will be used in our experiments to determine the levels of accuracy our SPR sensor can detect, samples of bovine immunoglobulin G need to be prepared. While preparing the samples, extreme care in the measurements must be taken to ensure accuracy for our final results. Our measurements will be measured in the microgram scale, which requires a lab precision grade scale to be able to measure to one microgram. Our plan is to seek permission from professors at the University of Central Florida to use their lab equipment when preparing our samples to ensure our measurements are as accurate as possible. If permission is not obtained, our second choice is to measure our samples in the milligram scale. This is much more feasible to do, as there are many low-cost scales available online that can measure to the milligram scale. Once we have a scale available to us, the following procedures will be followed for measurement of our samples:

1. Obtain samples of bovine immunoglobulin G from the company Jackson ImmunoResearch.
2. Obtain phosphate-buffered saline solution of pH 7.4 from the company Millipore Sigma.
3. Place a small sterile beaker onto the scale and use the TARE function on the scale to subtract the weight of the beaker from the measurement.
4. Pour a small amount of the bovine immunoglobulin G from the sealed vial onto a separate sterile beaker. This ensure the vial containing the analyte is not contaminated.
5. Using a sterilized 1 mL syringe, carefully transfer the bovine immunoglobulin G from the beaker and add to the beaker placed on top of the scale.
6. Once the proper amount of bovine immunoglobulin G is measured on the scale, move the beaker containing the sample aside.
7. In a separate sterilized beaker, pour a small amount of the phosphate-buffered saline solution.
8. Using a new sterilized 1 mL syringe, place the syringe in the sterilized beaker and measure out 1 mL of the phosphate-buffered saline solution.
9. Transfer the 1 mL of phosphate-buffered solution into the sterilized beaker containing the measured bovine immunoglobulin G.
10. The beaker containing both the bovine immunoglobulin G and phosphate-buffered saline solution will be used to place the measured sample into the SPR sensing chamber using a separate sterilized syringe to transfer the solution from the beaker into the chamber.

After preparation, each sample will be properly sealed and labeled with a temporary secondary label that details the solution being used and its concentration, the person who prepared the sample, the date the sample was made, and any safety hazards that are mentioned on the manufacturer's label for both the bovine

immunoglobulin G and phosphate-buffered saline solution. The prepared samples will then be placed in a refrigerator for storage until needed for our experimentations.

#### 4.H SPR Sensor Accuracy

An SPR sensor utilizes the phenomenon of surface plasmon excitation created when incident light is directed onto a noble metal to determine when molecular binding occurs in an analyte and ligand. Every SPR sensor has a certain level of accuracy it can obtain when analyzing this molecular binding interaction. SPR sensors measure their accuracy based on how low a concentration of a certain analyte can be and still be detected by the SPR sensing surface. This accuracy or sensitivity is determined by the quality of optical and electrical components used in the SPR device as well as the quality of the manufactured SPR chip being used as the disposable portion of the sensor. For our device, a set goal for the accuracy level of our SPR must be determined to guide us in deciding how efficient our product will be. To decide this accuracy level, several previously designed SPR sensors were researched to gain an educated idea on what is feasible to accomplish with our design. One such design was a smartphone based SPR sensor created in China in 2015 [Liu, Y. citation]. The smartphone based SPR sensor used multimode optical fiber for wave propagation of its incident light onto the SPR sensing location. The cladding of the fiber was cleaved to expose the core and gold nanoparticles were brushed onto its surface. Protein A was then functionalized onto the gold surface to create the SPR sensing location. A flow cell was then placed around the exposed core to create a chamber for the testing solution to remain during experimentation. The analyte and ligand used in their experiment was bovine immunoglobulin G and Protein A respectively, making this a favorable design for research purposes as we will use the same analyte and ligand in our experiments. For their analysis, they also tested their various concentration levels with a commercial SPR sensor to compare with the results found using their smartphone based SPR sensor. Doing so gives a clear comparison of the limits of detection for a cheaper, smartphone based SPR sensor when compared with a commercially designed one. Figure 8 below illustrates the results for both the commercial and smartphone based SPR sensors.

	Commercial SPR instrument(Biosuplar 6)	Smart phone SPR biosensor
Resolution	$2.7 \times 10^{-5}$ RIU	$7.4 \times 10^{-5}$ RIU
Limit of detection	15.7 nM	47.4 nM
Cost	220,000¥	240¥
Size (without computer/smart phone)	20 cm × 9 cm × 8 cm	12 cm × 6 cm × 2 cm
Weight (without computer/smart phone)	2.5 kg	40 g
Computer/smart phone and operating system requirements	PC, Windows 98/2000 or Windows XP	Smart phone, Android

**Figure 8.** Comparison of Smartphone Based SPR Sensor vs. Commercial SPR Sensor [Liu, Y. citation]

From the figure above, the limit of detection for the commercial SPR sensor was measured at 15.7 nanomolar concentration of the bovine immunoglobulin G combined in 1 mL of phosphate-buffered saline solution. On the other hand, the smartphone based SPR sensor was only able to detect concentrations of the bovine immunoglobulin G at 47.4 nanomolar. It was clear from the experiment that the commercial SPR sensor outperformed that of the smartphone based SPR sensor created by the researchers, indicating that a smartphone based SPR sensor utilizing multimode fiber has a lower sensitivity to binding processes compared to a commercial SPR sensor. This information will aid us in understanding the limitations our design may encounter when detecting molecular binding. Although we will use a prism-based system for our SPR sensor as opposed to multimode fiber, our components are not at a high precision level that are commonly used in commercial SPR sensors, making the detection limit of 47.4 nanomolar seen in the smartphone SPR sensor a realistic baseline for us to achieve with our SPR sensor.

For our experiment, we will design an SPR sensor with a level of accuracy that can detect concentrations of bovine immunoglobulin G combined in 1 mL of phosphate-buffered saline solution as low as 47.4 nanomolar. If the aforementioned goal is accomplished, and there is sufficient time, we will then attempt to enhance our limits of detection to that of the commercial SPR sensor, which is 15.7 nanomolar. This may be accomplished by purchasing higher quality components such as higher resolution CMOS sensors and SPR chips with a larger sensing surface. We may also upgrade our SPR sensing chamber to contain a flow cell attached to a pump which would allow the analyte solution to flow through the sensing location at a constant flow rate, which would provide our analyte with more opportunities to attach to the ligand immobilized on our SPR chip.

## **4.1 Power Delivery**

During the inception of our SPR device, we planned to use the internal camera of an Android smartphone to capture the information and process it. Now we have redesigned the device to use an exclusive camera mounted inside our SPR device. To control this camera module, we would use a low-power microcontroller unit. The ESP32-CAM was a perfect choice for its wi-fi and Bluetooth low-energy functionality as well as its compact size. The ESP32-CAM has two different powering methods, a 3.3v and a 5v input. The 5v method was selected to ensure reliability and a stable clock rate. The maximum current draw of the ESP32-CAM is 1200 mA but with our limited use and proper programming we expect our maximum current draw to be 500 mA. When prototyping the ESP32, it was observed that the device can draw 500 mA for startup before settling to a lower and more consistent current. The second power and final consuming device in our SPR system is the laser diode which has an accepted voltage range from 3v to 5v with an output power up to 50 mW.



Before changes were made to our SPR design, we had the smartphone mounted to the side of the device to use its camera as the primary CMOS image sensor. The touch screen display would still be usable, but this caused compatibility issues and could disturb the experiment if the device was moved too much. Our current design is to use an internal camera module inside the device with a microcontroller wirelessly feeding the captured data to a compatible computer or smartphone. Since our focus is no longer on the smartphone mount, we had to forgo the use of a smartphone battery to power the SPR device. Our current design is utilizing two 9v Alkaline by Energizer, one for each power consuming device. A linear regulator was used to drop the voltage from around 9v to a steady 5v with the use of two electrolytic capacitors. Although this was successful at properly supplying our microcontroller with enough power, the L7805 linear regulator is very inefficient, and we observed in our prototype that almost two thirds of the total energy released by our single 9v battery was released into the form of heat. After researching alternative methods, our next decision was to invest in an integrated switch or buck converter. If properly designed, we can increase our efficiency up to 95 percent without a negative effect on the microcontroller performance. Even in the worst case of drawing 500mA for an hour, we expect a single 9v Alkaline battery to satisfy the requirements of the microcontroller.

Further research will be done on the chemical makeup of batteries to narrow down the most appropriate choice for our microcontroller and laser diode. In order to avoid disturbances of the internal electronics and unnecessary waste, our next focus would be on rechargeable batteries. This will influence our decision on the battery's chemical makeup and the number of cells we use in the device. We will use a USB connection port for charging input, and it is unknown at the time if we are to use separate cells for the laser diode and microcontroller unit.

#### **4.J 3D-Printed Housing and Mounts**

The Surface Plasmon Resonance device will be housed in a hollow box made from biodegradable polylactic acid thermoplastic. All the devices such as the microcontroller unit, the camera module, the laser diode, the printed circuit board, the battery, integrated circuits and other common electronic components will have specialized mounts inside the plastic housing to ensure a locked position and minimal vibrational disturbances.

Polylactic acid is a popular thermoplastic used with fused deposition modeling (FDM) printers. It's cheap, abundant, and derived from fermented plant starch usually from corn. This thermoplastic has been chosen for its high tensile strength of 7,200 psi, biodegradable nature, and appropriate thermal resistance. The glass transition phase starts at 60 degrees Celsius; this phase is described by the thermoplastic's ability to deform and lose structural tension. The thermoplastic that will be used for our housing is a compound of polylactic acid to account for a better ability to dampen vibrations;

because the compound varies between manufacturer, we can only use the pure form of polylactic acid as a baseline for measurements.

#### **4.K Software Solutions**

The ESP32-CAM will be controlled by a get request through HTTP, we need an application to perform these requests in a timely manner. Our engineer requirement has the capture frequency at 0.5 seconds between captures. This is achievable with the chosen hardware with plenty of room for energy optimizations. The next responsibility for our software solution is to then process the captured data and create visual representations for the user to read and analyze. Processing the captured data at the same time as capturing the data does not need to be processed at the same time but it will greatly shorten the time between the start of the experiment and the moment the data can be readable from a visualization. Most modern hardware such as smartphones and laptops should be more than enough to do both tasks simultaneously, but no testing has been done on cheaper smartphones or weaker computers yet.

As stated previously, the main task for the software solution is to process the data gathered by the image sensor. When the processing happens has not been fully decided upon but the decision has little impact on the concept behind the processing. The expected behavior of the surface plasmon resonance phenomenon can be measured through the form of intensity modulation. To the CMOS sensor, the intensity can be described as 'brightness' when looking at the captured data. The data capture can be simplified by capturing only monochromatic images and interpreting perfect black as a value of 0 and perfect white as a value of 255 in reference to brightness. The caveat of our software solution is as follows, what decides the brightness of an image. There are three possible approaches that seem to give the best results for our situation: average brightness of the pixels, a histogram of brightness distribution amongst the pixels, or the root mean square value for all pixels. Each method can produce a different value, but one method may be better than the rest for our use case. Our first elimination was the average brightness of the total pixels, we expect interference noise and artifacts to be present on each captured image and that will distort the accuracy of our data. Root mean square can process undesirable information in the image, but the value would be more generalized and should prove to be more accurate for our needs. The histogram approach seems more desirable since we'll be able to ignore the values of some pixels that could be interpreted as noise or artifacts, but all three methods could still be sufficient during testing.

Once the image data has been captured and the software has finished processing all needed data, the user should be able to read the visualizations on screen and discern if excitation has occurred. Our sub-goal is to allow the user to know if excitation is occurring or not during the experiment, but this is not a requirement. The user should be

able to explore past experiments and export the data as needed. The software will have complete control over the microcontroller and therefore the entire device.

#### 4.L Different SPR Monitoring Methods

There are three classified forms of monitoring surface plasmon excitation: angular scanning, wavelength modulation, and intensity modulation. There is no perfect one, as each different form is based on the particular light being measured or the molecular binding that will be observed. In the following sections, we will discuss the three different modulations that are common in a commercial surface plasmon resonance sensor and the pros and cons of each.

##### 4.L.1 Angular Scanning

The most common modulation method used in commercial surface plasmon resonance sensors is angular scanning. In this method, a monochromatic light source is directed at different incident angles to the noble metal on the prism. As excitation of the surface plasmons is created, the detector will observe a dip in the intensity of the reflected light where the resonance angle is located. Figure 9 below illustrates the reflection spectra for an angular scanning method where two incident angles were measured and their respective dips in intensities were observed.

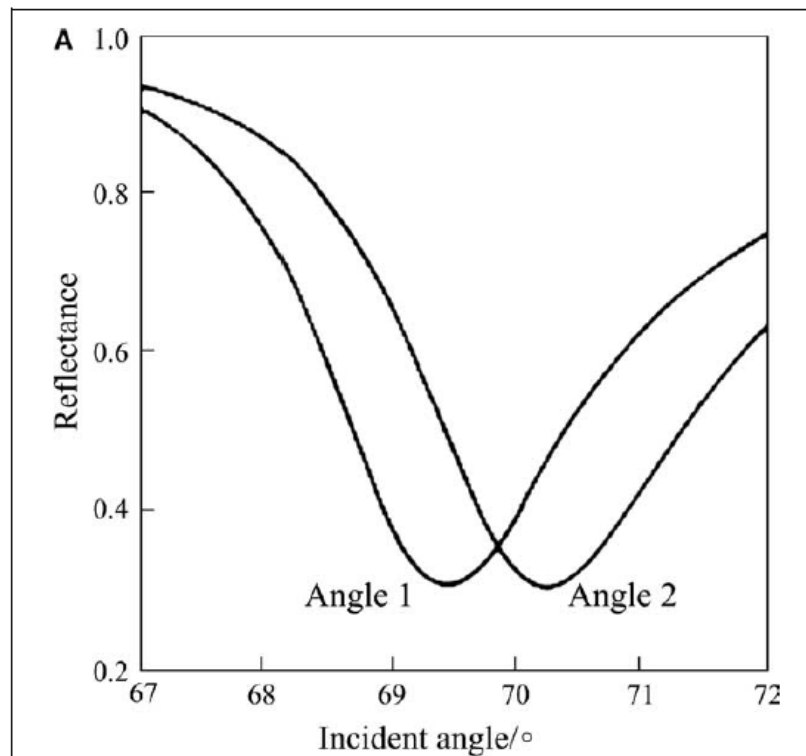


**Figure 9.** Reflectance Spectra for Angular Scanning.

This method is most widely used due to its high resolution and wide range of refractive index measurements as it scans a range of various incident angles to show the changes created by molecular binding. However, this setup can be costly due to the mechanical components required to allow the incident angle of your light source to change throughout the experiment. It also creates a more complicated optical setup as well, as you must consider the change of the incident angle also having an effect on the reflected light path. Many surface plasmon resonance sensors that utilize angular scanning use the Kretschmann configuration, which involves a light source directed at a prism to use total internal reflection as a method to excite the surface plasmons on the noble metal surface. This monitoring method therefore can be very useful but does greatly increase the cost and difficulty of the final surface plasmon resonance sensor.

#### 4.L.2 Wavelength Modulation

Another method to monitor surface plasmon excitation is with wavelength modulation. In wavelength modulation, the incident angle of the light source is fixed during the experimentation. However, unlike angular scanning, the light source is not monochromatic but has a spectrum of wavelengths. This is commonly done using a white light source and measuring the red, green, and blue wavelengths of the reflected light. When surface plasmon excitation is created, the intensity of the reflected light is at a minimum at the resonance wavelength [Liu, Xia citation]. Figure 10 below illustrates the reflectance spectra for wavelength modulation.

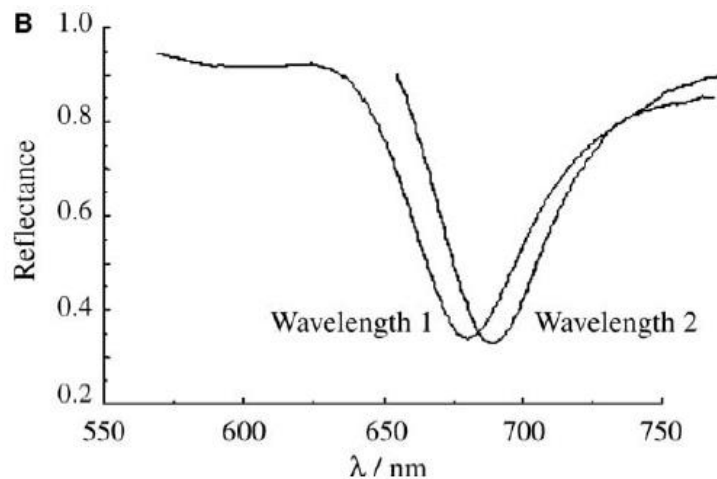


**Figure 10.** Reflectance Spectra for Wavelength Modulation.

The interaction of the molecules being observed can be monitored by measuring the shift of the resonance wavelength over time. This method is easy to miniaturize and is commonly used for low-cost surface plasmon resonance sensors that use a smartphone's white LED as the incident light source and optical fiber for wave propagation.

### 4.L.3 Intensity Modulation

The third method used for monitoring surface plasmon excitation is called intensity modulation. In intensity modulation, a monochromatic light source is fixed at a specific incident angle and the detector measures the intensity changes of the reflected light. Intensity modulation allows for a simple and low-cost setup for surface plasmon resonance sensors, but at the cost of the overall sensitivity of the device. Figure 11 below illustrates the reflective intensity curve created using different extinction refractive indexes with a 632.8 nm wavelength laser fixed at an incident angle of 74 degrees. As can be seen, the dip in intensity observed is much shallower compared to the one observed with wavelength modulation and angular scanning illustrated in prior sections.

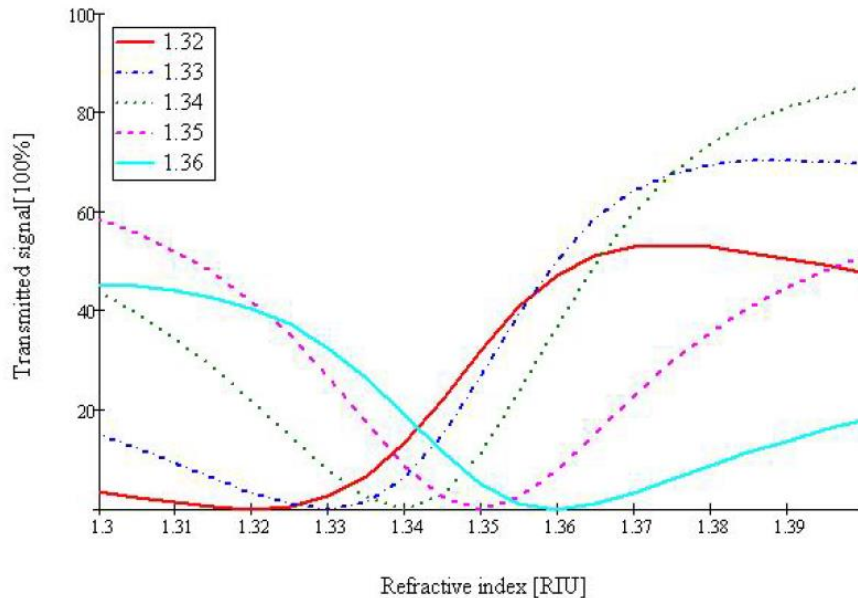


**Figure 11.** Reflection Intensity Curve for Intensity Modulation.

However, research has been done to combine intensity modulation with changes in the polarization state of the incident light to allow for more complex and higher sensitivity of molecular binding to be monitored [Sun, B. citation].

## 5. Constraints and Standards

A key aspect in project development is production under certain conditions. The constraints listed below will discuss the areas of development that are limited to specific criteria. These constraints can have a negative impact on the design process depending

on government issued regulations such as International Traffic in Arms Regulation (ITAR). The standards of optical components and computation of images, such as data processing will be noted in this section. Basic laser safety will be introduced as well.

## **5.A Constraints**

For every product design, there are a level of constraints that must be considered which can limit the final project. Common constraints such as financial and software are the first that come to mind, but a professional engineer should consider the more abstract constraints such as ethical and environmental to ensure their product is safe and sustainable for long term use. In this section, we will discuss the various constraints specific to our product and our plans to ensure our final design is in compliance with each one.

### **5.A.1 Financial**

Financial constraints stem from the limitations of college students. This project is not funded or sponsored by a third party, leaving the financial decisions and spending up to the developers. This allows for freedom of choice when applied to catalog browsing for the desired equipment but can be very costly. To keep the pricing to a minimum, some of the basic components will be purchased online through a third-party website for vendors, Ebay. The basic components purchased from Ebay will not be the highest quality but will function as intended and allow more lucrative spending on the more important components.

The financial goal for this sensor is a \$600 investment ceiling. Commercial SPR sensors have a cost estimate of \$40,000. Because of the financial disparity, this device will not provide as high of a sensitivity for surface plasmon detection as can be achieved using a commercial SPR sensor. This device can be seen as a more affordable option if mass manufacturing for consumerism is pursued. The total cost is anticipated to be within a 10% window of the \$600 investment goal. This is a result of the SPR sensor chip package being priced at half of the investment goal. Luckily the manufacturer the sensor chip is being purchased from has the most cost-effective sensor chip. This allows for the device to be less expensive, as other sensor chips on the market are priced around \$700.

### **5.A.2 Environmental**

The components will be housed inside of a 3D printed casing made from thermoplastic polyurethane. TPU longer lasting plastic that is more eco-friendly than other commercial plastics. Using this type of plastic for the device housing does not result in any sort of constraints, as it benefits the longevity of the project, and the

environment as polyurethane can be broken down using microorganisms without emitting toxicity.

### **5.A.3 Social**

Social constraints are limitations set upon a device's development that stem from the influence of social behaviors. Upon further inspection, a mobile surface plasmon resonance sensor has miniscule societal constraints that will prevent or limit development of such a device. The constraints that do exist pertain to government regulations on light sources.

### **5.A.4 Political**

Political constraints are limitations set upon development that stem from local to federal political climates that influence policies. Upon further inspection, there are no political constraints that are applicable to the surface plasmon resonance sensor being developed. However, political constraints can be applied towards regulation and importation of optical components from trade restricted regions.

### **5.A.5 Ethical**

Ethical constraints are limitations set upon development that involve and potentially intrude on user privacy, and safety. Ethical constraints do not apply to the sensor's anatomy but can potentially apply to app development. This can be resolved by asking the user to consent to any sort of involvement of privacy, such as accessing the mobile device's photo reel to read pre-recorded data if needed.

### **5.A.6 Health and Safety**

The light source used in the device is classified as a 3b laser source and has a power output of 10 milliwatts. The beam generated is bright and can potentially damage the eye's rods, cones, or retinas if proper eye safety is not taken into consideration during construction and operation. The specifics of the safety concern will be discussed in greater detail further down in the document.

SPR sensors detect molecular binding that occurs in specimens such as antibodies, proteins, bacteria, and other biological substances. Therefore, it is important that proper health and safety precautions are taken when using certain substances that can be harmful to humans or other living organisms. The substances we will observe with our SPR sensor are Staphylococcal Protein A and bovine immunoglobulin G. These substances are not harmful to humans as they can be found naturally in our bodies, making them ideal for testing our SPR sensor in a safe environment. However,

our SPR sensor can be used to detect other substances such as pesticides or bacteria's which could pose a health risk to those in close contact with them for an extended period of time.

### **5.A.7 Manufacturability**

Constraints on manufacturing limit the device's design that can hinder the device's mass production capabilities. One constraint can be found with the external camera's ability to transfer the captured images to the software application in a timely manner. Our external camera will capture an image every 0.5 seconds which could result in 1,200 captured images at 1080-pixel resolution if the device operates for 10 minutes, which is an average range of time for many SPR sensors to gather an accurate representation of molecular interactions. The camera, microcontroller unit, and Wi-Fi components would therefore need to be powerful enough to store and transfer this information in a timely manner. This constraint would cause the cost to increase and could affect the manufacturability of the final product.

### **5.A.8 Software Compatibility**

In the technology age, it is important to consider the constraint software can have on the versatility of your product. A successful product should attempt to be compatible with multiple operating systems to reach a larger audience. Our software application to control the SPR sensor will attempt to be compatible with Windows, Linux, Android, iOS, and MacOS. This will be done by using a cross platform Python framework that would be compatible with the inputs of different devices such as multi-touch, Windows Pen, and the macOS touchpad.

### **5.A.9 Sustainability**

When designing a product, it is essential to consider the longevity of the system after its initial completion. Sustainability requires one to consider the lifespan of the device and how reliable its results will be after prolonged use. A professional engineer should always consider sustainability when choosing components and any design decisions throughout the building process.

One sustainability constraint for our product will be measuring the concentration of the analyte solution to test with the SPR sensor. Our experiment will consist of measuring IgG concentrations in the microgram scale that are combined in PBS solution. Measuring to the microgram scale requires precision grade scales that may not be available to every customer wishing to use our product. Scales that measure to the milligram scale are much more affordable to most, with many in the price range of \$16-20. Therefore, along with our experiments measuring in the microgram scale, we can



also perform experiments with concentrations measured in the milligram scale to show the sensitivity of our product at this range as well.

Another constraint for our product is ensuring the chamber for SPR sensing is sealed properly to avoid any leakage. The solutions we will measure in the SPR sensing chamber will be in a liquid form when interacting with the SPR chip, which makes it a hazard to our sensitive electrical and optical components inside the 3D printed case. To avoid leakage, we will seal the base of our right-angle prism with 100% silicone sealant commonly used for bathrooms. A silicone sealant is safe to use on glass and plastic materials, making it a safe choice to interact with our glass prism and the plastic of our 3D printed case. However, the longevity of the sealant itself is something to consider for our final product. After a certain amount of time, the sealant may need to be reapplied to avoid any liquid from entering the rest of the device.

#### **5.A.10 Covid and the Global Semiconductor Shortage**

The global shortage of semiconductors was very influential on our decisions with electronic components. With our time constraints, there was only so much that can be done when one of the key components that was planned from the beginning has a production lead time over three months. In some extreme cases, these lead times can range from a few weeks to a couple years. Alterations to the overall design had to be made when there are no alternative components to be purchased without risking other portions of the project. Forethought had to be taken seriously when purchasing a component that could be damaged or dead-on-arrival. A prime example would be our camera module, the OV2640. This is a camera module manufactured by OmniVision that was released in 2005 but discontinued in 2009. This sensor was targeted to the mobile phone industry, so the production volume has been so large that they are still popular in IoT camera applications to this day. Texas Instruments is a very trusted manufacture of semiconductor devices and creates a lot of ease with their intuitive catalog organizing and WEBENCH Power Designer for development purposes. They are no exception when it comes to this global shortage. When searching for a proper switching regulator for direct current, it was easier to find something out of stock without a solid estimated time for resupply than it was to find something with a lead time that worked with our time constraints. Thankfully they have such a large supply of their integrated circuits that we were able to find components that we could work with.

#### **5.A.11 Time Constraints**

Time constraints is one of the main challenges for our design. With only two semesters to research, build, test, and finalize our device, many of our advanced and stretch features we would hope to accomplish will have to be discarded. We also must consider that one of our two semesters is during Summer, which is only twelve weeks

as opposed to fifteen weeks during Spring and Fall semesters. During this time, each of us has obligations that take away time we could otherwise dedicate to our design, which can pose a serious threat to our final project. If we were given more time to dedicate to our final project, there are various advanced and stretch features which were previously mentioned we would like to accomplish that would perfect the accuracy, response time, and longevity of our SPR sensor. The detailed explanation for our advanced and stretch features can be found in the section titled 2.A Features above.

### 5.A.12 Storing and Handling of Biological Samples

To test the accuracy of an SPR sensor, an analyte and a ligand must be present to observe the molecular interaction between the two substances. Both the analyte and the ligand to be used in our experiment are biological substances that will require some form of refrigeration during storage. The SPR chip we will be using during our experiment has been prepared with our chosen ligand Protein A immobilized on its surface. Protein A is sensitive to temperature changes and therefore must be stored at 4 degrees Celsius when not in use, as can be seen on the manufacturer label for the SPR chip shown in Figure 10 below.



**Figure 12.** Surface Plasmon Resonance Sensor Chip Manufacturer Label.

Our analyte, bovine immunoglobulin G, will also require refrigeration when not in use. This adds a constraint on our project as it requires us to have a refrigerator that can accommodate the specified temperature required for both the analyte and ligand substances. It also limits the movement of our biological samples as they cannot be in a low-temperature environment for too long. We will also be required to create various concentration levels of the bovine immunoglobulin G with phosphate-buffered saline for our experiments. These preprepared samples will have to be stored in a refrigerator in temporary containers. This will require us to have proper seals on the containers to

avoid any accidental spillage as well as proper labeling of our solutions and concentrations to avoid any accidental contamination.

Another constraint is in handling the analyte and ligand to be used in our experiments. The SPR chip is extremely sensitive, especially on the side that contains the immobilized Protein A. As can be seen in Figure 12 above, the manufacturing label warns of avoiding contamination to the functionalized side which contains the immobilized Protein A. To avoid any contamination, the surface of the chip must avoid contact with any surfaces not being used for testing. The surface of the chip is 9 mm by 9 mm, which makes the task of avoiding contamination much more difficult due to its very small size. Figure 13 is an image of the bare gold SPR chips we will be using when calibrating our SPR sensor. These are not functionalized with the Protein A we will use during our experiments and therefore are safe to use when testing the location of our optical components before including the analyte.



**Figure 13.** Image of Gold Coated SPR Chip.

As can be seen in the figure above, the SPR chips are very small. This will require us to wear gloves to avoid damaging the chip with oils from our skin, as well as using precision instruments such as tweezers that have been sterilized with alcohol and air dried before use. Extreme caution must be taken when transferring the SPR chip from its package onto the base of the right-angle prism to avoid damaging or contaminating the surface of the chip. We will also be required to fix the SPR chip onto the base of the prism with superglue, which will also be a constraint to consider as this can become difficult to perform without damaging the surface of the chip. The glue must

be placed in a way that ensures the chip remains fixed on the prism during experiments while also not interfering with the surface. When performing the experiment, measures must be taken to ensure nothing bumps or disturbs the surface of the SPR chip when attached to the prism. A chamber will be created to protect the SPR sensing location, as well as provide a dark environment to ensure the only light interacting with the molecular binding is the light emitted from the laser diode. But when cleaning or transferring different solutions into the chamber, the risk of contamination is once again present. This constraint is one of the most important to consider during our entire design process, as contamination of our SPR chip can not only be a costly error but also a damaging one to our final results. Similar care must be taken when handling the analyte substance, the bovine immunoglobulin G. For our experiments, various concentrations of bovine immunoglobulin G will be combined with phosphate-buffered saline solution to test the sensitivity of our SPR sensor. When we begin our experiments, care must be taken when transferring the combined solutions onto the SPR sensing chamber for analysis. Proper equipment such as sterilized syringes or pipets should be used to avoid any contamination of our substances. Clean and sterilized glassware, such as beakers, should be used when storing the combined materials and properly handled to avoid contamination from the environment. As well, proper procedures for handling chemicals in a laboratory setting must be followed to ensure the safety of those involved in the experiment. Although our substances are not toxic or otherwise irritable to the skin, they are biological samples that should be treated with care, nonetheless.

## **5.B Standards**

Standards are a necessary requirement for every industry, providing safe and reliable methods for designing and manufacturing industry components. A set of standards ensures common appliances such as light fixtures or computer hardware can work together even across different industries. Without them, many components we rely on would not work cohesively and could pose a health and safety risk in some instances.

Each industry has its own set of standards that manufacturers follow to allow for easy communication between the consumer and creator. Some standards may involve safety guidelines and procedures that are universal in certain industries. These guidelines must be understood and followed to ensure we minimize and safety hazards that could be present in our work environment. It is good practice as engineering students to learn about the various set of standards in our respective fields and how to design products following these guidelines. Below we will discuss various standards that are relevant to our project and how we plan to follow these standards throughout our design process.

### **5.B.1 Laser Safety**

Lasers can be classified into multiple distinct categories for safety purposes based on their emission characteristics. Most lasers are required by the law to classify lasers using the IEC 60825-1 and 60601-2-22 standard. The five categories are listed below.

- Class I: The output power is less than 0.39 milliwatts. This laser is not capable of producing dangerous levels of light.
- Class II: Has a visible beam that has a power of less than 1 milliwatt. Only applicable to visible light lasers.
- Class IIIa: The output power ranges from 1 to 4.99 milliwatts. Generally safe but recommended to view with proper eye equipment.
- Class IIIb: The output power ranges from 5 milliwatts to 499.99 milliwatts. The beam is hazardous if directly viewed without proper viewing equipment.
- Class IV: Output power of 500 milliwatts or greater. Beam can cause irreparable damage even if indirectly viewed.

The laser in this device is classified as a IIIb laser. The output power of the device's laser diode is 10 milliwatts. While operating the laser, proper eyewear must be worn to prevent eye injury. Eye protection will not be necessary once the laser diode is mounted within the casing.

The eye protection necessary for operating this type of classification will assist in filtering out 532 nanometer wavelength light to prevent any devastating damage to the eyes. The placement of the neutral density filter will also assist in protecting the eyes while the diode is not encased.

### **5.B.2 Surface Quality of Optical Components**

The surface quality of optics is important because it is an evaluation of faults on the surface of the optics. One of the standard classifications for surface quality is known as the scratch-dig metric. The United States Military Performance Specification MIL-PRF-13830B documentation, as seen in Figure 11, describes and classifies the surface quality of optics using the scratch-dig metric. The document states that all optical elements, components and systems must comply with the scratch-dig metric for military use.

A scratch, as defined by section 3.5.2.1 of the document is a mark on the surface of the optics. The surface marks can be ranked on their brightness using these arbitrary numbers: 10, 20, 40, 60 or 80. The assigned value increases as the brightness of the scratches increases. The values for classification are arbitrary because the number is not an exact measurement but are a subjective comparison between component and calibration. The maximum permissible scratch size is one fourth of the optical

component's diameter. If a maximum permissible scratch size is on the surface, the sum of the scratch numbers multiplied by the ratio of their length with respect to the diameter must be below one half of the maximum scratch number. When there is no maximum sized scratch, the sum multiplied by the ratio must stay below the maximum permitted scratch number. Scratches on optical coatings that do not interfere with the surface of the glass must also abide by these guidelines.

A dig, unlike a scratch, is a measurable value. A dig, as classified in section 3.5.3.1 of the document, is the diameter of defects allowed, specified in units of 1/100mm. The maximum dig size permissible is one per each 20mm of diameter, or a fraction of that optical surface. Any digs with a diameter size of less than 2.5 microns are negligible. The If the optical material has a bubble within the surface it is classified as a dig. The maximum size of surface bubbles allowed is one per 20mm of light travel, under the impression that this is placing arbitrary normal reference point on the optical axis. For example, if a BK7 prism, such as the one in this device was arranged so that the light penetrates the hypotenuse to transmit through the glass, bubbles within the glass are only permissible for every inch of travel inside of the prism. If nonsymmetrical shaped digs occur on the surface of the optic, then the diameter will be accounted for as the average of the maximum length and width on the surface. In the case of bubbles, irregular shapes will be considered as one half of the sum of the maximum length and width. Figure 14 illustrates the scratch-dig for optical devices and their various optics specifications. This figure informed us on the proper scratch-dig that would be required for our optical setup. Table 5 below shows the scratch-dig specifications and their application for practical use from the company Newport Optics.

Focal planes and near focal planes			Central zone 1/2 diameter of surface		Outer Zone	
Beam diameter (mm)	Magnifying power	Focal length (mm)	Scratch	Dig	Scratch	Dig
Over 5.....	.....	.....	80	50	80	50
4-5.....	.....	.....	60	40	60	40
3.2-4.....	.....	.....	60	30	60	40
2.5-3.2.....	.....	.....	40	20	60	40
2.1-2.5.....	.....	.....	40	15	60	30
1.6-2.1.....	.....	.....	30	10	40	20
1.0-1.6.....	.....	.....	20	5	40	15
0.6-1.0.....	.....	.....	15	3	30	10
0.4-0.6.....	.....	.....	10	2	20	5
0.2-0.4.....	.....	.....	10	1	15	3
0.2.....	20-10	12.5-25	10	1	15	3
0.4.....	10-5	25-50	10	2	20	5
0.6	5-3.3	50-75	15	3	30	10
1.0.....	3.3-2	75-125	20	5	40	15
1.6.....	2-1	125-250	30	10	40	20

**Figure 14:** Scratch-dig table from the MIL-PRF-13830B. This table is approved for public release from the AMSC N/A FSC 6650, and distribution is unlimited.

Scratch-Dig	Quality	Applications
60-40	Low	Commercial use
40-20	Standard	Imaging and low power lasers

20-10	High	Laser mirrors and high-power lasers
10-5	Highest	High energy applications

**Table 5:** Scratch-dig specifications and some of their applications for practical use (Newport)

The scratch-dig metric is important in optical manufacturing because it forces manufacturers to construct their optical components fit within certain specifications for sales. The benefits of following the scratch-dig metric when it comes to component shopping is being able to determine which specification is more appropriate for the system being built. The scratch-dig metric helps determine the amount of internal scatter since the tighter the specification, the lower the scatter. For example, if a system does not have a need for reducing scatter or the scatter is negligible, a 60-40 scratch-dig specification is optimal. If the system needs minimal scatter due to the amount of precision needed, such as a laser system or an imaging system, a 20-10 or 40-20 scratch-dig specification is best. The prism in this device has a 40-20 scratch-dig specification making it a good choice because the device will be recording images of the laser after the beam contacts the SPR sensor chip. Table 3 above describes some applications based on the scratch-dig specification of the optics.

### **5.B.3 Communication Standards**

The Surface Plasmon Resonance device will utilize the wireless capabilities of our chosen microcontroller unit to expand compatibility amongst all devices that can function with the following IEEE wireless communication standards.

#### **5.B.3.1 IEEE 802.11**

The IEEE 802.11 is part of the IEEE standards for local area network technical standards. The wireless local area network standard is used for implementing communication between the microcontroller unit and the computational device used for processing the data retrieved from the CMOS image sensor. The IEEE standard describes the compatible wireless communication bands of 2.4 GHz and 5 GHz that will be used by the system on chip Wi-Fi module.

#### **5.B.3.2 IEEE 802.15.1**

The IEEE 802.15.1 covers wireless personal area networks such as Bluetooth and is intended to expand the functionality of the SPR device with multiple forms of wireless communication [x]. Although Bluetooth is not the primary wireless communication standard, the option of use for Bluetooth Low Energy mode which

operates at a frequency of 2.4 GHz can greatly expand the device's battery life without compromising performance.

#### **5.B.4 Software Standards**

The Surface Plasmon Resonance device relies entirely on the collection of data during experimentation and the software must follow strict standards set by recognized organization to ensure reliability in our experiments. If we cannot be confident in our software due to bugs or unintended features, then we cannot be confident in the accuracy of our processed data. These standards are applied to the communication features, electronic connections controlled by the software, and the source code itself.

##### **5.B.4.1 Agile Development Method**

The Agile Development Methodology is based on iterative development by communicating with the targeted user or customer, developing in phases while adapting to changes in the design requirements. This method will ensure the software to be useful for prototyping without being full completed, creating a greater ease when reassessing the design to satisfy the requirements more precisely. Since the software is made up of multiple functions and has a final goal of interpreting data visually for an enhanced user experience, a lot of the functionality of the software can be completed without the reliance on other features. By utilizing this method, our team will be able to communicate more thoroughly with a schedule that's made to ease adaptability.

##### **5.B.4.2 Android Developers Core App Quality**

The Android Developer's Core App Quality is a set of guidelines used to help ensure the quality of the application [x]. They are very commonly used in the community to set a standard for the user experience and to avoid unintended features. These guidelines work like a checklist which covers a large variety of topics such as visual design and navigation, notifications, popups, privacy and permissions and even performance on varying devices.

##### **5.B.4.4 IEEE 830.1998**

The IEEE 830.1998 is part of the IEEE standards for recommended practices for software development. The standard is a rubric for assessment of software requirements and is intended to be used as a scoring guide [x]. This standard will have direct influences on our development environment and how the software will behave on both mobile devices and personal computers. Since the SPR device is intended for commercial use for the industry and possible everyday consumers, then it is very important these standards are utilized to ensure proper uniform scaling and a streamlined development process.



### **5.B.5 Battery Standards**

IEEE 1625-2008, a standard on rechargeable batteries for multi-cell mobile computing devices. The established criteria are intended to be used for design analysis for quality, reliability of the battery system, and qualifications of the battery itself. It provides methods for quantifying the operational performance of the batteries and their control systems. The battery technologies covered in this standard are limited to lithium-ion polymer. This does include the battery's electrical and mechanical construction such as the system, pack, cell level charge and discharge controls as well as the battery status communications. The follow topics are the focus of this standard: qualification process, manufacturing process control, energy capacity and demand management, levels of management and control in the battery systems, packaging technologies, and finally the considerations for end-user notification for the battery's status [x].

### **5.B.6 Microcontroller Standards**

IEEE 1118.1-1990 is part of the IEEE standards for microcontroller system serial control bus. A serial control bus for interdevice as well as intrasite interconnection of microcontrollers is described. The bus, which is defined for microcontrollers and devices with limited reprogrammability, provides a multidrop bit-serial communication protocol that will allow the interconnection of disturbed independently manufactured devices. The protocol is optimized for instrumentation, disturbed data acquisition systems, control devices, and test and measurement. Specifications for a common architecture, generic bus services, system wagement, data link, and several physical media are provided [x].

### **5.B.7 Chemical Laboratory Safety in Academic Institutions**

Whenever chemicals or biological samples are used in a laboratory setting, certain standards must be followed to ensure the safety of everyone involved. It is crucial that the standards decided upon remain the same in every laboratory setting to ensure that everyone understands the hazards and safety procedures required when handling toxic or otherwise dangerous materials. The American Chemical Society for Lab Safety has devised a set of standards and procedures that can be adapted to various environments, from academic to professional settings. The purpose of these guidelines is to promote safe, ethical, responsible, and sustainable practices that are accessible through educational training provided by the society to all academic and professional laboratories [Society, A.C citation]. The 8<sup>th</sup> edition of the American Chemical Society Safety in Academic Chemistry Laboratories will provide us with guidance on the best practices to perform when handling the various biological samples we will use in testing the accuracy of our surface plasmon resonance sensor. Below are

certain sections from the text that are applicable to us throughout the design process of our project to ensure our laboratory settings are as safe as possible for those present in the laboratory environment.

### **5.B.7.1 Personal Protective Equipment (PPE)**

Personal protective equipment is one of the fundamental ways to protect yourself when in a laboratory setting. It is used to avoid exposure to hazardous materials you may encounter when working on an experiment in the laboratory. PPE can include items such as gloves, eyewear, and lab coats that protect sensitive areas of your body from exposure to chemicals that may be used during an experiment [Society, A.C. citation]. For our experiment, PPE such as eyewear should be worn when interacting with the biological samples as they are being mixed and added to the surface plasmon resonance sensor sensing chamber. This is to avoid any of the liquid chemicals being used from entering the eyes in the event of any splashes or spills. The types of chemicals being used determine the type of protective eyewear that should be used. For our experiment, since we will not be using any toxic or hazardous chemicals, regular goggles that cover both the front and side of our face are appropriate for protection. Gloves are also appropriate for our experiment, as it protects the wearers hands from interacting with the liquid materials. It also protects the various chemicals and biological samples being tested from the oils on our skin, such as the SPR chip which is immobilized with Protein A which can be damaged if in contact with our skin. The length of the gloves and the type of material they are made of is another factor to consider when choosing the correct gloves for your experiment. For our experiment, disposable gloves made of latex are acceptable for our purposes, although any members of the group who are allergic to latex should avoid using gloves of this material and instead use ones made of neoprene or butyl rubber that are acceptable as well for our purposes. The length of the gloves can be up to our wrists for this experiment, as we will not be dealing with any substances that can cause burning or irritation to the skin when in contact. In circumstances where one uses chemicals that have negative effects to exposed skin, gloves that cover the entire arm or at least the forearm should be used. As we will be using disposable latex gloves, proper safety procedures dictate that the gloves should not be reused to avoid any contamination from chemicals that may have interacted with the gloves in the previous experiment without notice.

Other forms of PPE include what is appropriate to wear when in a laboratory environment. Loose-fitting clothing such as long sleeves should be avoided as it can be a hazard to any open flames or toxic chemicals that may be present in the laboratory [Society, A.C. citation]. The material the clothing is made of should also be considered if you will be dealing with open flames or chemicals in a liquid form. The most appropriate clothing to wear is materials made of cotton or other natural fibers which can be less

dangerous in case of fires compared to polyester materials that can cause serious burns when melted. Other clothing one should consider is the type of shoes to wear in a laboratory. Closed toed shoes are always recommended even for the least hazardous experiments to avoid not just chemicals from interacting with exposed skin but any glassware or other lab equipment that could break and cause damage to exposed skin. In our experiment, we will not be using flames or chemicals that can damage clothing when exposed to certain materials. However, clothing such as closed toed shoes should be always worn in the laboratory to protect the wearer from lab equipment that could be broken in an accident during the lab, such as beakers or other glassware we will use to transfer our samples. It also protects us from any other chemicals that may be present in the lab from previous or current experiments without our knowledge.

### **5.B.7.2 Maintaining an Organized Environment**

When in the laboratory, it is essential to maintain an organized environment that is free of obstructions and other obstacles. This is to minimize any tripping hazards from the floor and any spilling hazards from a cluttered workbench [Society, A.C. citation]. This also ensures that in case of an emergency, the walkways are free and easily accessible so that everyone can safely evacuate the lab in a timely manner. Part of maintenance includes cleaning the floor and tables of any spills that may have occurred during the experiment as soon as possible. Not only can these become tripping hazards, but they can also lead to dangerous chemical or biological interactions if they interact with substances on the floor or workbench that were not properly cleaned by a previous group performing an experiment. Should any glassware break during an experiment, proper cleaning and glass disposal procedures should be taken to avoid any injury. Glass should never be disposed of in a regular trash can, but instead should be placed in a separate receptacle designated for broken glass. Each laboratory contains specific procedures for disposal of glass or chemical and biological substances and should be followed to ensure the safety of everyone that enters the lab. During our experiment, all the procedures involved in maintaining a clean and organized laboratory environment should be followed at all times to ensure everyone that enters the lab during or after our experiment is safe.

### **5.B.7.3 Labeling Chemicals**

During an experiment involving chemicals, various vials or beakers may be used to store any samples used or created. These samples can become a danger in the laboratory environment if not properly and clearly labeled with what type of substance was used. Without proper labels, substances could be wrongly mixed in a dangerous or sometimes deadly manner. Labeling chemicals is one of the most important procedures to follow when in a lab setting and should be handled with care during each experiment. Labels used in laboratory settings fall into two categories: manufacturer and secondary

[Society, A.C citation]. Manufacturer labels are ones that are found on the container of the substance to be used that was sold by a manufacturer. These labels are not to be damaged, covered, or changed in any way until the container is verified to be empty, due to the wording and information on the label being essential for understanding any interactions that substance could have with other chemicals found in the laboratory. In some circumstances, empty containers that once contained chemicals are reused for other experiments. Before any container can be reused, the label on the verified empty container should be removed completely and the container should be thoroughly cleaned and allowed to air dry. This ensures that no chemical to be placed in the reused container can interact with past chemicals. Under no circumstances should a marker be used to write over an existing manufacturer label and no container should be more than one label present. The second category is secondary labels. These are temporary labels used during an experiment on substances that were mixed or created in a laboratory environment. At a minimum, the secondary label for temporary storage of a chemical substance should contain the name of the chemical or chemicals being used, the name of the person who filled the container, the date it was filled, and the hazards for the chemical. Should the container be used for long term storage, the label should follow the standards of the Globally Harmonized System of Classification and Labelling of Chemicals (GHS) [Society, A.C. citation]. Our experiment will include creating multiple samples of our bovine immunoglobulin G analyte combined with our phosphate-buffered saline solution. This will require us to create multiple secondary labels for our samples that must follow the guidelines described above. The containers our chemicals arrive in will contain manufacturer labels that must remain undamaged and clearly legible throughout our entire experiment to avoid any cross-contamination from occurring in and outside of the laboratory setting.

#### **5.B.7.4 Cleaning Glassware and Disposal of Chemicals**

Once an experiment is complete, disposal of the substances used must be considered. Proper handling of chemical waste is an important part of incident prevention, leading to very strict rules that must be followed for disposing of chemicals [Society, A.C. citation]. When disposing of chemical waste, different containers should be used for disposal of different classes of chemicals. This is to avoid any cross-contamination from occurring accidentally, which could result in adverse reactions that may cause fire or other serious damage. The containers used for disposing waste should follow the labelling procedures described above to avoid any confusion as to which container should be used when cleaning. In some circumstances, reactions created in experiments can be neutralized to help reduce waste handling. When disposing of chemicals, the following guidelines should be followed [Society, A.C citation]:

- When disposing of chemicals, each class of waste chemical should be placed in its specific disposal container that is properly labeled. The label should be read carefully before disposal and the cap replaced securely on the container after disposal.
- Never pour chemicals into a sink or down a drain unless instructed to by an instructor or lab assistant certified in laboratory safety guidelines. This is to avoid chemicals from entering the sanitary sewer system which could cause adverse effects.
- Materials contaminated with chemicals, such as paper towels used to clean spills during the experiment, should be disposed of in special containers marked for this use.
- Broken glass should be placed in disposable containers specially marked for glassware. If the glassware contained chemicals used during the experiment, a separate waste container should be used to properly dispose of the contaminated glassware. Should any hazardous materials be exposed from broken glassware, such as mercury, the on-duty lab instructor should be notified immediately and proper cleanup procedures for hazardous materials should be followed.

Once chemicals are disposed of in their proper waste containers, they are now subject to hazardous waste regulations regulated by the local state government and the federal Environmental Protection Agency (EPA) [Society, A.C. citation].

After all chemicals are properly disposed of, the glassware and other laboratory equipment used should be properly cleaned. Dirty glassware should be cleaned using hot water with environmentally acceptable cleaning agents in a laboratory sink. Chemical splash goggles should be worn while cleaning laboratory glassware to avoid any chemicals from splashing into your eyes. Care should be taken while cleaning, such as not forcing a brush into the glassware or using a high-velocity stream of water, as this can cause the glassware to break and create a hazardous environment. Should the glassware break, use a pair of cut-resistant gloves, tweezers, or tongs to remove the broken pieces of glass from the sink [Society, A.C. citation].

For our experiment, both the procedures mentioned for disposal of chemicals and cleaning of glassware must be followed. We will be experimenting with biological samples that must be disposed of following proper guidelines described by the Florida Department of Environmental Protection, the federal Environmental Protection Agency, and the University of Central Florida Environmental Health and Safety department. Our biological samples will be transported in glassware, such as beakers, that must be properly cleaned and stored once the experiment is completed.

### **5.B.7.5 Safety Procedures for Using Electrical Equipment**

In many chemistry laboratory settings, electrical equipment may be used for equipment used for measurements, Bunsen burners, and other necessary equipment for the completion of an experiment. It is therefore crucial to ensure that all electrical equipment is in good and working condition to avoid using anything that could pose a fire hazard. Before beginning an experiment, all insulation on the electrical cord for each equipment must be inspected to ensure no wires are exposed [Society, A.C. citation]. If any liquids are being used during the experiment, all liquids should be placed far enough away from any wall outlets or other live electrical wires that could pose a safety hazard. Our experiment will include chemicals in a liquid form that will be close to multiple electrical components, namely laser diodes, microcontrollers, other various electrical components. Care should be taken to avoid any spillage of our liquid samples that could cause damage not only to ourselves but to our electrical components as well.

### **5.B.7.6 Refrigerating Chemical or Biological Samples**

Some substances used in chemical laboratories require low-temperature storage when not in use. These substances will normally contain a required temperature on their specific manufacturer label to ensure the longevity of the product. Any chemicals or other substances that require refrigeration should be properly labeled in a fridge designated for chemical or biological storage. Some substances may be flammable and should be stored in fridges rated for storage of flammable materials [Society, A.C. citation]. Food and beverages should not be stored in the same refrigerator that chemical or biological samples are stored to avoid accidental consumption. Our experiment contains some substances that require refrigeration, such as our SPR chip that contains immobilized Protein A and therefore must be stored in a refrigerator at 4 degrees Celsius. Proper care and labeling of our biological material must be taken to avoid any accidental consumption or cross-contamination from occurring.

### **5.B.10 NASA-STD-8739.3**

NASA's technical standards on soldered electrical connections does not represent formal requirements but acts as guidance to use when preparing or evaluating process procedures for the manufacture of mission critical hardware [x]. Although the focus of these standards is for space flight and ground support equipment, the same practices can be followed when soldering electrical connections and to ensure a less susceptible product due to rough handling as well as implementing safety methods.

## 6. Project Hardware Design Details

The hardware components of our design relate to the physical parts that will aid us in manipulating the light in our system, measuring the final output of our sensor, providing power to the entire system, and housing the entire setup. The following sections will discuss the design calculations done to determine the components and direction of our project, how these components evolved since our initial design idea, and how we decided on our present project design based on research and testing.

### 6.A Design Calculations

The purpose of design calculations is to determine relevant values to our optical subsystems. These calculations were performed using relevant equations and software that simulates optical results to aid us in determining the best components and specifications for our project.

#### 6.A.1 Optical Design Calculations

In our surface plasmon resonance sensor, the core optical phenomenon observed is total internal reflection created using a right-angle prism and a 532-nanometer wavelength laser diode. As we know, total internal reflection only occurs when light travels from a medium of high refractive index to a medium of low refractive index. These refractive indices, as well as the incident angle, play a key role in the critical angle which determines when we will experience total internal reflection. Using Snell's Law, we can determine the relationship between the directions our light will travel in these two mediums. Equation 3 below is Snell's Law rearranged to determine the critical angle our light will travel.

$$\theta_2 = \sin^{-1}\left(\frac{n_1}{n_2} \sin \theta_1\right)$$

**Equation 3.** Formula for Critical Angle

The standard material used for glass in optics is N-BK7 due to its high purity and is why it was chosen as our material for the right-angle prism. Using the equation above, our first index of refraction is the N-BK7 glass which has a standard refractive index of 1.52 with a 532-nanometer wavelength, and the second index of refraction is air which has a value of 1. When light is incident on a medium with a lower refractive index, the ray is directed away from the normal, so the exit angle is greater than the incident angle. The exit angle approaches 90 degrees for some critical angle value, where incident angles greater than the critical angle create total internal reflection. Using the values given above, it can be determined that the critical angle of the prism is 41.81 degrees.

From our calculations, total internal reflection should be observed when the incident angle of our light is greater than the critical angle. To better determine when we should see total internal reflection occurring, the software called WinSpall was used to simulate the reflectivity curve created using a 532-nanometer wavelength laser and a N-BK7 right-angle prism. WinSpall was developed to simulate surface plasmon resonance curves based on the Fresnel formalism. It allows one to add various layers that the rays will travel through, specifying their real and imaginary parts of the dielectric constants, to output a theoretical reflection curve at each angle. In our experiment to determine total internal reflection, there are only two layers the light will travel through: the right-angle prism and air. For the prism layer, the real part of the dielectric constant is 2.29 which corresponds to a refractive index of 1.5. The imaginary part is zero because there is no absorption of our light from the glass prism. For the second layer, air, the real part of the dielectric constant is 1 which corresponds to a refractive index of 1. The imaginary part is zero as well because there is no absorption of our light when in air. The parameters used to simulate the reflectivity curve for total internal reflection using WinSpall can be seen below in Figure 15.

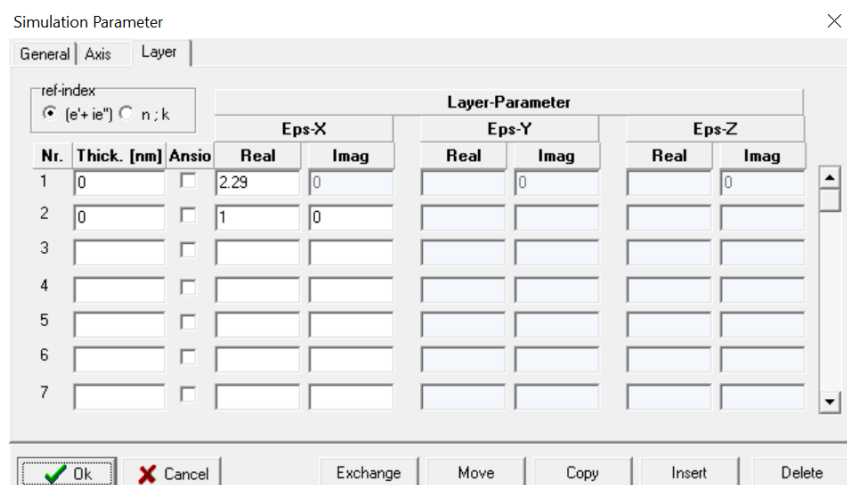


**Figure 15.** Simulation Parameters to Simulate Total Internal Reflection using WinSpall.

With our parameters in place, a simulation of the reflectivity curve we should observe was created. The simulated reflectivity curve can be seen below in Figure 16.



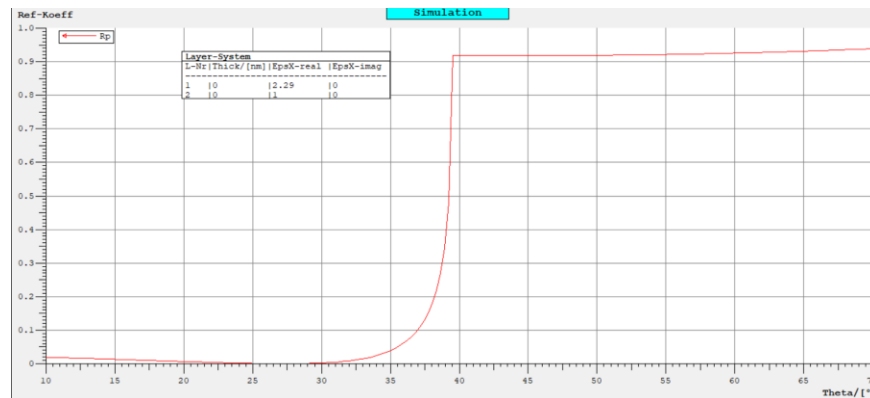


**Figure 16.** Simulation of Reflectivity Curve for Total Internal Reflection using WinSpall.

From the simulated reflectivity curve, at angles lower than 30 degrees, all light is transmitted through the prism without any reflection. After 30 degrees, more and more of the light is reflected until at 39.47 degrees where total internal reflection is reached. This simulation, while not able to consider every real-world parameter, gives us a useful estimate of at what angles we should expect to see total internal reflection occurring based on the wavelength of our laser diode and the material chosen for our right-angle prism.

## 6.B Initial Designs and Related Diagrams

Our initial design idea for the surface plasmon resonance sensor began with the document “Divide and Conquer”. The purpose of this document was to lay out a blueprint for our project which could later be built upon as we continued to research and modify our goals and objectives. Figure 17 shows the initial block diagram that was created which later became the portable surface plasmon resonance sensor.

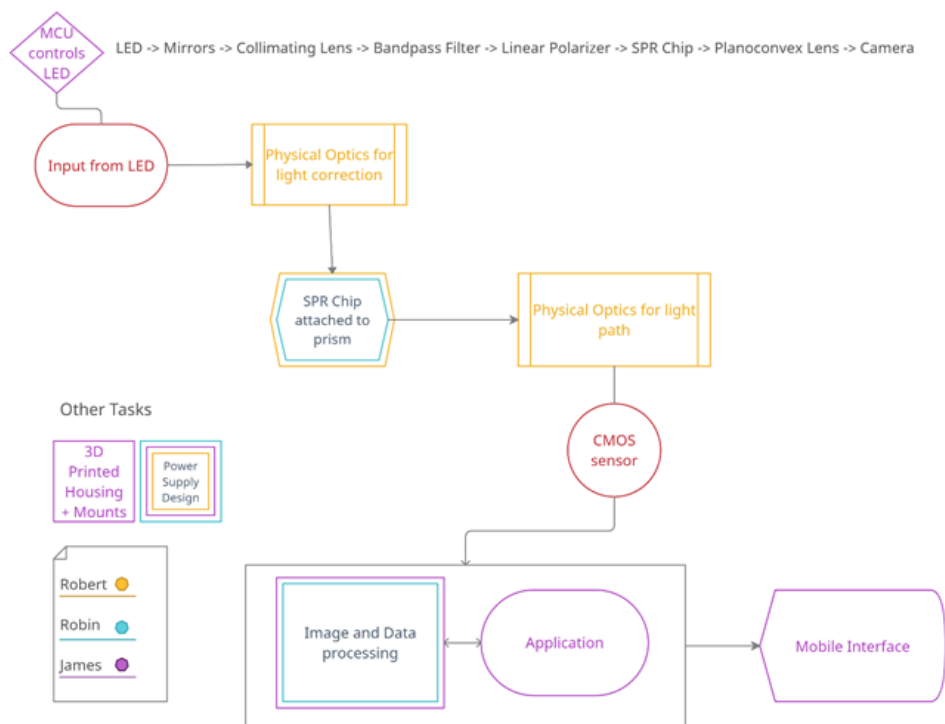


**Figure 17.** Initial Divide and Conquer Block Diagram for Surface Plasmon Resonance Sensor

The final design for our project has evolved since we created the initial block diagram above, with many of the technologies illustrated having changed or been discarded altogether. Nevertheless, this initial diagram provided us with a basic concept of what we wanted to accomplish and how we could go about it. A crucial point in any project is its initial design, which serves as the backbone of the finished product. The research into past technologies, the different optical and electrical components used, and the final design all were based on the original figure above. Although basic in design, it allowed us to begin the plans for our finished product.

The following sections serve as a journal of the evolution of our hardware components for the project. Through research and testing, the final concept for our project was formed to ensure our device was as efficient as possible.

### 6.B.1 Initial Design Idea – Smartphone Based SPR Sensor

When we first decided upon the idea for our senior design project, our initial thought was to utilize a smartphone device to act as the controller and sensor for our surface plasmon resonance sensor. This idea came from past low-cost surface plasmon resonance sensors that would mitigate the overall cost by taking advantage of the high-powered CPUs and high-resolution cameras that come with most smartphone devices

today. Our initial idea was to use multimode optical fiber as a way to direct the incident light onto the sensing surface and towards the detector. But after careful consideration, we decided that a prism-coupled SPR sensor would fit better for our purposes. This was due to the simplicity that a prism-based system provides, where surface plasmon excitation is created using the phenomenon of total internal reflection and the evanescent wave created that travels the boundary between the prism and air. Figure 18 below shows our original illustration for the surface plasmon resonance sensor using this design idea.

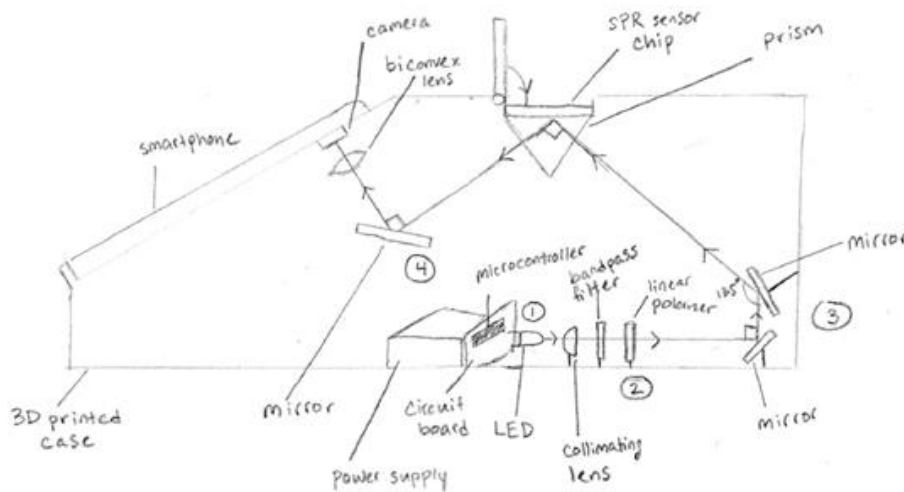


**Figure 18.** First Illustration of the SPR Sensor Prototype

In the illustration above, a green LED would be connected to a microcontroller that would allow the smartphone application to communicate with the system and determine when the light turns on or off. A battery-powered power supply would be used as a power source for the LED and microcontroller. The light from the LED would be manipulated by a 532 nm bandpass filter and linear polarizer, which are used to narrow the range of the LEDs wavelength spectrum and change our incident light into a transverse magnetic wave respectively. This would ensure our incident light was monochromatic and transverse magnetically polarized so that the wave may resonate with the wave created by surface plasmon excitation. Two mirrors would then be used to direct the light onto a right-angle prism. This is where the surface plasmon detection occurs. By angling our incident beam to a 45-degree angle using mirrors, we could create the phenomenon called total internal reflection as the beam hits the right-angle prism. This coupling of the light using the prism creates a perfect situation where surface plasmon excitation can occur as most of the energy from our incident light will be absorbed by the metal/dielectric interface on our SPR chip. This leads to a decrease in intensity of our received light onto the smartphone's CMOS camera. The decrease in intensity of our received light indicates that excitation occurred, and molecular binding took place. The smartphone device would be placed in a mounted area with its screen facing outward. A small hole would allow for the back facing camera of the smartphone

device to interact with the optical path of the SPR sensor found inside the casing. The entire structure would be designed using 3D printed components made of thermoplastic polyurethane.

### **6.B.1.1 Light Source Design**

The design described began to change as we continued to research the various technologies we would utilize and the pros and cons of each. The green LED as our light source at the time seemed a cheap solution for us to use in our product while also providing a light source that was separate from the smartphone as opposed to using the LED flashlight on the smartphone which would constrain how much we could manipulate the optical path. However, we discovered that trying to collimate the light from an LED source is very difficult and results in much of the light being lost. This led to us having to reassess what we would use as our light source that was both cost efficient and could be collimated easily. Our final decision was to use a 532 nm laser diode module as our light source. Laser diodes are semiconductor devices that provide a beam that is fully collimated. The wavelength 532 nm was chosen due to its steadier output power. To produce the 532 nm wavelength, a Neodymium gain medium is doped by a 1064 nm diode. When this occurs, the second harmonics of the 1064 nm radiation emitted by the Neodymium gain medium produce the 532 nm wavelength that exits the laser diode. These lasers are well suited for applications which require a good beam quality and high-power stability. For our purposes, the intensity of our light source must remain constant throughout the experiment to avoid any fluctuations being interpreted as molecular binding occurring. However, using a laser diode as opposed to an LED as our light source brought new challenges. A laser diode is a very efficient light source but also a very powerful one. The light that will be directed onto the SPR sensing location and the detector would emit an output power in the range of 5 to 10 mW of power. At this level, damage could be done to the detector and to the biomolecular solution being tested. To avoid any potential damage, a neutral density filter would be needed in the optical path. Based on our research, a neutral density filter with an optical density of 1.0 would be sufficient to ensure the output power directed onto the detector and SPR sensing location would be low enough to avoid damage. An optical density of 1.0 would ensure that only 10% of incoming light would be transmitted, making the final output power onto the detector and SPR sensing location be in the range of 0.5 to 1 mW. Another challenge the laser diode brought to our design was the method we would use to ensure the beam intensity remained constant. One of our design goals is to provide a portable SPR sensor which requires us to provide a power source that is battery powered. A detailed explanation of the various technologies and solutions for powering our laser diode using batteries can be found in the subsection titled Power Delivery in the Research section of the document.

### **6.B.1.2 SPR Detector Design**

As can be seen in our initial design illustration above, the original design was to have the smartphone's CMOS sensor act as the detector for our SPR sensor. Doing so would mitigate the cost of purchasing a separate camera with a high enough resolution to properly image the intensity changes seen during molecular binding. But this requires the smartphone device itself to be a part of the optical path, which brought a certain amount of constraints to our product. In order for the SPR sensing device to work, the smartphone used by the consumer would require the back facing camera be in the same position as the smartphone we will use for designing our project. This is to ensure that the camera is in the correct location for the captured images to properly visualize the transmitted beam from the prism after surface plasmon excitation. Many smartphones vary in the location of their back facing camera, which would therefore limit the type of smartphones that would be compatible with our finished SPR sensor. To ensure our project was more versatile, we discarded the idea of using the smartphone's camera as the detector and chose an external CMOS sensor instead. This removed the smartphone altogether from the optical path, ensuring that we no longer had a hardware compatibility issue for the type of smartphone device used. However, this removed our ability to use the high-resolution CMOS sensor that most smartphone devices provide, forcing us to find a sensor that provided similar specifications at a reasonable price. After careful consideration, the ESP32 microcontroller with the OV2640 camera module was chosen due to its low price, its 1600 x 1200 pixel resolution, its wireless features such as Bluetooth low-energy and Wi-Fi, and onboard JPEG encoder that would offload the processing power to reduce memory on the microcontroller. The sensor also provides fast processing time, which became another factor to consider as the camera must capture and transmit its captured images to the software application in a timely manner. With the CMOS sensor described, we will be able to image the intensity changes seen during our experimentation to provide an accurate measurement of when surface plasmon excitation takes place.

## **7. Project Testing and Prototype Construction**

After the initial design is created for a project, the next step is to begin testing the functionality of the various hardware and software components. Before any time, money, and resources are spent on the first fully functional prototype, one must ensure that each component is the correct choice for the particular goals and objectives for the project. The following sections describe the hardware as well as software testing done for the completion of our project, as well as the multiple prototypes built for our final product.

## **7.A Hardware Testing**

Testing is a key element of any prototype, ensuring that each component chosen is the most efficient decision for the final output of the product. The following sections will describe the testing done for the electrical and optical components of our hardware that have aided us in deciding the direction our final prototype will take.

### **7.A.1 Microcontroller and Power Supply Testing**

The chosen microcontroller has two particularly important jobs that both have major influence over the results of our experiment. The first and most taxing responsibility is to capture an image from the CMOS sensor, process and compress the JPG file, then upload it to an asynchronous web server that is hosted by the microcontroller unit itself. This process must be completed in under 500 milliseconds to reach our engineering requirement. The second responsibility is to control the switching behavior of the power source to the laser diode through the use of a MOSFET, acting as an on / off switch.

The ESP32-CAM does not have an onboard USB port and instead uses UART, universal asynchronous receiver and transmitter. This required the use a special adaptor that would plug into a USB port of a computer and breakout into 4 pins. Power, ground, transmit, and receive with the latter being the data lines. The decision to not have an onboard USB port was to decrease the size of the device, but at the cost of extra modification in order to use the GPIO pins corresponding with the UART pins to be used for anything but UART. With the limited pins for free use, especially when using the CMOS sensor, this was a must.

Our original power source was a 9v Energizer battery connected to a linear voltage regulator to lower the voltage from 9v to 5v. Two capacitors were installed in parallel with the input and the output power from the regulator to smooth out any fluctuations. Two 9v batteries were used in total to ensure enough current went to our two power consuming devices, in the figure below, the second laser diode is replaced with a blue LED, so it was unnecessary but still used with two 9v batteries. The original switching circuit for the laser diode, or LED in this case, was using two MOSFET transistors, one P-channel and one N-channel. Figure 15 depicts the microcontroller testing with the L805 voltage regulator and the 9V battery.

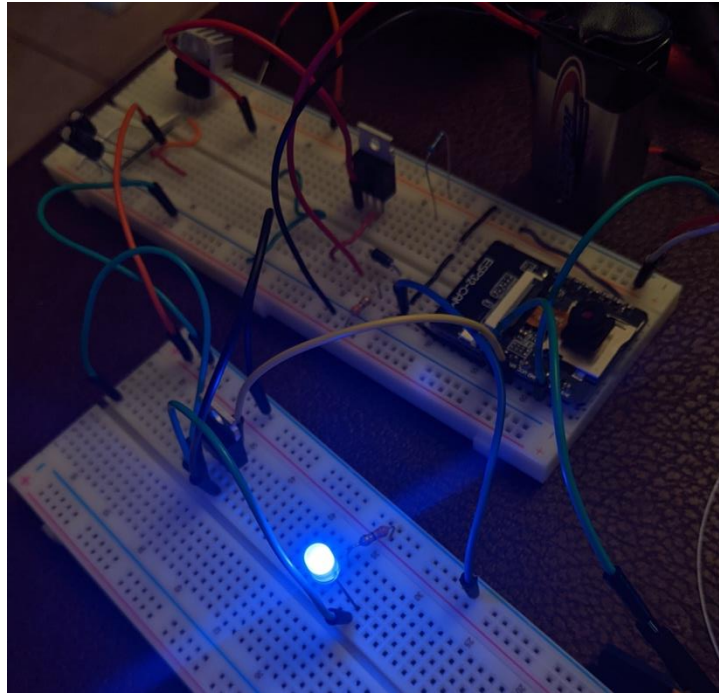


**Figure 19.** Microcontroller Testing with L805 Voltage Regulator and 9v Battery.

Although the 9v battery proved to be appropriate in the initial testing, the rate of voltage drop-off was starting to cause issues and eventually the microcontroller unit ceased to turn on. Although a 9v battery has a capacity rating of 500 mAh, this was when our team learned how the capacity rating was measured and how it changes depending on the current draw. There was no reason to continue using 9v batteries without being extremely wasteful and buying 9v batteries by the bulk.

The power source was changed to a 2-cell 7.4v lithium polymer rechargeable battery rated for 40 Amps with 1600mAh capacity. It was designed for the use of consumer RC cars which most have high potential for large spikes in current consumption. This can be considered 'overkill' for our power requirements, but this ensures we have room for expansion and high efficiency for our engineering requirements.

Another discovery that was made just before switching away from 9v batteries was the inefficiency of a linear voltage regulator. Unfortunately, about two thirds of the energy was dissipated as heat through the voltage regulator. With our marketing and engineering requirements, this was a large drag on our power consumption, and we decided to move away from it at the cost of moderately complicating the power supply design. The move was made to a LM2596 switching regulator purchased from TI that has a potential max efficiency of 96 percent. This required the use of a diode, two electrolytic capacitors for smoothing out spikes in voltage, and an inductor to properly regulate the feedback loop of the switching regulator.

The original switching circuit for the laser diode was simplified to only use a single N-channel MOSFET that can be seen in Figure 20 below.

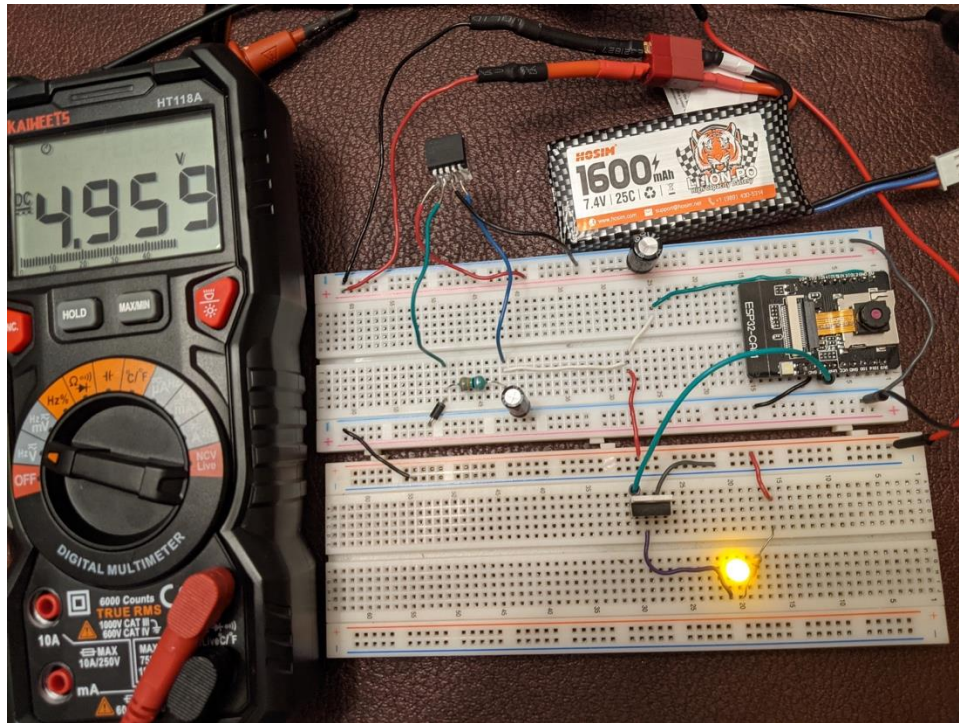


**Figure 20.** Microcontroller Testing with LM2596 Switching Regulator and 7.4v LiPo

Below in Figure 21 is an example of the ESP32-CAM capturing an image and uploading to the asynchronous webserver hosted by the microcontroller. At any point, if the IP address of the device is used for an HTTP GET request with the “/capture” route, the microcontroller will be instructed to both capture and upload the image upon loading the request on the client side. There seems to be inconsistencies with the timing of the capture function, it is unknown if it is a memory or energy complication, but the average is 200ms which is below our 500ms engineering requirement.



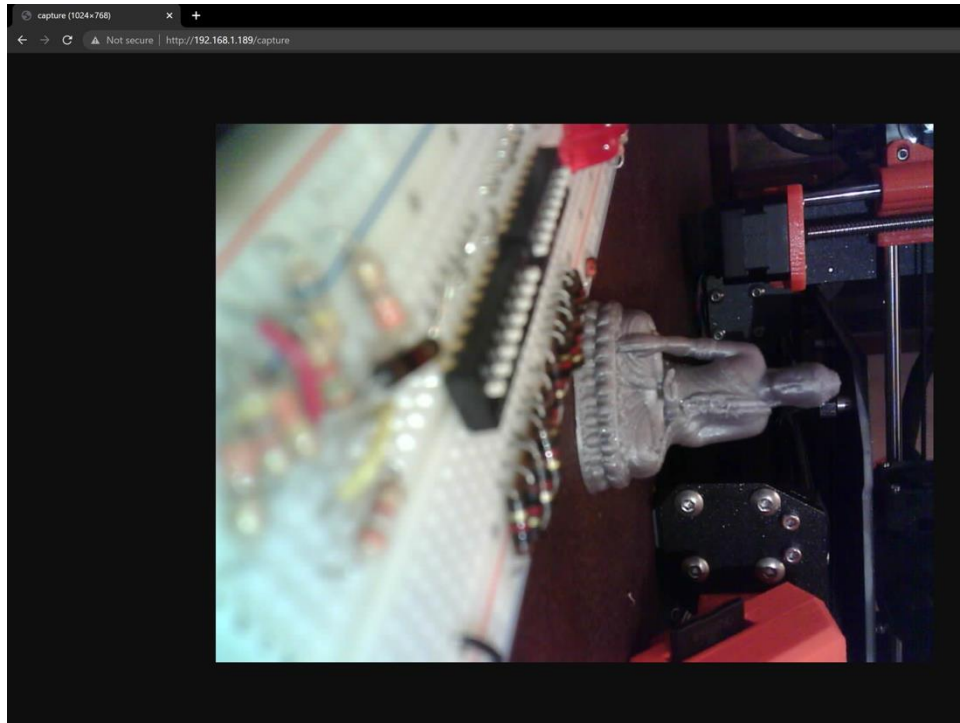


**Figure 21.** Capture Test with Microcontroller

In Figure 22 below, an asynchronous webserver is being used similar to the figure above, but the HTTP route is changed to “/laser” in this scenario. When the GET request is sent to the webserver, it will return the current state of the laser

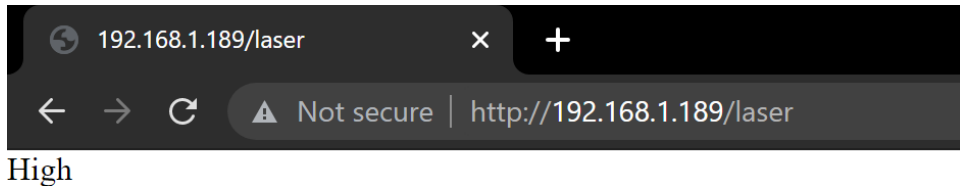


**Figure 22.** Async Webserver Test with Microcontroller

The original switching circuit design did not account for the current load on the laser diode as the prototype version in the figures above were only powering a single LED. The IRF510 MOSFET had too low of a drain current for the 3.3v from the GPIO of

the ESP32CAM for proper saturation. To properly supply the 200 mA to the laser diode, the voltage from the ESP32CAM would have to be boosted or a new MOSFET would be used for the switching circuit. Figure 23 below shows the correlation of the applied voltage and drain current.

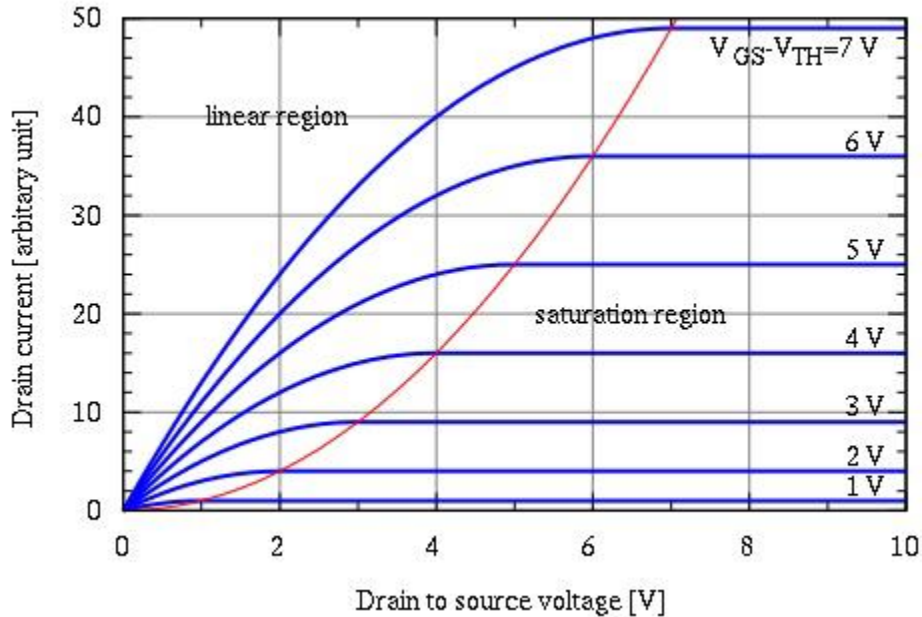


**Figure 23.** Drain Current and Voltage Saturation Graph

The power supply design needed to be expanded to accommodate for an AC-DC wall adaptor through the use of a 3-pin chassis-mounted DC jack. We wanted to be able to unplug the SPR device from the DC jack and have the battery supply instantaneously take over as the power supply of the system as well as plug the device in and switch to the DC jack as the power supply. The battery will be always kept inside the device with a USB cable extending through a hole in the 3D printed housing to be used for charging. We ordered a 7.5v / 800 mA AC-DC wall adapter to be used alongside the battery but what we received was a 10.5v AC-DC wall adapter. To accommodate the extra voltage that needs to be bucked, a second LM2596 was added to the circuit, this one being adjustable. Using the datasheet provided by TI, the feedback resistor values were calculated to buck the 10.5 volts down to 8 volts. This will be fed into the second voltage regulator that will behave the same as if the power was coming from the battery. This will ensure a much higher overall efficiency of the system to further reach our engineering requirement. Figure 24 below is the schematic designed in Altium for easier analysis and an easier time soldering to perforated board.

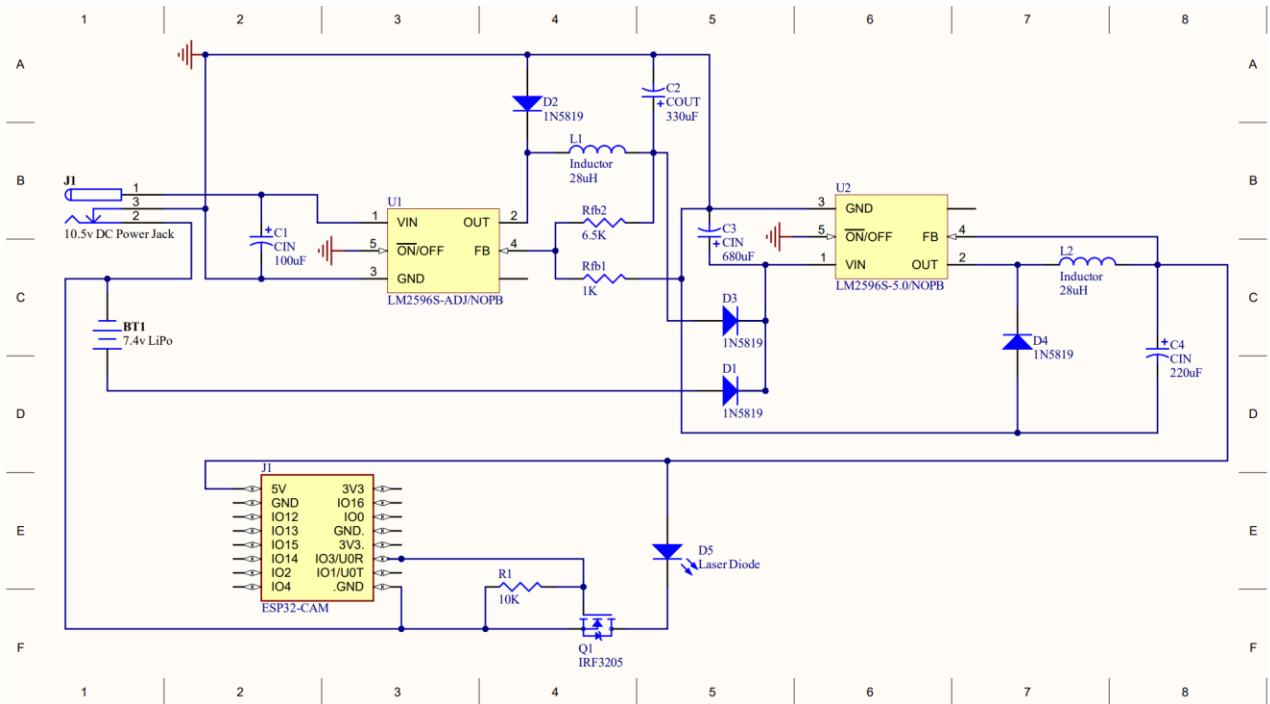
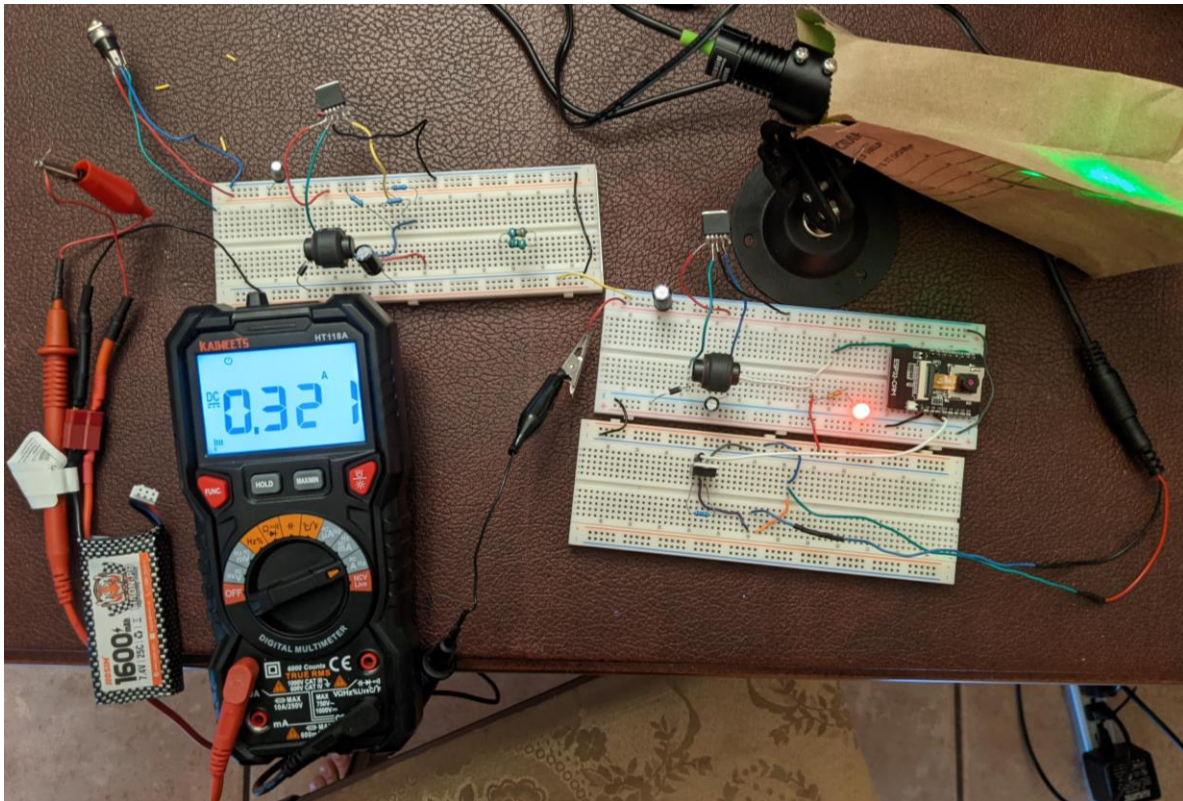
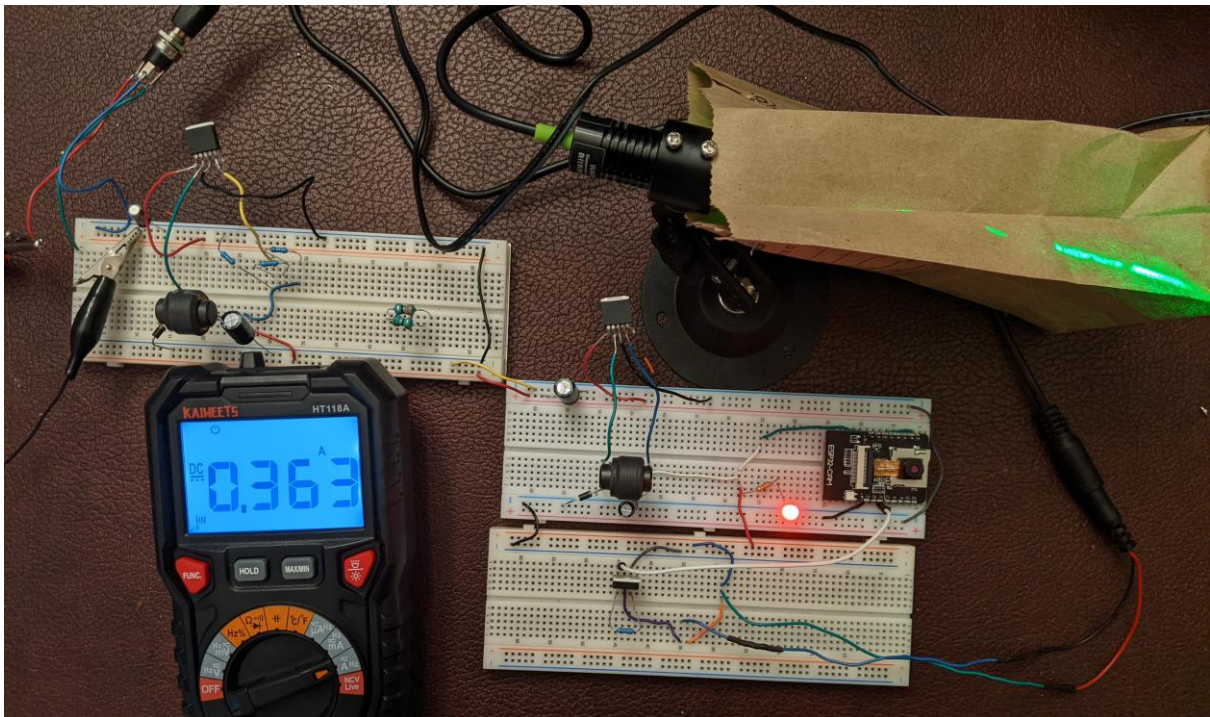


Figure 24. Final Schematic for Power Design



**Figure 25.** Battery Powered System Test

Figures 25 above and below shows the final power circuit design on a breadboard. The red LED indicates the ESP32, and laser is powered, the current draw is negligible for the LED. The inductors here are used as a choke and were found as scrap from Skycraft Surplus, they have been tested to roughly equal the desired inductance and were tested to handle the expected current draw. The DC power jack is also a part that does not have a manufacturing number or any identifying details, but the internals work very similar to the power jack show in the schematic. For context: the laser is shrouded in a paper bag for safety reasons, it is not strong enough to combust but is strong enough to damage eyes.



**Figure 26.** AC-DC Adaptor Powered System Test

### 7.A.2 3D Printed Housing / Mounts

To ensure a compact size and decreased cost in materials, we chose to 3D print the housing of the device and as much of the mounts as we can. Our goal is to make the device as portable as possible, which means we must isolate the inside as much as we can from the outside environment. Although not temperature sensitive, all optic components including the camera sensor must be free from any disturbances such as vibration, noise, or unnecessary light. This means we must measure every dimension of

every component that will be housed and tolerances of the FDM printer will have to be calculated to allow a proper fit. The design software used is Fusion 360 from AutoDesk.

Figure 27 below showcases the first housing we designed when we expected to use a 9v battery for the power supply. This was used to protect and stabilize the camera during initial testing. Figure 28 further below is a demonstration using an older design of the same housing, this one having the camera held at a different angle.

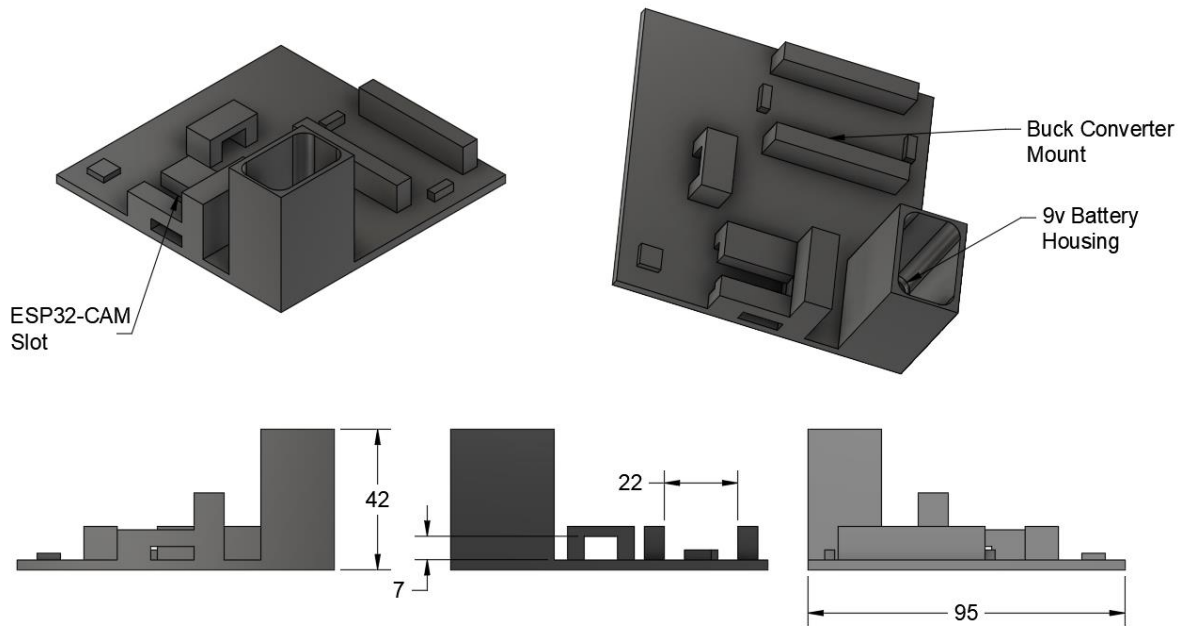


**Figure 27.** First iteration of ESP32-CAM housing using a 9v battery

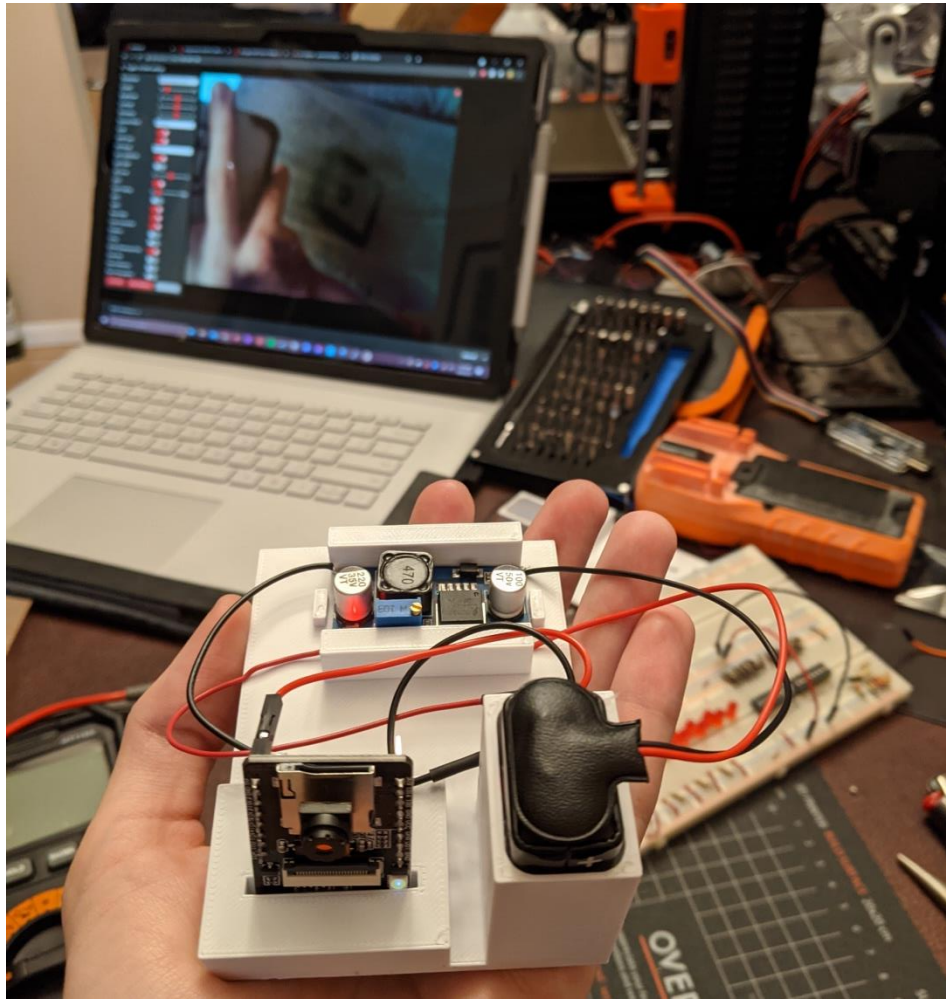


**Figure 28.** First test using housing

The design process of the ESP32-CAM housing had to be done completely from scratch. Fusion360's community has several extensive catalogs of 3D models to freely download, most of which are popular electrical components such as microcontrollers. There were several ESP32 models available but due to ESP32-CAM's relatively recent inception, there was none available to download. A housing for this device was especially important to protect the camera from unnecessary stress and to dampen as much vibration as possible to ensure the cleanest data we can. To do the measurements, a caliper was used on the ESP32-CAM for the dimensions of any extrusion or indent. A surrounding shell was made from the model and printed in halves with overlapping sides to give a moderately loose seal. This will later be modified to fit into the permeant housing, most likely using M3 screws. Figure 29 illustrates the semi-final variation of the ESP32-CAM mount.

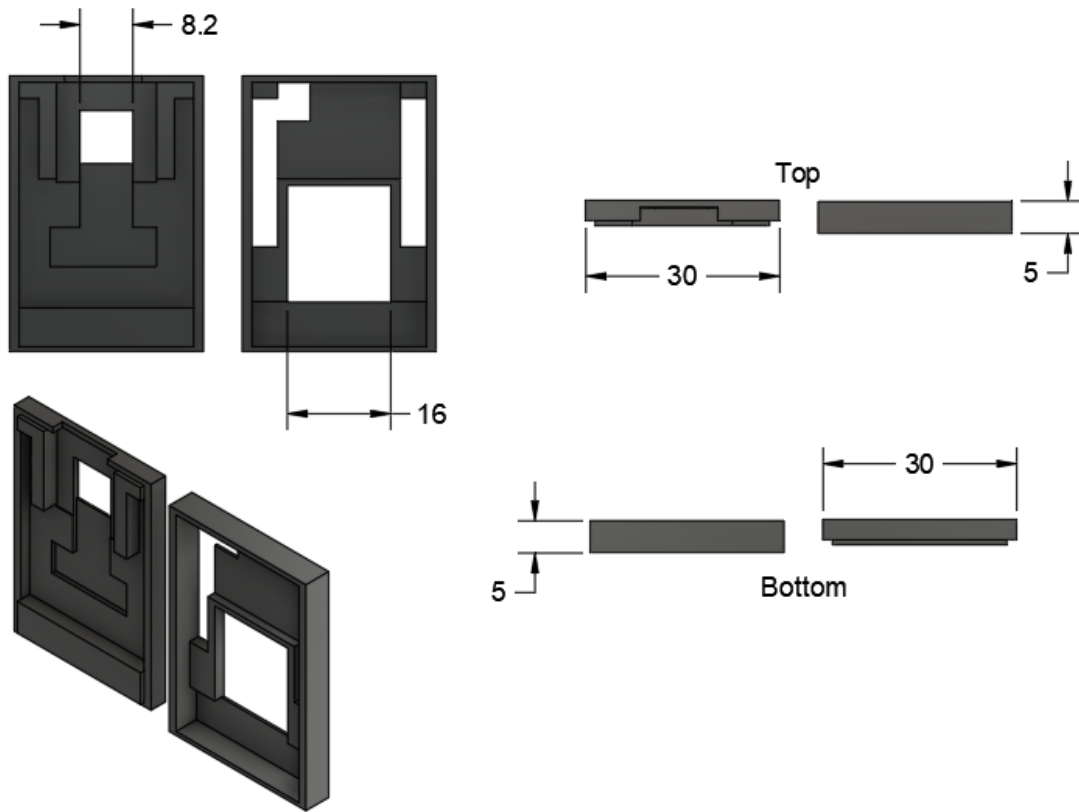


**Figure 29.** Semi-final variation of ESP32-CAM mount

Figure 30 shows a 3D rendering of the laser diode and a 3D printed mount that will be used to stabilize and dampen the laser. This is a critical aspect of the experiment because we expect perfect control over the angle of the light beam and do not account for any misalignments. This is a prototype design and was only used for an easier experience with handling and to gather tolerances on the dimensions.

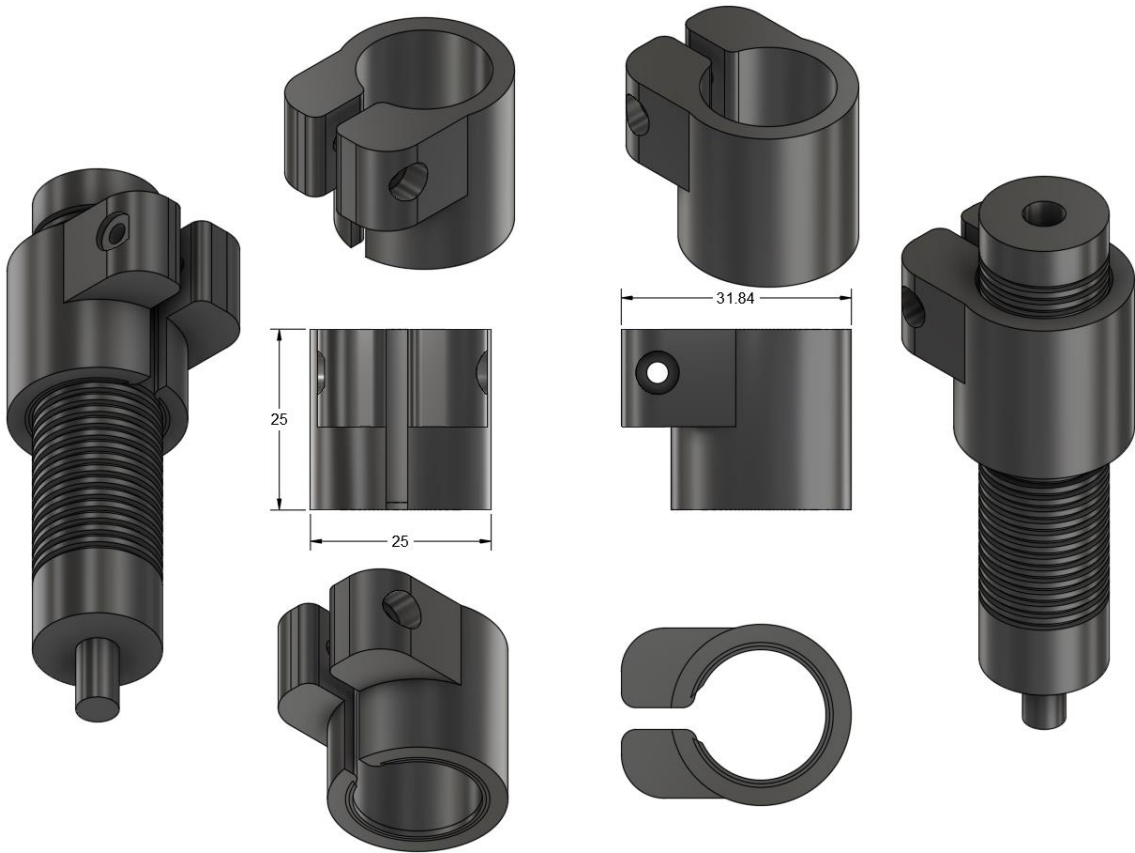


**Figure 30.** Prototype mount of laser diode

### 7.A.3 Laser Diode Testing

The laser diode plays a crucial role in our SPR sensor, providing the energy that will create the surface plasmon excitation needed for molecular binding to occur. As described in previous sections, specifications such as the central wavelength, output power, beam divergence, and polarization of our laser diode were all parameters that must be determined based on our particular needs. We concluded that a 532 nm wavelength laser diode module from the company LaserLands would best serve our purposes, both for its good beam quality and lower cost compared to other laser diodes of similar wavelength on the market. Once the laser diode was delivered, we began by testing its various properties in the CREOL Senior Design optical lab. Our first test was using an optical power meter to measure the output power the laser diode emitted when plugged in. The measured output power of the laser diode was 43.7 mW, a much higher value than the 10 mW that was expected based on the laser diode specifications from the manufacturer. Figure 31 below shows the optical power meter and the calculated output power of the laser.



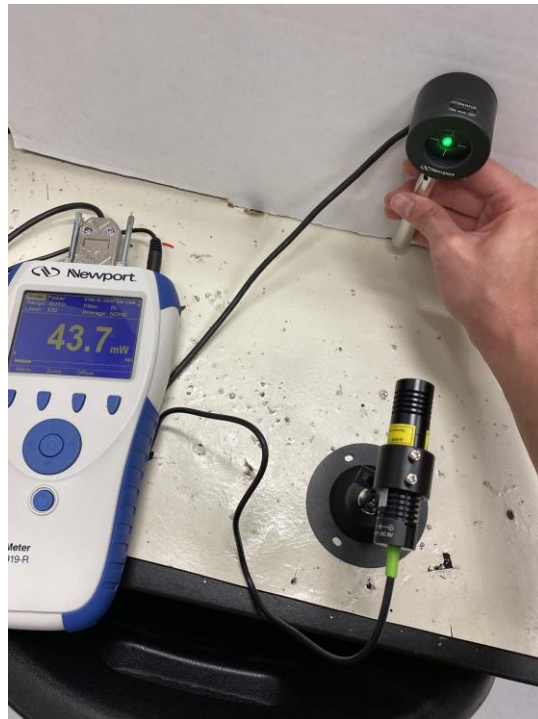


**Figure 31.** Output Power of Laser Diode from LaserLands

The laser diode from LaserLands included a mount which we assembled to use for our optical tests to ensure the laser was secured and the beam would not accidentally stray from the optical path and create a safety hazard. With the laser mounted in the assembled mount, we began to align the beam using two pinhole irises. We would close the iris of one pinhole while opening the other and adjust the position of the laser to direct the beam through the iris. This was done multiple times, opening and closing the two irises until the beam was traveling through both irises when both had a small aperture. Figure 32 below shows the laser diode after the alignment process, with the beam being directed through the bandpass filter, neutral density filter, and right-angle prism. It can also be seen that the phenomenon of total internal reflection was established by rotating the rotation stage to an angle of 46 degrees.

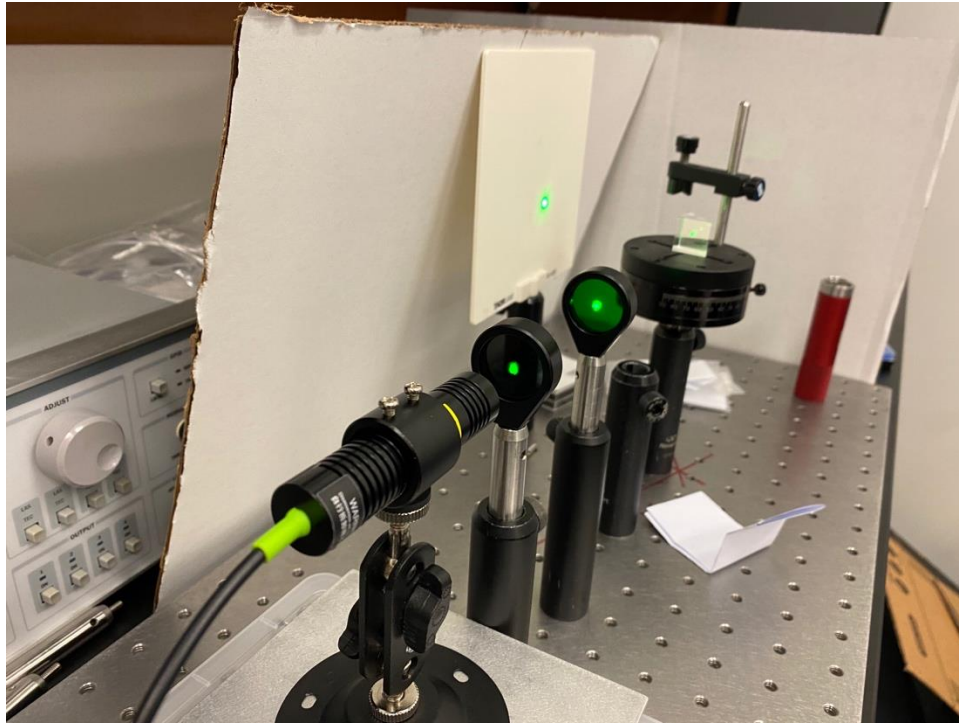


**Figure 32.** Initial Optical Setup with Laser Diode and Prism

However, during the alignment process of the laser diode, it was observed that the mount included with our laser diode made aligning the beam difficult. This was due to the mount not being able to be fixed onto the optical breadboard we were using for testing our optical equipment, making it difficult to fix the mount at an angle relative to the rest of our optical equipment that could be secured into the holes on the optical breadboard. Figure 33 illustrates the optical setup described and how the mount for the laser was not designed to be secured to the optical breadboard.

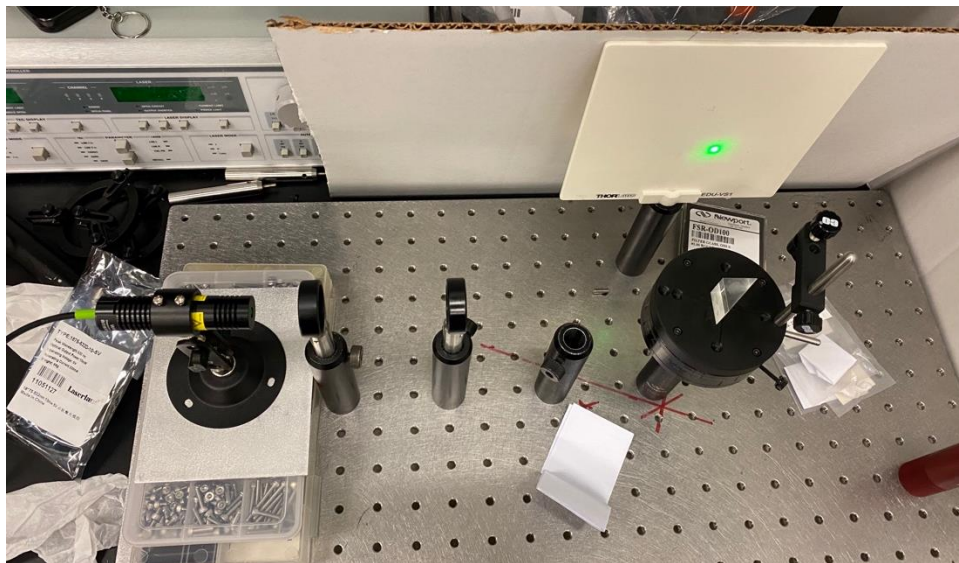


**Figure 33.** Laser Diode Test Experimental Setup.

This proved to become a complication for our testing purposes, as any movement to the laser or bumping of the workstation could misalign the laser. A decision was made for us to use another 532 nm laser diode module that is similar to the one we have purchased but can be properly secured to the optical breadboard. This decision was made for us to continue testing our optical setup and design the optical demo required for the end of the Senior Design I semester. Once the optical demo is complete, we will design a proper housing for the laser diode we have purchased to ensure it remains secured to avoid any misalignment.

The laser diode we chose that is similar to the one purchased is a 532 nm laser diode module from Edmund Optics. This laser was borrowed from the undergraduate lab in CREOL to use for the completion of our optical demo. The laser is capable of emitting an output power of 5 mW and a beam divergence of less than 1 milliradian.

Using the optical power meter as before, we measured the output power of the laser diode from Edmund Optics. The measured output power of the laser diode was 5.70 mW which was close to the 5 mW output power expected based on the laser diode specifications from the manufacturer. Figure 34 below shows the optical power meter and the calculated output power of the laser.



**Figure 34.** Output Power of Laser Diode from Edmund Optics

The next test for our laser diode was to determine the polarization of the emitted light. This is important to determine because for surface plasmon excitation, we will

need to manipulate the polarization of our incident wave to only allow p-polarized light to interact with the gold film. To determine the polarization of our light, we used a mounted linear polarizer and a power meter to measure the output power as we changed the axis of our polarizer to find the maximum and minimum output power and their specific rotation angles. To begin, we set the rotation angle of the mounted linear polarizer to 0 degrees and began slowly increasing the rotation angle in increments of 5 degrees, monitoring the measured output power from the optical power meter placed after the light exits the linear polarizer, until we found a maximum output power. Once the maximum output power was found, we recorded the measurement and the rotation angle of the linear polarizer. We then rotated the linear polarizer to 90 degrees from the angle where maximum power was found. This was done to find the minimum output power reading for the orthogonal polarization. The measurements were done five times and the results were averaged. The results can be seen below in Table 6.  $P_{max}$  represents the maximum power found for each rotation angle, while  $P_{min}$  represents the minimum power found. Ellipticity is the square root of the ratio of  $P_{min}$  divided by  $P_{max}$ .

Experiments Performed	$P_{max}$ (mW)	Polarizer Rotation Angle at $P_{max}$ (degrees)	$P_{min}$ (mW)	Polarizer Rotation Angle at $P_{min}$ (degrees)	Ellipticity
1	3.57	130	1.38	220	0.622
2	3.36	136	1.37	226	0.639
3	3.25	135.5	1.37	225.5	0.649
4	3.26	130	1.36	220	0.646
5	3.13	128	1.34	218	0.654
Average	3.31	131.9	1.36	221.9	0.642

**Table 6.** Experimentation to Determine Polarization of the Laser Diode.

From our results, we could see that the minimum output power never decreased below 1.34 mW. This informs us that our emitted light from the laser diode is elliptically polarized, due to the amplitudes of the maximum and minimum power being of different values but the minimum never reaching an output power of zero. If the light was linearly polarized, the minimum output power detected would be zero or close to zero. If our light was circularly polarized, the amplitudes of both minimum and maximum power measured would be the same. This information is very useful for later experiments to determine the rotation axis of our linear polarizer when we will want only p-polarized light entering our system.

#### 7.A.4 Simulating the Surface Plasmon Resonance Curve

When surface plasmon excitation occurs, a dip in the measured intensity of the reflected beam can be seen. This dip occurs at a certain angle known as the resonance angle or SPR angle. The angle where this dip occurs is related to the changes in the refractive index of the metal being used, as well as other parameters such as the wavelength of the incoming light, the illumination angle, the evaporation process used when depositing

the metal, and the refractive index of the prism, metal, and the various layers being tested. The software WinSpall used previously for simulating total internal reflection was now used for simulating surface plasmon resonance curves based on the Fresnel formalism. Using this software, we can calculate a resonance curve specific to our parameters and compare the theoretical results with our experimental results.

Before beginning our experiments, we created a simulation using the software WinSpall to mimic the expected resonance curve based on our specific parameters. In this simulation, the only layers that our light will travel through is the glass prism, the gold film, and air. The real and imaginary dielectric constants for the glass and air layers remain the same as the ones used for simulating total internal reflection. The gold layer will have a thickness of 50 nanometers due to the manufactured SPR chips we purchased having a gold film thickness of 50 nanometers. The real dielectric constant of the gold layer is  $-12.45$  while the imaginary dielectric constant is  $1.3$ . The real and imaginary dielectric constants are typical values for gold film but can vary slightly based on the evaporation process used by the manufacturers to deposit the gold film onto the chip. Figure 35 below shows the simulation parameters used for simulating the resonance curve with the gold SPR chip.

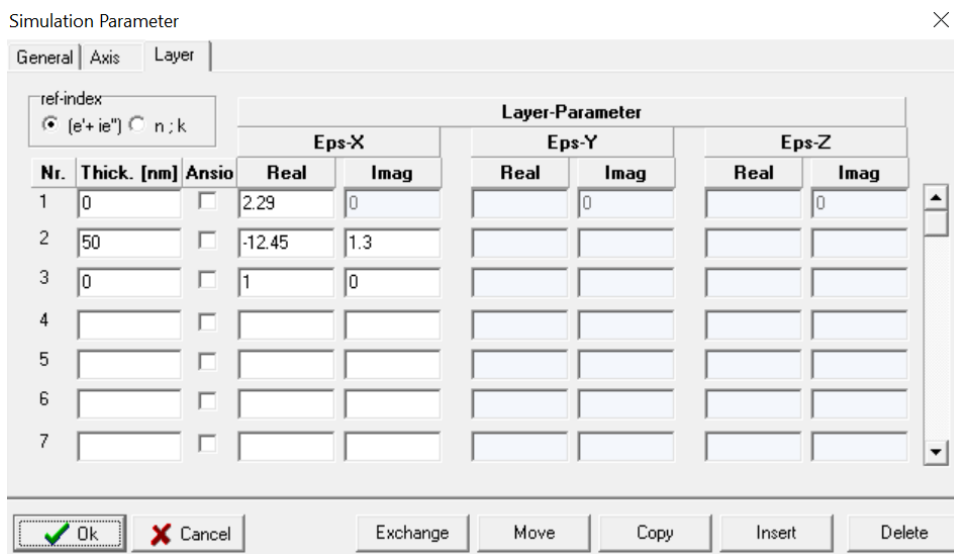


**Figure 35.** Simulation Parameters for the Resonance Curve of Gold Film using WinSpall.

Using the parameters specified, a simulation of the resonance curve for a gold film of 50 nanometers was created. Figure 36 below illustrates the resonance curve that was observed.

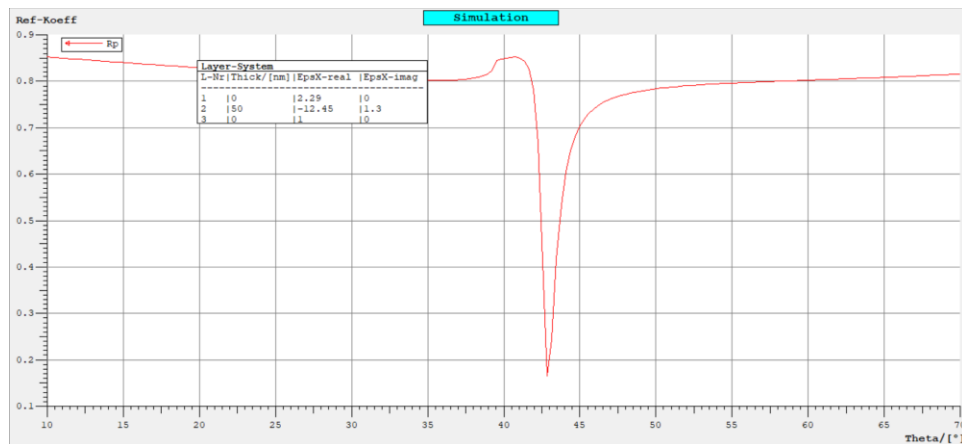


**Figure 36.** Simulation of Resonance Curve of Gold Film using WinSpall.

From the simulation, it can be seen that the increase in reflectivity where total internal reflection occurs at 39 degrees is much shallower compared to the previous simulation for total internal reflection using only a glass prism in air. This shallow increase is due to the reflective properties of the gold film itself. Another key observation from the simulation is that there is a sharp dip in the reflectivity at 42.84 degrees. This dip is due to majority of the laser beam's intensity is bound in the surface plasmons, stopping the light from being reflected. This simulation informs us that when using a laser diode with a wavelength of 532-nanometers directed at a right-angle prism, we should observe surface plasmon excitation at a resonance angle of 42.84 degrees. Knowing this theoretical resonance angle will better aid us in finding the resonance angle during experimentations and comparing our results with the simulated ones.

## 7.B Software Testing

Initial software testing was done with a simple Python script running on a desktop, this does not represent the application running on a smartphone, but it creates an easier environment to test out proper scheduling methods to reach our engineering requirement of 2 captures per second. The ESP32-CAM is capable of capturing images much faster than every 0.5 seconds, but this gives diminishing returns to the accuracy of our data and causes unnecessary stress on the system. While the 2 captures per second is an engineering requirement, it may prove to be more often than is needed to reach our accuracy requirement but due to the conceptual nature of our project, this is still in the testing phase.

There are multiple scheduling methods that can be used to reach our engineering requirement of 2 captures per second. Each method comes with its own drawbacks and can influence the power draw of the device. Most methods are reliant on the clock cycles of the microcontroller unit, so if we continue to keep a lowered clock rate then the capture rate could be negatively affected.

A table is shown below to show how the clock rate correlates with the capture rate. There will be no scheduling method used for this testing scenario but instead the C program will poll the CPU as fast as possible and produce an average processing time. This processing time also includes the upload through Wi-Fi which takes a very small and much more consistent amount of time to perform.

Clock Rate	Pixel Resolution	Captures per Second	Average Processing Time	Maximum / Minimum Processing Time
240 MHz	1600 x 1200	12.2	79 ms	209 ms/ 73 ms
240 MHz	800 x 600	25.6	40 ms	61 ms/ 38 ms
160 MHz	1600 x 1200	11.9	83 ms	162 ms / 74 ms
160 MHz	800 x 600	27.1	39 ms	98 ms / 42 ms
80 MHz	1600 x 1200	8.3	112 ms	185 ms / 67 ms
80 MHz	800 x 600	25.6	39 ms	72 ms / 34 ms

**Table 10.** ESP32-CAM Capture vs Clock Frequency

What the table above does not show is the variation in processing time and capture rates, they seem to get worse as the clock rate is lowered so it seems to be in our best interest to keep the clock rate at the fastest recommended frequency at the cost of a moderately significant power draw increase.

Unrelated to the consistent variation in processing time and capture rates is that the ESP32-CAM has been observed to experience massive capture rate drops, most likely an issue with the pseudostatic random-access memory or the frame buffer needing to be reset. What exactly causes these rate drops is unknown and seem to be correlated with higher capture rates as only the 800 x 600-pixel resolution tests experience the issue, albeit inconsistently. These capture rate frequency drops are important to consider when designing the software to call on these captures and must be prepared to accommodate for the improper timing. Not only does the capture rate drop but it can also have rare moments where it's much faster than intended, this is something that might only exist when the processor is being consistently polled so the software should not have this issue.

## 7.C Prototype Construction

The following section will be dedicated towards the prototype presentation for the UCF CREOL college of optics and photonics that occurs towards the end of the first semester of the senior design capstone sequence. The initial prototype will be an optical set up using a laser, two pinholes, the linear polarizer, a rotation stage that has the prism and a thin gold film glued to one of the faces of the prism, and a screen. The reasoning behind a minimal set up is that most of the optical components are not necessary to display surface plasmon excitation and the resonance of these surface

plasmons. To achieve surface plasmon resonance, a technique called total internal reflection must be utilized. When total internal reflection is achieved, a side effect called evanescent waves are created along the surface where the incident light impacts and reflects away. As the incident light reflects, a small amount of light penetrates the second medium at the surface, thus creating a ripple like wave along the boundary of the two mediums. The two mediums being the prism, and the gold film. Surface plasmons can be observed on the screen at an angle greater than the angle of total internal reflection. This optical design will also use the Brewster's Angle to transmit p-polarized light through a linear polarizer while s-polarized light is reflected off the linear polarizer surface and separated from the transmitted light.

The initial testing was done using a 632 nanometer Helium Neon (HeNe) laser. The purpose of using this laser is that it is easier to align as there are places to adjust the X and the Y axis of the laser diode, and that the dip in intensity is wider than a 532-nanometer diode as can be seen in Figure 38 and 39 below. This wider dip in intensity relates to surface plasmon excitation occurring at a particular angle, but unlike the simulated resonance angle for a 532 nm wavelength laser, the 632.8 nm wavelength laser would have excitation occurring for a slightly longer duration. Therefore, it would be easier for us to find where the resonance angle is during our experiments using the HeNe laser at first. It is also important to note that red light is easier to observe than green light, making this diode more visually appealing when attempting to confirm surface plasmon excitation for the first time. A simulation was ran using the software WinSpall using the wavelength of the helium neon laser diode to describe the dip in intensity where surface plasmon excitation occurs and following images will display the light before and after exceeding the critical angle of the prism where power loss occurs. It is uncertain whether surface plasmon excitation occurred or not due to the lack of clarity in the transmission of light. The following power loss could be glue induced or a result of internal scattering within the prism against the glue. This will be investigated further during the second half of the senior design capstone course.

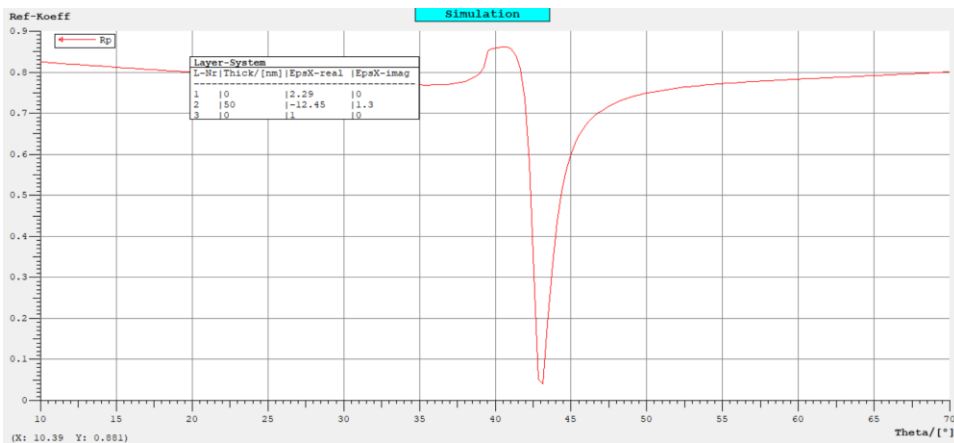


**Figure 37.** Simulation of Resonance Curve of Gold Film with 632.8 nm Wavelength using WinSpall.



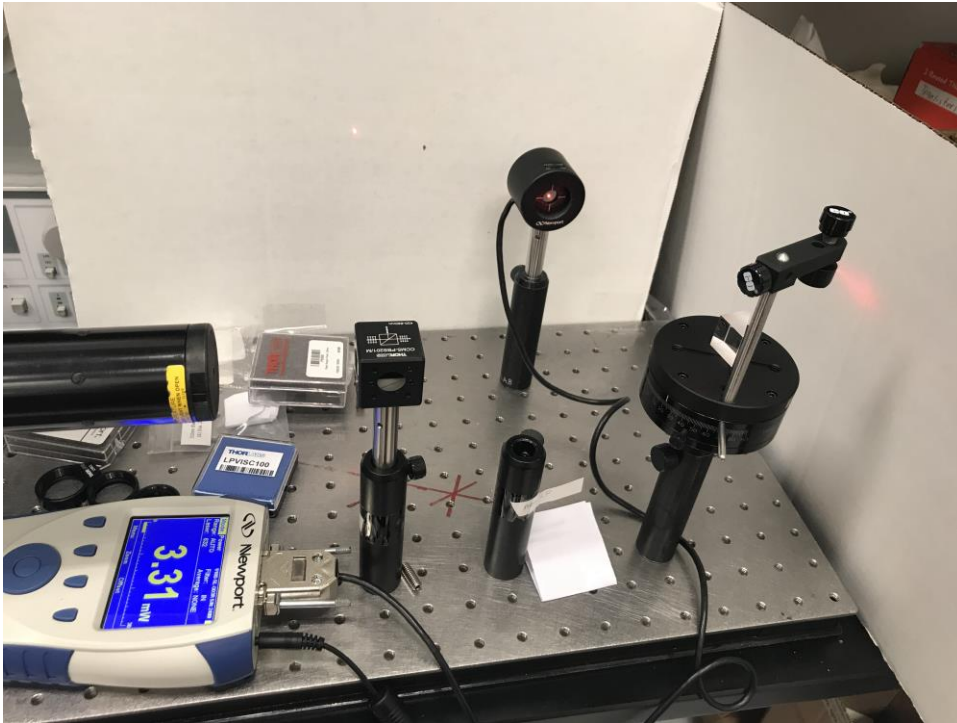


**Figure 38.** Experimental set up that displays an angle smaller than the critical angle.



**Figure 39.** Experimental set up that displays an angle beyond the total internal reflection angle that results in power loss.

Figure 38 displays the prism set at an angle smaller than the calculated value of the critical angle. When we increased the angle of our prism, total internal reflection was seen and a drop in the output power was observed which can be seen in Figure 39. There is a 55% loss in power at this angle. It is hard to note what the angle of the laser is hitting the prism because the prism had to be moved around to make sure there is contact between the light source and the gold film, but the prism did not move from this exact spot between photos.

The prototype demo will utilize a 5-milliwatt laser with similar specifications as the diode from Edmund Optics listed above in section 3.2.B. The reason this laser is chosen for the demonstration is because it was borrowed from the CREOL undergraduate learning laboratory and was readily available for use as well as having an attached mount and holder, allowing ease of alignment along the optical surface. The laser purchased for the device has a smaller diameter and is unmounted so with consideration of the time constraints upon the team members, this prevented the creation or purchase of an adequately sized laser diode mount. To begin the prototype, the laser was aligned using the two pinholes to locate the beam in the near field and far field of the optical system to ensure that the beam travel path will lead directly into the area of the prism necessary for total internal reflection. The laser diode has limited movement in the x-z plane because the mount is attached to the diode, so the direction of the beam can only be manipulated through changes in the angle of the diode with respect to the optical axis. The prism is placed upon a rotation stage to allow angular changes so the beam can transmit through the prism at different angles to find the appropriate angle for total internal reflection. Figure 40 is a photograph taken of the bare optical system with the laser turned on to show the occurrence of total internal reflection.



**Figure 40.** Initial Prototype Optical Setup.

Next, the optical filters were placed into the system to confirm that the optical components are operating properly within the environmental conditions. The pinhole irises were removed from the optical setup as the beam was now properly aligned and their use was no longer necessary. The linear polarizer was placed directly after the laser diode to provide the p-polarized light to the system. After the linear polarizer, the beam is directed onto the right-angle prism on the rotation stage. For the first part of our experiment, the SPR chip is not placed on the prism so that we can establish the correct angle where total internal reflection occurs before excitation. The prism was placed onto the rotation stage so that the beam of our laser diode is incident at 0 degrees to the side of the prism. Moving our rotation stage until only reflected light was emitted from the prism and no light was transmitted, we measured our rotation angle where total internal reflection occurs at 42 degrees. This matches where total internal reflection should occur in our prism based on the calculated critical angle. As mentioned prior, for angles of our incident light greater than our critical angle, the glass boundary of our prism will act as a mirror and the incident light is totally reflected. This matches the measured angle where total internal reflection was found, as 42 degrees is a greater angle than 41.81 degrees.

Once total internal reflection was established without the SPR chip, it was time to add the SPR chip to the prism to determine the resonance angle for surface plasmon excitation to occur. To attach the SPR chip to the prism, clear silicone glue was used. This was chosen based on the SPR chip manufacturers recommendations for use with biological samples and because silicone glue can be removed safely from glass

surfaces. Figure 41 illustrates the process of attaching the SPR chip to the right-angle prism.



**Figure 41.** Attaching the SPR chip to the Right-Angle Prism.

The glue was allowed to set for one hour to ensure the chip remained fixed to the glass surface. After the glue was set, we placed the prism back onto the rotation stage and aligned it so the beam is incident at 0 degrees to the prism side. We moved our rotation stage until we observed total internal reflection occurring. Total internal reflection began to occur when the prism was at an angle of 46 degrees. Unfortunately, the intensity of the emitted beam on our screen did not seem to decrease when observing with the naked eye. Therefore, we could not be certain if surface plasmon excitation was occurring when the incoming light interacts with the anti-phase light back-scattering from the gold metal film.

To determine if the intensity was decreasing at any point, an optical power meter replaced the location of the screen to allow us to monitor the changes in optical power measured after the incident light interacts with the gold surface. However, we realized that the SPR chip needed to be removed from the right-angle prism in order for us to measure the difference in output power when the chip was on or off the prism to properly determine when surface plasmon excitation is occurring. A 40 mm right-angle prism from the undergraduate lab was borrowed to replace our prism that had one of the SPR chips attached to its surface with glue. This 40 mm prism would be used instead for the remainder of our optical demo experiments.

To begin our experiments in determining why we were not experiencing surface plasmon excitation, we removed our 20 mm right-angle prism that has the SPR chip and placed the 40 mm right-angle prism onto the rotation stage. The prism was aligned so the laser beam is incident at 0 degrees relative to the prism side. Our issues could be with multiple components in our design: the polarization axis of our linear polarizer or the SPR chip purchased. Various experiments would be done to determine which of these is causing our transmitted light not to create surface plasmon excitation.

### 7.C.1 Determining the Polarization of our Incident Light

One possible reason for our incident light not to be destructively interfering with the back-scattered light from the gold metal film is the polarization of the incident light is not polarized correctly. For the light to interfere with the evanescent wave created beyond the boundary of the prism, the light must be p-polarized meaning that the light must have an electric field polarized parallel to the plane of incidence. Reflective linear polarizers, such as the one we used for this experiment, will transmit the desired polarization while reflecting the others. The linear polarizer used in our experiments is mounted with a rotation axis which allows us to easily see which angle the polarizer is rotated to. The mounted linear polarizer used can be seen in Figure 42.

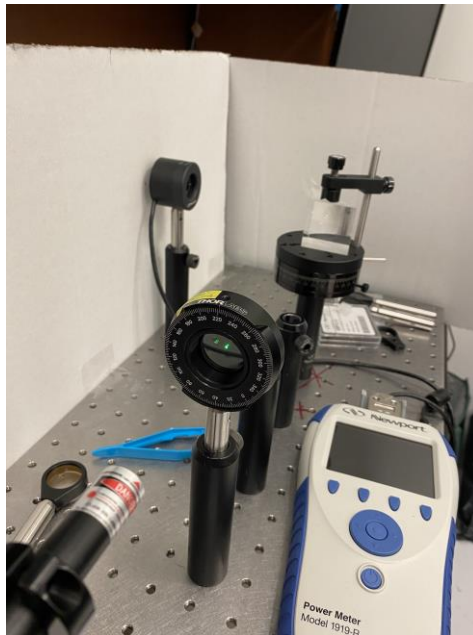


**Figure 42.** Mounted Linear Polarizer for Optical Demonstration.

To determine which angle is appropriate for us to only allow p-polarized light into our system, we began by testing the measured output power of the beam after passing through the right-angle prism without the SPR chip attached while changing the rotation angle of the linear polarizer and then once again measuring the output power of the beam at the same angles with the SPR chip attached. This would provide us with a

reference measurement of output power with and without the SPR chip included in the optical setup.

The first experiment was with the right-angle prism without the SPR chip included. The prism's rotation stage was moved until total internal reflection was established, which was at an angle of 42 degrees. We then set the rotation angle of the mounted linear polarizer to 0 degrees and began slowly increasing the rotation angle in increments of 5 degrees, monitoring the measured output power from the optical power meter placed where the reflected light from the prism was emitted, until we found a maximum output power. Once the maximum output power was found, we recorded the measurement and the rotation angle of the linear polarizer. We then rotated the linear polarizer to 90 degrees from the angle where maximum power was found. This was done to find the minimum output power reading for the orthogonal polarization. The measurements were done five times and the results were averaged. It was determined that at a rotation angle of 133.2 degrees, the maximum output power of our laser was 2.99 mW. The minimum output power of our laser was 1.23 mW at a rotation angle of 223.2 degrees.

The next experiment to perform was to attach the SPR chip to the prism and measure the output power at the rotation angles found in the previous experiment to compare any changes to the power readings. For these experiments, we used clear packing tape to attach the SPR chip to the prism in a way that allows us to easily remove the chip and not have any excess glue on the prism itself. The tape was placed at the top corner of the SPR chip to avoid the tape from interfering with the location of the chip where the beam would interact. An image of our SPR chip attached to our prism with the tape can be seen in Figure 43 below.

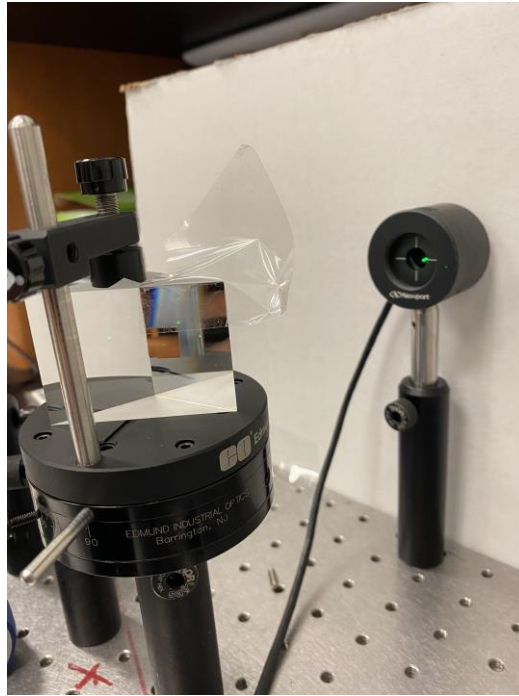


**Figure 43.** SPR Chip Attached to 40 mm Right-Angle Prism

Once the SPR chip was attached, we rotated the rotation stage of our prism until total internal reflection was observed, which was measured to be at a rotation angle of 42 degrees. We then changed the rotation axis of our linear polarizer to the previously found angles and recorded the output power at the various minimum and maximum output locations. The measurements from each experiment mentioned to determine the polarization axis for our experiment can be seen below in Tables 7 and 8.  $P_{\max}$  represents the maximum power found for each rotation angle, while  $P_{\min}$  represents the minimum power found.

Experiments Performed	$P_{\max}$ (mW)	Polarizer Rotation Angle at $P_{\max}$ (degrees)	$P_{\min}$ (mW)	Polarizer Rotation Angle at $P_{\min}$ (degrees)
1	3.12	134	1.22	224
2	2.98	136	1.24	226
3	3.01	134	1.25	224
4	2.96	130	1.22	220
5	2.87	132	1.23	222
Average	2.99	133.2	1.23	223.2

**Table 7.** Experimentation for Determining Polarization Axis for SPR Effect: Right-Angle Prism without SPR Chip Attached.

Experiments Performed	$P_{\max}$ (mW)	Polarizer Rotation Angle at $P_{\max}$ (degrees)	$P_{\min}$ (mW)	Polarizer Rotation Angle at $P_{\min}$ (degrees)
1	2.98	134	1.24	224
2	2.35	136	1.26	226
3	2.76	134	1.24	224
4	2.81	130	1.21	220
5	2.82	132	1.23	222
Average	2.74	133.2	1.24	223.2

**Table 8.** Experimentation for Determining Polarization Axis for SPR Effect: Right-Angle Prism with SPR Chip Attached.

From our experiments, there was no moment during the changes in rotation of the linear polarizer that we noticed a significant drop in output power intensity. Nevertheless, this experiment did provide us with the rotation angles where the maximum and minimum power transmitted through the linear polarizer occur. In a linear polarizer, the maximum transmission of incident light occurs when the axis of the polarizer is parallel to the plane of polarization while the transmission is minimum when the axis of the polarizer is perpendicular to the plane of polarization. From our previous test, we know that the laser diode is elliptically polarized. We can then conclude that at a rotation angle of around 133.2 degrees the incident light from our laser diode will be parallel to the axis of the polarizer.

Determining when our incident light is p-polarized using only a mounted linear polarizer became time-consuming and other avenues to ensure we have only p-polarized light in our system were investigated. This led to the discovery of the polarizing beam splitter. A polarizing beam splitter is a device that uses the idea of the Brewster's Angle to create a phenomenon where only the p-polarized light directed at a medium is transmitted through while the s-polarized light is reflected. To do this, two right angle prisms are cemented together to create a cube shape. The cube is coated with a dielectric coating along the diagonal interface between the two right angle prisms which will reflect s-polarized light and transmit p-polarized light. The extinction ratio of the polarizing beam splitter is 1000:1 in favor of p-polarized light, ensuring that the emitted beam has the highest polarization purity possible. This device is perfect for our surface plasmon resonance sensor because it will ensure that the optical components of our experiment are correct since only p-polarized light will be emitted from the beam splitter. This will aid us in eliminating the possible issues that are causing us not to have surface plasmon excitation occur. Figure 44 is an image of the polarizing beam splitter used in our experiment, where a diagram etched onto the device can be seen that shows the s-polarized light will be reflected to the left relative to the plane of incidence while the p-polarized light will be transmitted through.



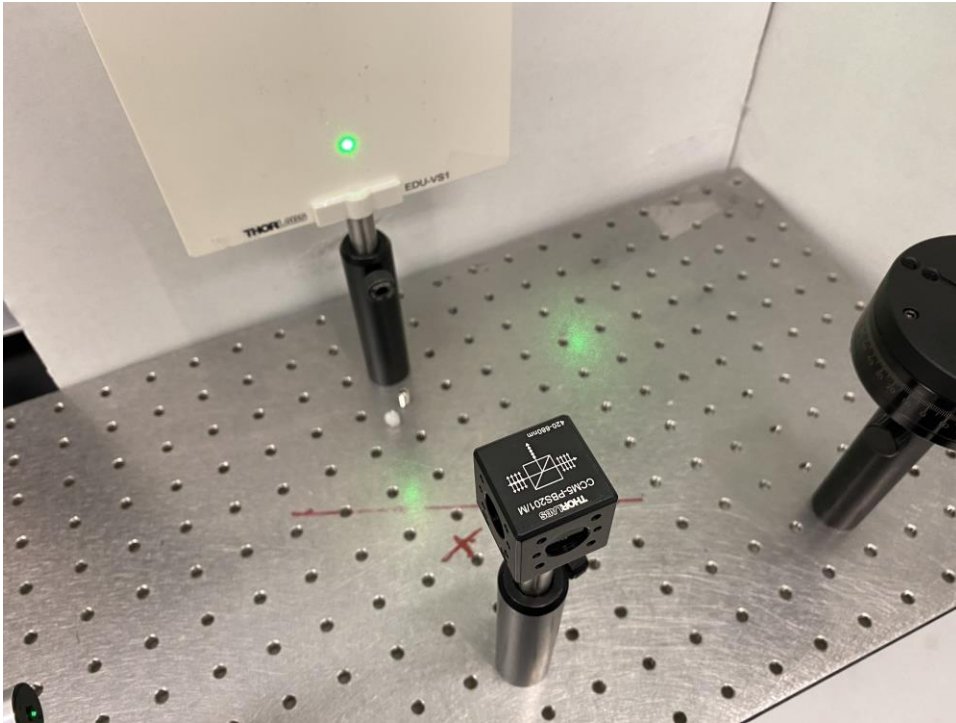


**Figure 44.** Polarizing Beam Splitter for Transmitting P-polarized Light.

The polarizing beams splitter was placed between the laser diode module and the rotation stage where our prism was placed. A white screen was placed to the left of the polarizing beam splitter to block the s-polarized light reflected from the dielectric coating inside the beam splitter itself. Before beginning our experiments to determine if surface plasmon excitation is now occurring when the p-polarized light from the beam splitter is directed onto the prism, we first measured the output power of the laser diode before and after the light enters the beam splitter. Using our optical power meter, the output power measured before the light enters the polarizing beam splitter was 6.10 mW. Figure 45 below shows the output power measured on the optical power meter.

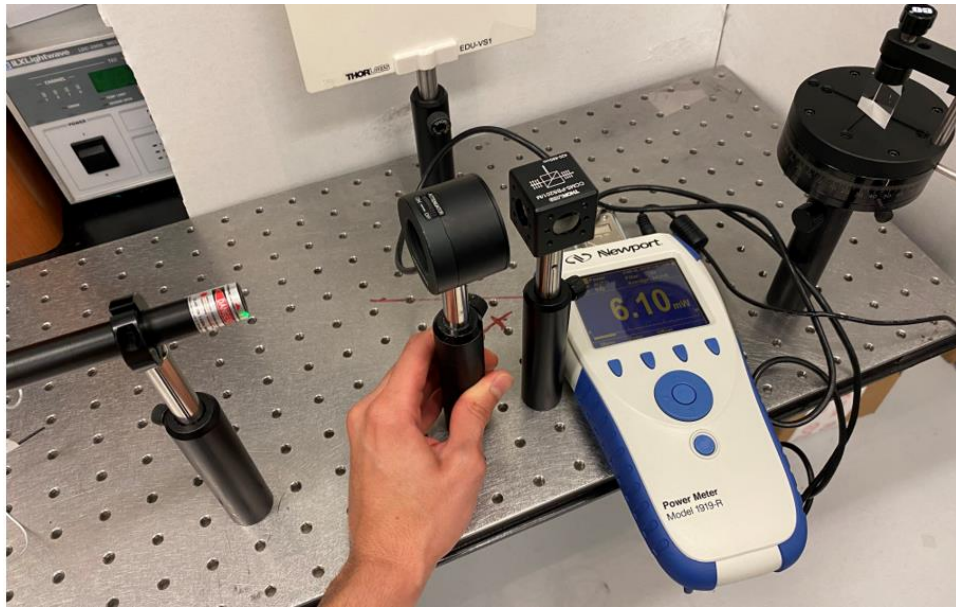


**Figure 45.** Measured Output Power before Polarizing Beam Splitter.

We then measured the output power of our beam after only p-polarized light is allowed to transmit through. Once again using the optical power meter, the output power of our p-polarized light was found to be 4.18 mW. Figure 46 below shows the output power measured on the optical power meter.

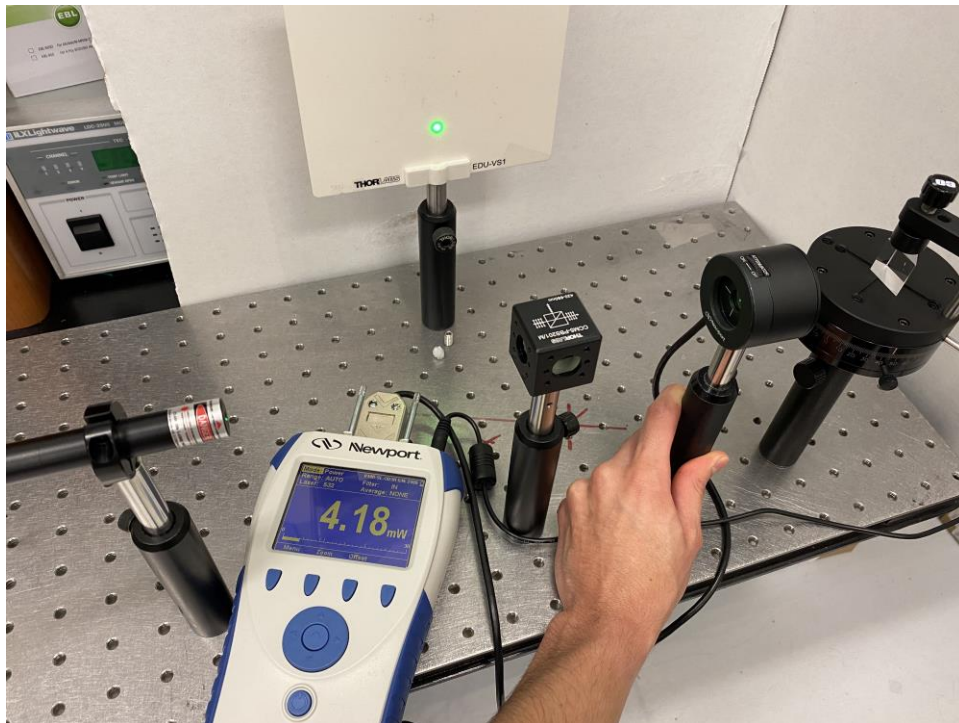


**Figure 46.** Measured Output Power of P-Polarized Light.

We also measured the output power of the s-polarized light to determine how much of our light was being lost due to the s-polarization of our incident light being reflected. Using our optical power meter, the output power of our s-polarized light was found to be 1.524 mW. Figure 47 below shows the output power measured on the optical power meter.



**Figure 47.** Measured Output Power of S-Polarized Light.

From the measured output power, it can be seen that our p-polarized light is about 1.5 mW less than our emitted light from the laser diode module. This also shows that our elliptically polarized light from the laser diode contained a majority of p-polarized light. It should also be noted that this decrease in output power is still sufficient enough power to create surface plasmon excitation.

Our next experiment was to measure the output power of our beam after interacting with the SPR chip attached to the prism at different angles of rotation to determine if surface plasmon excitation is occurring. The right-angle prism was once again placed so the laser beam is incident at 0 degrees relative to the prism side. We then rotated the rotation stage until total internal reflection was observed, which was found at the rotation angle of 42 degrees. The optical power meter was then placed to capture the emitted light that is reflected off the prism's surface in order to measure the output power as we slowly rotated the prism by 0.5 degrees until total internal reflection was no longer observed. The measured output power for each rotation angle can be seen below in Table 9.

Angle of Rotation Stage, degrees	Output Power (p-polarized light), mW
42	4.18
42.5	4.16
43	4.20
43.5	4.23
44	4.21
44.5	4.21
45	4.22
45.5	4.20
46	4.15
46.5	4.13
47	4.15
47.5	4.12
48	4.13
48.5	4.11
49	4.12
49.5	4.15
50	4.10

**Table 9.** Experimentation to Measure Output Power with Polarizing Beam Splitter.

From our experiment, no significant drop in output power was measured when rotating our right-angle prism. Therefore, as we have now ensured that our beam is polarized correctly and that the angle is allowing for total internal reflection to occur, the reason surface plasmon excitation has not happened must lie with the SPR chip itself.

### 7.C.2 Investigating the Properties of our SPR Chip

For surface plasmon excitation to occur, one must consider certain parameters. The SPR chip must be within a nanometer of contact with the prism used. This includes the glue or epoxy used to mount the chip on to the prism. A proposed solution to this crucial parameter is using index matching gel to mount the SPR chip on to the prism. The index matching gel will have the same index as the BK7, also known as crown glass. This will prevent any light deviation from occurring as the beam will interpret the gel as part of the prism. The prevention of deviation is important to this device because the light must hit the surface connecting the prism and the SPR chip at a specific angle, and any refractive index change along the optical path will result in either a greater or lesser change in angle. Using any sort of glue, such as Elmers or a higher-grade silicon glue will result in a randomized angle of incidence on the SPR chip. This was displayed during the prototype demonstration for the College of Optics and Photonics, as surface plasmons could not be displayed on the provided screen due a lack of contact between the chip and prism as well as the silicon glue's index of refraction being unknown. The refractive index could be tested however the testing and calculation of the refractive index is strenuous and time consuming compared to the alternative of purchasing index

matching gel, which will be demonstrated during the second half of this capstone course.

Another important property that is necessary for surface plasmon excitation to occur is chip dimensions. During the testing phase to investigate the occurrence of surface plasmon excitation, it was noticed that as the angle of incidence grew as the rotation stage was turned the incident light would exceed the size of the gold chip. This resulted in constant adjustments of our prism to maintain contact between the beam and the chip. The prism dimensions are 20x20x20 mm and the chip dimensions are 10x10x0.3 mm. The chip was glued directly to the center of the hypotenuse of the prism, limiting the amount of angular change in the system. Any time the stage was rotated far enough that the light no longer contacted the chip, the prism had to be moved to retain contact. Any slight change in the prism's orientation affects the generation of surface plasmons as the angle of incidence gets changed during the movement. The chosen solution to surpass this is to purchase another set of gold chips that similarly sized to our prism to maintain contact throughout the angular changes.

Our plans for the Fall semester will be to use the index matching gel purchased from Thorlabs to attach the 20x20x20 mm bare gold SPR chip to the base of our prism. This should ensure that our chip and prism are in close contact to allow surface plasmon excitation to occur. Once we are able to excite the surface plasmons using the index matching gel as an adhesive, we can investigate other methods besides using an adhesive to press the chip firmly against the prism during experimentations. One method we will investigate is by 3D printing a flow cell where our analyte solution will go which will have a spring mechanism on it to mechanically press the SPR chip against the prism during the entire experiment. This way the user does not need to use any adhesive to create the close contact needed for surface plasmon excitation to occur. Once the angle is found, it will be translated into the device by mounting mirrors on to a fixed platform that allows the light to reflect into the mirror at said angle. With these fixes in place, the design should operate as intended for data collection.

## **7.D Reassessment of Research Post Prototype Construction**

The initial research towards the construction of the prototype was appropriate but the initial optical effect must occur before adding in components for clarity. It is important to be able to capture surface plasmon excitation before specifying and altering the characteristics of the beam. Unfortunately, our prototype did not sufficiently display what was promised. The benefit to this, however, is the discovery of different solutions to resolve multiple problems that were occurring. The biggest problem that occurred was due to the characteristics of the gold film discovered through the prototype phase, surface plasmon resonance was not confidently detected. This problem can be resolved through having a flow cell or index matching gel to reduce the distance between the

chip and the prism. The light source may have to change from a 532-nanometer diode to a 632-nanometer diode as the helium neon laser diode was easier to observe and operate with, and the simulation graphs insinuate that the surface plasmon excitation time is longer with red light than green, making the imaging process slightly easier and less time restraining.

Due to the conceptual nature of our surface plasmon resonance device, we are not fully aware of what will be seen by the CMOS imaging sensor, but we do know that the change in intensity is the most significant information to be recorded. With this, we do have an idea of what to look for but not how often we have to look; or in this case, capture the images. The best thing to do is plan for the most extreme scenarios to avoid any under planning and modify the components or features as necessary to properly reach our engineer and marketing requirements of power draw and accuracy. Although the hardware should never need to be modified, the software will have to adapt with our needs before we can call this a consumer device.

## **8. Block Diagrams**

Our final design will consist of optical components, computer hardware components, and software components to ensure we have a fully functional SPR sensor. To accurately represent each piece in our design, three block diagrams were created to illustrate the various components and how they all work cohesively together. Figure 48 shows the optical design for our SPR sensor and how the final output from our CMOS sensor will connect to the computer hard components that will deliver the captured images to the software application. Each block is color coded to illustrate how the responsibilities of each device have been divided among the group members. A separate section in the bottom left illustrates other components such as the power supply and 3D printed case which will be a part of our final product but are not directly linked to any one component in the block diagram. Figure 49 explains in more detail the software application we will design and its various functions available to the user when operating the SPR sensor. This provides one with a simple illustration detailing how our software application will ask the user for information and how it will be delivered.

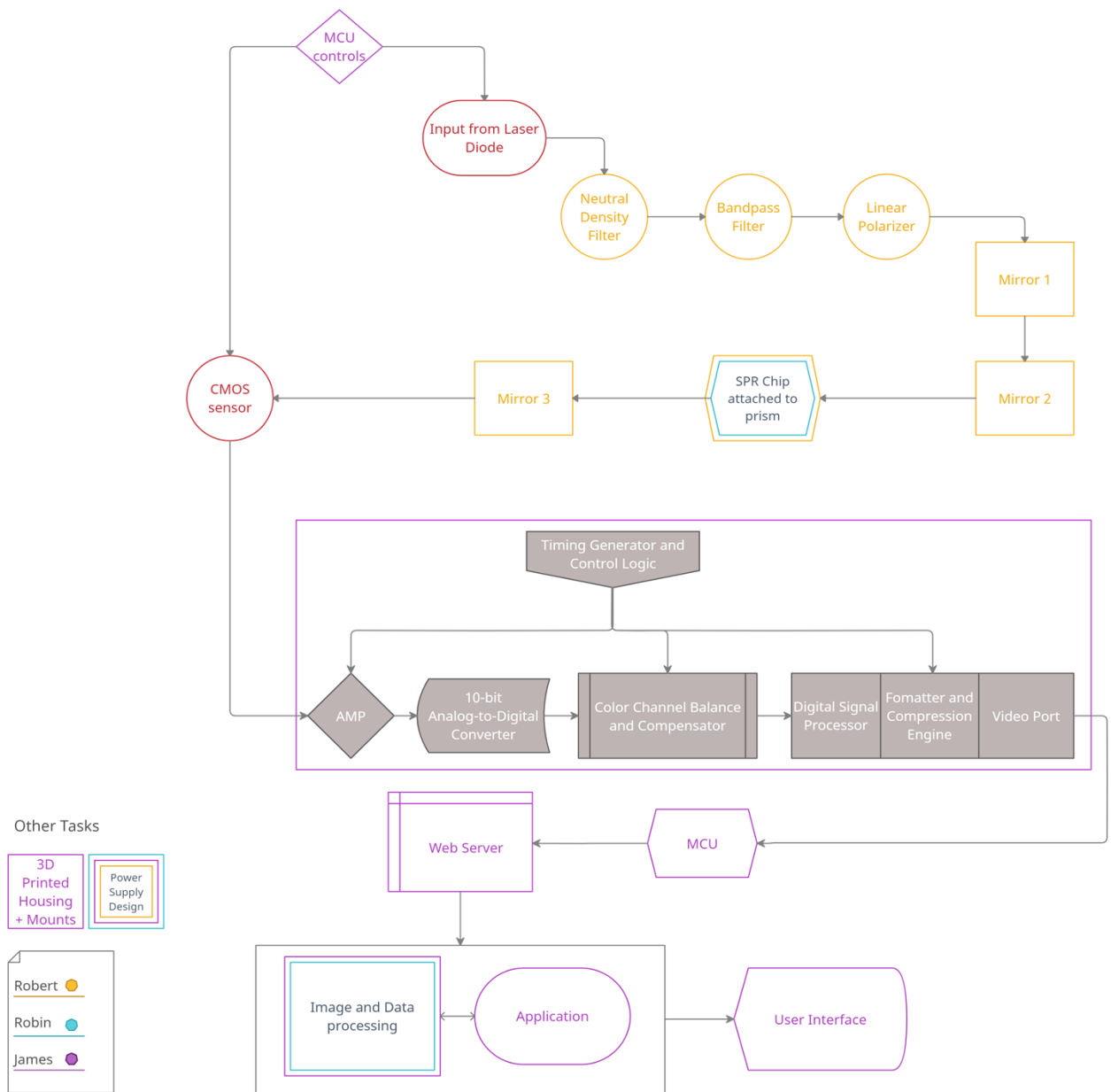


**Figure 48.** Block Diagram of Optics (top) and Computer (bottom) Hardware Interactions

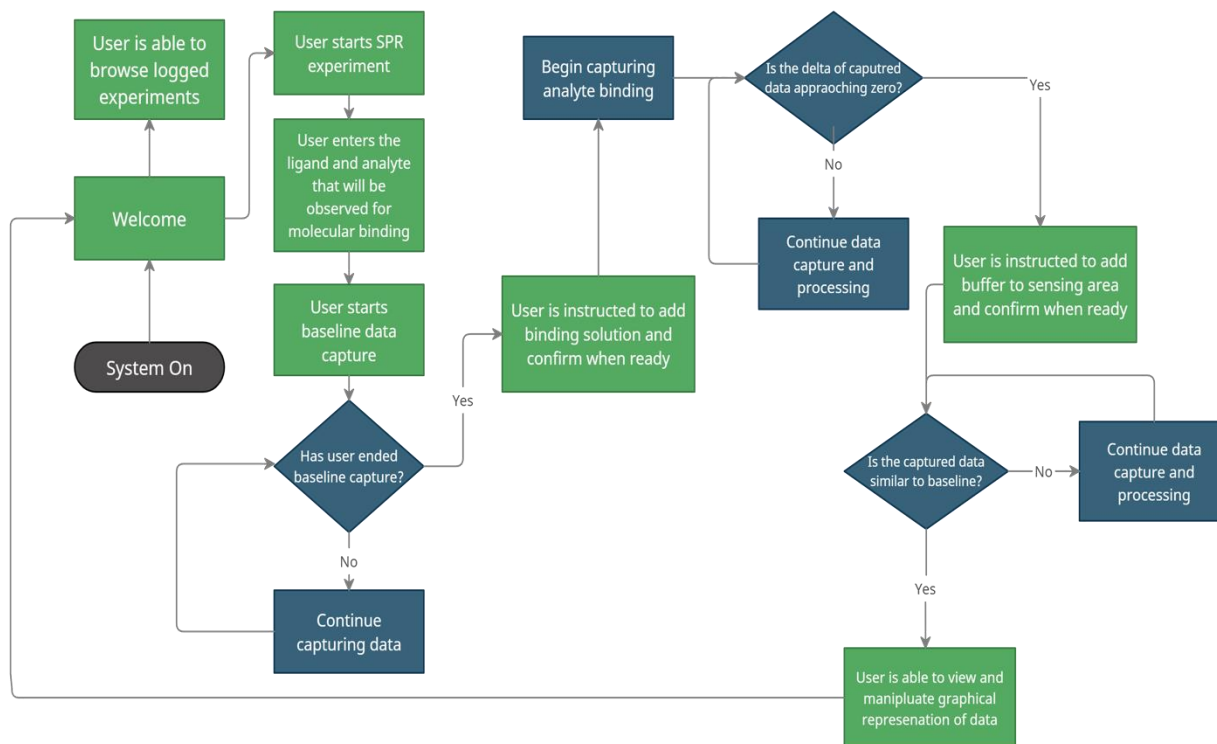


Figure 49. Use Diagram of Application

## 9. Bill of Materials

This section will provide a table of the various optical, electrical, computer, and biological components used for the completion of our SPR sensor. Table 5 provides information on each component, where it was purchased, how much each component cost, and the total cost of the project. This provides one with a clear representation of the cost of our entire project and how affordable it may be for future replication.

Item	Quantity	Price \$	Seller	Purchased	Est. Arrival
Right-angle Prism	1	97.00	Newport <a href="#">Link</a>	Y	Arrived
Bandpass Filter	1	9.41	eBay <a href="#">Link</a>	Y	Arrived
Polarizing Beam Splitter	1	282.44	Thorlabs <a href="#">Link</a>	Y	Arrived
Plano Mirror(s)	4	39.00	eBay <a href="#">Link</a>	Y	Must reorder. Complications
Laser Diode	1	23.50	Laser Land <a href="#">Link</a>	Y	Arrived



Absorptive Neutral Density Filter	1	38.00	Newport <a href="#">Link</a>	Y	Arrived
25.4 mm Fixed Filter Mount(s)	3	47.07	Thorlab <a href="#">Link</a>	Y	Arrived
0.5" Mirror Mount(s)	3	99.00	Newport <a href="#">Link</a>	Y	Arrived
MC and CMOS Camera	1	18.00	Amazon <a href="#">Link</a>	Y	Arrived
9V Battery Cable Clips	1	3.99	Amazon <a href="#">Link</a>	Y	Arrived
USB to UART Serial Adaptor	1	10.99	Amazon <a href="#">Link</a>	Y	Arrived
SPR Sensor Chip	3	255	Sofchip <a href="#">Link</a>	Y	Arrived
LM2596 – 5 / NOPD	1	5.21	TI <a href="#">Link</a>	Y	Arrived
LM2596 – ADJ / NOPD	1	3.66	TI <a href="#">Link</a>	Y	Arrived
10V / 1A AC Wall Adaptor	1	8.99	Skycraft (Local)	Y	Arrived
7.4V 1600mAh 25C Li-Polymer Rechargeable Battery	1	26.99	Amazon <a href="#">Link</a>	Y	Arrived
T Plug Connectors	1	7.99	Amazon <a href="#">Link</a>	Y	Arrived
Total Cost		<b>910.44</b>			

Table 11. Project Financing Table

## 10. Project Milestones

In this section, the project milestones for our project are shown in Table 6 below. Each week, from the initialization of our project design to the final presentation of our prototype, is represented below alongside the week each task should be completed. This table serves as a clear guide to ensure we remain on track to complete our final prototype by the end of the Fall 2021 semester.

Week	Description
<b>1-12</b>	<b>Senior Design I</b>
1	Project Conception
2 - 3	Research and Role Discussion
4 - 5	Initial Project Documentation Draft

5 - 6	More Research
7 - 8	Initial Project Documentation Final
9 - 10	Order Parts
11 - 12	Build and Present Project Demo
	End Of Summer Session
<b>13-27</b>	<b>Senior Design II</b>
13 - 14	Build Prototype
15 - 16	Testing and Redesign
17 - 18	Finalizing Design
19 - 20	Fine Tuning
20 - 21	Peer Presentation
22 - 26	Finish Report
27	Presentation

**Table 12.** Project Milestones Table

Over the course of the first senior design course the project milestone timeline changed from our initial plan. Our parts were ordered early because of purchasing through third party vendors and arrived anywhere between week 5 and 8. This time range results from inconsistencies in purchases and incorrect shipping information. The mirrors for our device were never retrieved as the United State Postal Service sent the package with the mirrors back to China within 24 hours of delivery because the address was incorrect and did not contact the group member who purchased the mirrors before doing so, resulting in the mirrors being reordered. The project demo was designed around week 8 and was continuously tested until week 12. The rest of the timetable parallels the progress made over the course of the semester.

## 11. Conclusion

Smartphone-based SPR sensors provide an effective tool for analyzing substances outside of traditional lab settings. The simple yet highly sensitive process that SPR sensors use allow for real-time antibody testing that can provide tools for disease detection to remote and lower income locations across the globe. Unlike many smartphone-based SPR sensors, our device allows for easy replacement of the disposable SPR sensor chip without requiring realignment of the optical components, as is needed for optical fiber-based SPR sensors. This provides our device with a longevity that previous SPR sensors lacked. The conception of this device involved using an LED light source with multiple lenses, filters, an optical fiber with gold film attached, and a smartphone camera as the detector. Over the course of the first part of the senior design capstone class these components have either been removed or replaced for something more optimal. The Light source was changed to a laser diode from an LED because LED light sources tend to have a fair amount of power loss as the light travels

through the system. A laser diode provides a more consistent power output and reduces the number of optical components required in the system because collimating and focusing lenses are no longer a necessity. This also frees up room to adjust the distances between each of the utilized components. The optical fiber was also removed from the system and replaced with a right-angle N-BK7 glass prism with a customized surface plasmon resonance chip attached to one of the faces. This replacement was necessary as the optical fiber must be replaced after every test due to contamination on the surface of the part of the fiber where the cladding is removed for the gold film. A prism is easy to clean, and the surface plasmon resonance chips can be used a maximum of three times before needing a replacement. We have also removed the smartphone from the optical system and instead will use an external CMOS camera for our detector. This allows our final product to be much more versatile compared to previous smartphone based SPR sensors developed as it allows any smartphone or computer with our application installed to control the SPR sensor and receive detailed graphs detailing any molecular binding that took place. Many past smartphone based SPR sensors were limited by the type of smartphone used due to the location of camera's varying widely from smartphone to smartphone. While our experiment will prove the sensitivity of our SPR sensor to molecular binding of SPA and IgG, our device can be repurposed to detect various other substances such as salmonella and pesticides by simply changing the SPR sensor chip to one that contains the necessary bound protein for molecular binding to occur with these other substances.

The optical prototype demonstration will be constructed on a miniature optical table and will use a different diode than the device. This is only because time constraints prevent the construction of an adequate mount for the device's diode for the free space optical system. A thin gold film was glued to one of the faces of the prism as the location of the surface plasmons. When light makes contact with the film, evanescent waves are created along the surface and are detectable on the screen at an angle greater than the angle of total internal reflection. Once surface plasmon excitation was detectable, the optical components were placed into the system to verify that the process was still occurring.

The device housing will be 3D printed with proper distances between components to ensure no issues while collecting data. The device will have a separate chamber for the solutes for antibody detection in various concentrations. This chamber will also make it easier to exchange damaged or dirty sensor chips for fresh sensor chips. Once the light reflects off of the gold film it will enter into the CMOS sensor. The sensor will photograph the light every half second at a resolution of 1600x1200 and the intensity profile will be detected and analyzed using python through the self-developed application. The molecular binding concentration will be computed and displayed on the screen with an intensity map. This intensity map will first be created using MATLAB. Certain functions such as 'improfile' will be used on the captured images from the CMOS sensor to determine the pixel value across a x-y line segment across each

image. This line segment will tell us the intensity of each pixel, which can be compared with the other images captured during the experiment. During molecular binding, the pixel values will change as the resonance angle changes due to refractive index differences as the analyte binds to the ligand. The program will collect the various pixel values measured for every image and determine the changes in the angle measured. The changes in the angle throughout the experiment will then be plotted on a graph showing the change in the resonance angle versus time. This graph will then be shown to the user to visually represent when and for how long surface plasmon excitation occurred and molecular binding began between the observed analyte and ligand. The MATLAB program will then be converted to Python so that the software application can be created for multiple operating systems including Windows, Android, MacOS, iOS, and Linux.

In a time where viruses such as COVID-19 affected the world in such a catastrophic way, medical equipment that can speed up the drug development process are crucial. Surface plasmon resonance sensors are seen as a lab-on-a-chip devices that can effectively and quickly determine the efficacy of a drug based on the molecular binding observed. SPR devices are a highly sensitive tool used in early drug discovery tests to determine how quickly a drug's effects will occur, how long of a duration these effects will last, and what dosage is needed for the required effects to take place. Understanding these effects can aid scientists in determining the best course to take during the drug development process to create an effective vaccine in as fast a time as possible. With our device, we have shown that SPR sensors can be designed to be low-cost and portable to allow on-site detection to be possible for remote and low-income areas, paving the way for future drug development to be possible regardless of location constraints or funding.

## **Appendix A – References**

\*To be filled in with endnote citations\*


IEEE 1118.1-1990 - IEEE Standard for Microcontroller System Serial Control Bus. Retrieved October 30, 2019. From [https://standards.ieee.org/standard/1118\\_1-1990.html](https://standards.ieee.org/standard/1118_1-1990.html)


Kosap, S. O. (2013). Chapter 3-4. Semiconductor Science and Light-Emitting Diodes. In *Optoelectronics and Photonics: Principles and Practices* (2nd ed., Ser. International Edition, p.240,282). Pearson.

Hecht E. (2017). Chapter 8. Polarization. In *Optics Fifth* (5<sup>th</sup> ed., p.330-331) Pearson.

## Appendix B – Permissions

The following are the various forms of permission and their current status for use of citations and figures in our documentation. Approval status for various sources mentioned below are pending.

 Contact Us Summary



**Dear Customer,**

Thank you for contacting us via your recent comments on [Newport.com](https://www.newport.com). A member of the Newport team will be in contact with you as appropriate in response to this inquiry.

---

**Subject Category:**  
Other

**Comments:**  
Hello, I'm a Photonics engineering senior at CREOL UCF. I am in my capstone class to graduate and am wondering if I can use information from your optical surfaces web page and a graph from one of the products I purchased in my document. This paper will not be purchased for monetary gain. The following links below contain information I would like to use.  
Thanks! <https://www.newport.com/n/optical-surfaces>  
<https://www.newport.com/p/FR-OD100>

**Name:**  
Robert Jacob Ballentine

New message from: [mei-2014](#) (1,167 ★)

Dear friend

The BG9 picture you can use, because it is the picture we drew when measuring our products. But LB1 picture and JB470 picture are not from us, we use them for reference. you can easily get these pictures on the internet.

Best regards

Reply

### Your previous message

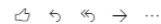
Hello,

I'm an undergraduate photonics engineering student at UCF. I am in my capstone class to graduate with my undergraduate and am wondering if I can use some of the graphs on your products in my research paper. The graphs I am requesting permission to use are the BG39 shortpass filter, the LB1 bandpass filter, and the JB470 long pass filter. The filters I have not purchased may be purchased in the future if my capstone project needs a different filter. The following images are the graphs I would like to use. Thank you.

-Robert B



Safa Kasap (Professor) <[sok533@usask.ca](mailto:sok533@usask.ca)>  
Wed 7/7/2021 9:42 PM  
To: Robert Ballentine



Yes, you can.

I don't think you would need permission for use in an academic report/thesis and it is a very small fraction of the book so it would also go under "fair use"

SK

On 7/7/2021 7:38 PM, Robert Ballentine wrote:

**CAUTION:** External to USask. Verify sender and use caution with links and attachments. Forward suspicious emails to [phishing@usask.ca](mailto:phishing@usask.ca)

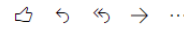
...

Hello Dr Kasap,  
I'm an undergraduate photonics engineering student at the University of Central Florida. I am in my capstone class to graduate with my bachelor's degree. I am writing to you today to ask permission to use some figures from your book Optoelectronics and Photonics 2nd edition. The figures I would like to use are figure 3.29 on page 240 and figure 4.1 on page 282. Figure 3.29 is an energy band diagram of a p-n junction before and after an applied bias and figure 4.1 is a figure about absorption, spontaneous emission, and stimulated emission. These figures will not be used for monetary gain.

Thank you,  
Robert Ballentine



Robert Ballentine  
Wed 7/7/2021 9:52 PM  
To: hecht@adelphi.edu



Hello Dr Hecht,

I'm an undergraduate photonics engineering student at the University of Central Florida. I am working on my research paper for my senior design capstone class. I am emailing you to ask for permission to use a figure and some information from your textbook Optics 4th edition. I would like to use some information from section 8.1.1, Linear Polarization, and figure 8.1 to show linear light. This paper will not be used for monetary gain.

Thank you,  
Robert ballentine

Reply | Forward

## Permission for [Liu, Y. citation]

### Rights and permissions

This work is licensed under a Creative Commons Attribution 4.0 International License. The images or other third party material in this article are included in the article's Creative Commons license, unless indicated otherwise in the credit line; if the material is not included under the Creative Commons license, users will need to obtain permission from the license holder to reproduce the material. To view a copy of this license, visit

<http://creativecommons.org/licenses/by/4.0/>

To: info@nicoyalife.com

Hello, my name is Robin Howell and I am a Photonics Engineering senior at the University of Central Florida. I am designing an SPR sensor for my capstone class for graduation. In our project documentation, I would like to mention your OpenSPR device as a commercial SPR sensor in the market today. Specifically, I would like to use the image below that I found on your website that illustrates your OpenSPR device. I wanted to ask if I could have your permission to use the image below in our final documentation of our project? This paper will solely be used in an academic environment and will not be used for monetary gain. Thank you for your help and I look forward to hearing from you.

Robin Howell

Below is the mentioned image.



Dear Robin:

Thank you very much for contacting ACS. Yes, ACS is granting you a permission to cite Safety in Academic Chemistry Laboratory (SACL) 8/e as a source documentation of your project. Please include the following ACS copyright credit line whenever the SACL as is quoted or excerpts are used:

***Quoted/ used with permission from ACS Safety in Academic Chemistry Laboratory 8<sup>th</sup> edition , Copyright 2017, American Chemical Society. Not to be used for commercial purposes.***

There is no charge for this one time use.

Please let me know if I can be of any help to you.

Marta Gmurczyk

**Marta U. Gmurczyk, Ph.D.**

Senior Safety Programs Manager| Scientific Advancement Division

Dear Robin Howell,

Thank you for placing your order through Copyright Clearance Center's RightsLink® service.

#### **Order Summary**

Licensee: University of Central Florida  
Order Date: Jul 8, 2021  
Order Number: 5104310924117  
Publication: Sensors and Actuators B: Chemical  
Title: A smartphone based surface plasmon resonance imaging (SPRI) platform for on-site biodetection  
Type of Use: reuse in a thesis/dissertation  
Order Total: 0.00 USD

View or print complete [details](#) of your order and the publisher's terms and conditions.

Sincerely,

Copyright Clearance Center



## 1. Analytical methods

0.00 USD

Article: A smartphone-based surface plasmon resonance platform

Order License ID	Pending	Publisher Portion	RSC Publishing Page
ISSN	1759-9679		
Type of Use	Republish in a thesis/dissertation		

[Hide Details](#)

### LICENSED CONTENT

Publication Title	Analytical methods	Publication Type	e-Journal
Article Title	A smartphone-based surface plasmon resonance platform	Start Page	4732
Author/Editor	Royal Society of Chemistry (Great Britain)	End Page	4740
Date	01/01/2009	Issue	39
Language	English	Volume	10
Country	United Kingdom of Great Britain and Northern Ireland	URL	<a href="http://www.rsc.org/Publishing/Journal...">http://www.rsc.org/Publishing/Journal...</a>
Rights holder	Royal Society of Chemistry		

## Copyright

Copyright © 2018 ChenGuang Zhang et al. This is an open access article distributed under the [Creative Commons Attribution License](#), which permits unrestricted use, distribution, and reproduction in any medium, provided the original work is properly cited.



Study on intensity-modulated surface plasmon resonance array sensor based on polarization control

Conference Proceedings: 2010 3rd International Conference on Biomedical Engineering and Informatics

Author: Boshu Sun

Publisher: IEEE

Date: Oct. 2010

Copyright © 2010, IEEE

### Thesis / Dissertation Reuse

The IEEE does not require individuals working on a thesis to obtain a formal reuse license, however, you may print out this statement to be used as a permission grant:

Requirements to be followed when using any portion (e.g., figure, graph, table, or textual material) of an IEEE copyrighted paper in a thesis:

- 1) In the case of textual material (e.g., using short quotes or referring to the work within these papers) users must give full credit to the original source (author, paper, publication) followed by the IEEE copyright line © 2011 IEEE.
- 2) In the case of illustrations or tabular material, we require that the copyright line © [Year of original publication] IEEE appear prominently with each reprinted figure and/or table.
- 3) If a substantial portion of the original paper is to be used, and if you are not the senior author, also obtain the senior author's approval.

License Number 5121060960650

[Printable Details](#)

License date Aug 02, 2021

#### Licensed Content

Licensed Content Publisher	Elsevier
Licensed Content Publication	TrAC Trends in Analytical Chemistry
Licensed Content Title	Wavelength-modulation surface plasmon resonance sensor
Licensed Content Author	Xia Liu, Daqian Song, Qinglin Zhang, Yuan Tian, Lan Ding, Hanqi Zhang
Licensed Content Date	Nov 1, 2005
Licensed Content Volume	24
Licensed Content Issue	10
Licensed Content Pages	7

#### Order Details

Type of Use	reuse in a thesis/dissertation
Portion	figures/tables/illustrations
Number of figures/tables /illustrations	1
Format	both print and electronic
Are you the author of this Elsevier article?	No
Will you be translating?	No

#### About Your Work

Title	Portable Surface Plasmon Resonance Sensor for Immunoglobulin G Antibody Testing
Institution name	University of Central Florida
Expected presentation date	Dec 2021

#### Additional Data

Portions	Figure 1
----------	----------